FLUID, THERMAL AND AEROSPACE SCIENCES

ENGINEERING DIVISION

CASE INSTITUTE OF TECHNOLOGY

LIQUID GAS CYCLONE SEPARATION

by

Sanford Fleeter and Simon Ostrach

UNIVERSITY CIRCLE • CLEVELAND, OHIO 44106

FTAS/TR-66-12

LIQUID GAS CYCLONE SEPARATION

by

Sanford Fleeter and Simon Ostrach

AFOSR Technical Report Number
AFOSR 66-1400

June 1966

ABSTRACT

This paper considers the secondary-flow of a liquid-gas mixture in a cyclone separator. By means of a momentum integral method, an engineering approximation to the secondary (heavy fluid) flow rate is obtained which makes use of an experimental velocity profile determined by ter Linden. This flow rate approximation is physically realistic and is partially verified in the laboratory.

Tests were run on a separator to determine the effect of the variation of certain operating conditions and geometric factors on the separation of a liquid-gas mixture. The effect of these variations on the efficiency of separation and pressure drop across the separator as functions of the Reynolds and Weber numbers is presented.

ACKNOWLEDGMENTS

This research was made possible by the financial support of the Air Force Office of Scientific Research (AF-AFOSR-194-66).

TABLE OF CONTENTS

LIST OF FIGURES

List of Figures (continued) Page

List of Figures (continued) Page

LIST OF TABLES

U. S. DEPARTMENT OF COMMERCE
Bureau of Public Roads

Experimental Form No.

Report Number:

Research and Development Studies

0379

ABSTRACTING AND EVALUATION WORKSHEET

Report Title & Date: Stabilization of Silty Soils in Alaska, Part II, Interim Report

Author(s): H. R. Peyton and J. W. Lund

Program Area: D-3 (4651-042)

Financing:
(HPR-PR-Adm.) HPR-1(2)

Conducting Agency: University of Alaska

State Study Ident. No: 12470

Sponsoring Agency:

BPR Study Ident. No: 5

[3] Year of a: [ ] year study

(x) continuing

Project Status: Active

(Approved, active, inactive, dropped, completed or accepted)

1. Abstract: original by: D. G. Fohs

Date: 1/27/66

edited or
reviewed by: E. B. Kinter

Date:

This brief interim report describes a laboratory study of the effects on the permeability and frost heave characteristics of an Alaskan silt, AASHO Classification A-4(8), produced by adding Portland cement, tetra-sodium pyrophosphate (TSPP), tri-sodium phosphate, calcium chloride, and sodium hexametaphosphate. Frost heave tests were performed to measure the effectiveness of polyvinyl membrane to prevent the detrimental effects of frost.

TSPP (0.3 percent) caused a large decrease in permeability and also proved most effective in reducing frost heave. Portland cement applied at rates from 1 to 3 percent did not greatly affect permeability and, for the soil tested, increased frost heave. The polyvinyl membrane prevented frost heave but caused redistribution of the water to the top of the specimen indicating the possibility of serious loss of strength in the upper layers of the pavement.

LIST OF SYMBOLS

A	Cyclone Inlet Width
B	Cyclone Inlet Weight
D	Cyclone Diameter
d	Overflow Diameter
E	Boundary Layer Velocity Parameter
$\vec{F}$,	Body Force per Unit Mass
F_1, F_2, F_3	Components of Body Force Vector in X, Y, Z Directions Respectively
f	Underflow Diameter
F_r	Froude Number
K(x)	Velocity Distribution
L	Characteristic Length
L_1	Dimensionless X Coordiante of Heavy Fluid Exit (ratio of underflow diameter to cyclone diameter)
ℓ_1	X Evaluated at the Heavy Fluid Exit
P	Pressure
p	Dimensionless Pressure
$\dot{q}_H$	Heavy Fluid Fow Rate in Boundary Layer
R	Radius of Surface of Revolution
R_o	Cyclone Radius
R_e	Reynolds Number
U,V,W	Velocity Components in X,Y, and Z, Directions Respectively
u,v,w	Dimensionless Velocity Components

List of Symobls (continued)

W_e	Weber Number
X	Arclength along Generators of a Surface of Revolution
Y	Orthogonal Trajectories of Surface Generators
Z	Coordinate Normal to the Surface of Revolution
x,y,z	Dimensionless X,Y,Z, Coordinates
β	Inlet Angle
$\vec{\gamma}$	Dimensionless Body Force Vector
δ	Boundary Layer Thickness
δ	Dimensionless Boundary Layer Thickness
η	Dimensionless Coordinate Normal to Surface in Boundary Layer
η_{RL}	Efficiency of Removal of Heavier Fluid Components
θ	Semi-apex Angle of Cones
ν	Kinematic Viscosity of the Liquid
σ	Surface Tension of the Liquid

ERRATA

Page	Line	Should Read
2	4	properly
9	13	subsequent
14	11	pressure
15	19	consideration
17	3	$u \frac{\partial u}{\partial x} - \frac{v^2}{\partial x} + w \frac{\partial u}{\partial z} = \ldots$
17	11	Solution
27	6	value of $.621 \frac{\delta_1}{L_1} > .621 (Re)^{1/2} \ldots$
37	19	separator
51	8	23 and 24 with Figures 25 through 28.
70	2	($\ell_1 = f/d$)
78	9	See Figures 37 and 46.

CHAPTER I

INTRODUCTION

I.1 Cyclone Separation

In the operation of a cyclone separator, a mixture, consisting of either two fluids or a solid and a fluid, is introduced tangentially into a cylindrical chamber. It is this tangential injection which causes the mixture to enter into a vortex-like motion which, in turn, produces a centrifugal force field. This force field causes the heavier component of the mixture to move outward - toward the surface of the cylinder. The lighter component remains in the center portion of the cylinder. See Figure 1.

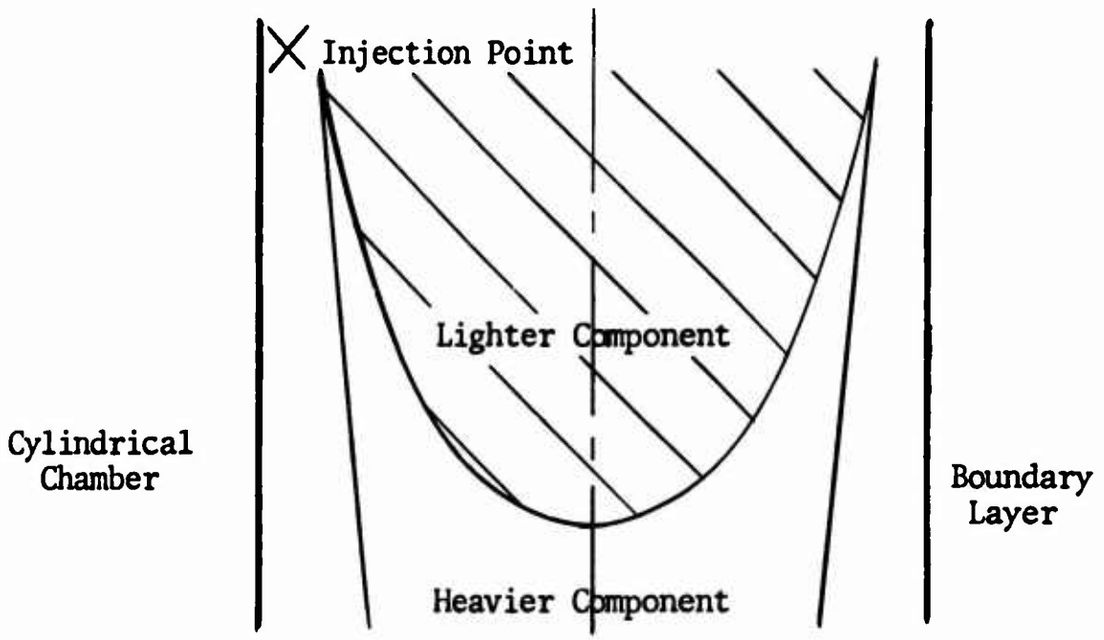

Figure 1

The initial concept of operation was that the heavier component would exit downward only because of gravity, while the lighter component would exit upward from continuity considerations. Ostrach [1] indicated, however, that by a propely shaped exit for the heavier component, e.g. a concial section, a secondary flow would be generated. Ostrach based his concept on a generalization of the work of Taylor [2] who showed that for the rotating flow of a single fluid in a cone, secondary flows do exist. This rotational flow together with the body force field determines the pressure distribution in the boundary layer which, as discussed by Lawler [6] and Taylor [2], is directed towards the apex of the cone. The boundary layer fluid is retarded by viscosity and, therefore, does not have sufficient inertia to maintain a circular path above the cone axis. The pressure gradient then directs this retarded fluid towards the cone apex where it exits.

Thus the discharge of the heavier component of a mixture in a cyclone separator is the result of both gravity and a secondary flow. The relative importance of this secondary flow is noted by ter Linden who states that cyclone dust collectors have been efficiently operated in an inverted position and by Lawler and this author who operated a liquid-gas cyclone separator successfully, but not efficiently, in an inverted position. See Figure 2.

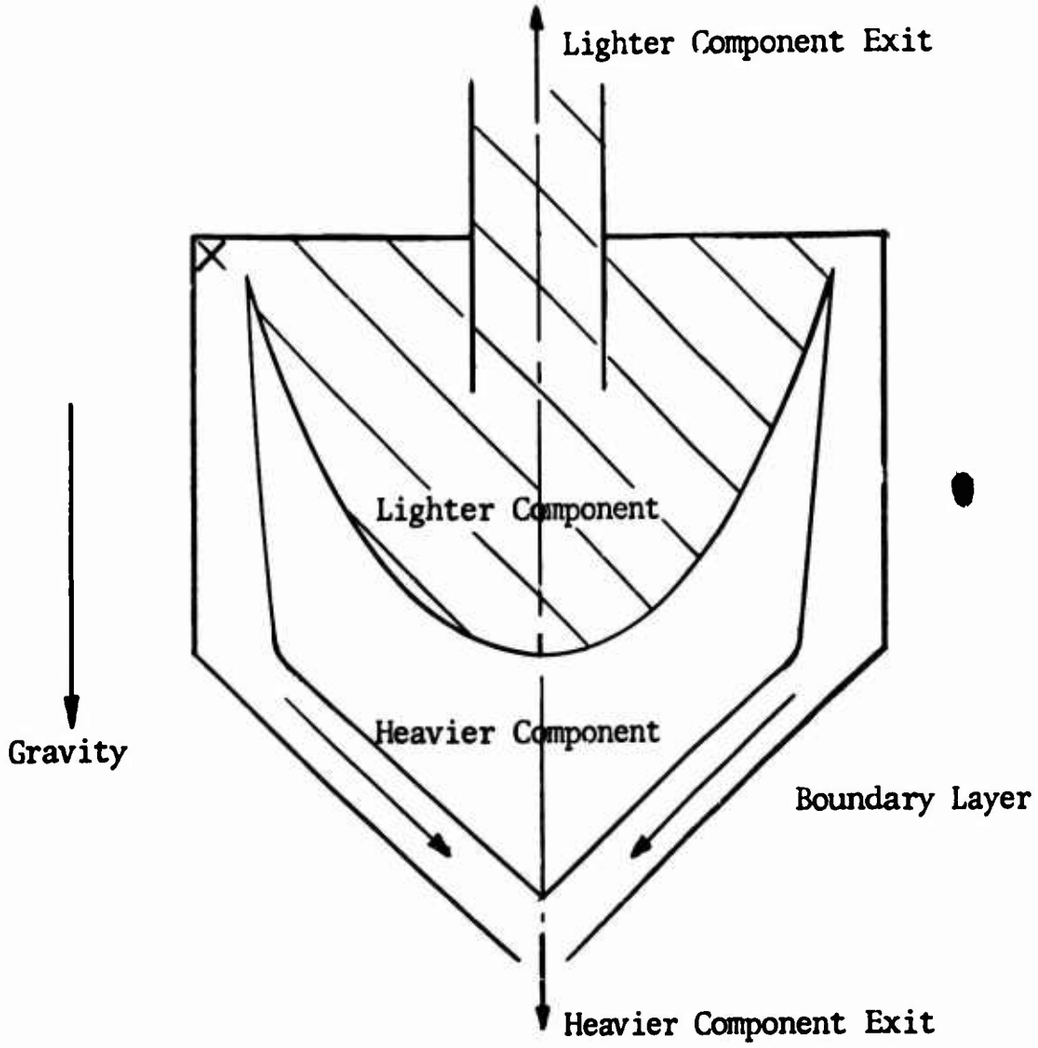

Figure 2

This operation of the cyclone separator in the inverted position makes such a cyclone a possible means of delivering the heavier component of the mixture to its exit in micro - or zero gravitational environments. Also, the fact that a cyclone separator has no moving parts makes it attractive for space applications.

I.2 Previous Work

This paper is concerned only with the case of liquid-gas separation, that is, the case where a liquid is separated from a mixture which is primarily gaseous. Therefore, in this section, a review of only liquid-gas separation work is presented. For a complete review of the work done on the other separation possibilities, such as gas-gas, liquid-liquid, or gas-liquid, the reader is referred to Lawler [6].

The principle analytical contribution to cyclone separation is that due to Ostrach who described the discharge mechanism as discussed in Section I.1. Lawler, in his paper, assumed that the flow in the conical section of the separator was that of a potential vortex. A momentum-integral method was then used to predict secondary flow rates. These predicted flow rates serve only as an upper bound approximation, as noted by Lawler, because of two assumptions: (1) The velocity of the outer edge of the liquid boundary layer is taken to be the same as that of the inner rotating gas core; (2) The flow can be represented by a potential vortex.

There exists a gaseous boundary layer between the inner gaseous core and the liquid boundary layer. Hence the velocity of the outer edge of the liquid boundary layer is lower than that of the inner rotating gas core. A potential vortex flow implies that as the axis of the separator is approached, the flow tends to infinity. In actuality, however, the flow at the axis approaches a large but finite velocity. Thus, in Lawler's approximation too large a value for the

velocities both at the axis of the separator and at the outer edge of the fluid boundary layer have been assumed, leading to an upper bound predicted flow rate.

Stromquist [1] experimentally investigated the effect of varying the inlet flow rate and mass fractions of the components of the mixture on a separator of fixed geometry. Data are presented for both pressure drop and efficiency of removal. These data are of questionable value as there were two design limitations: (1) there was a guide vane normal to the surface of the separator; (2) the heavy component exit was located on the side of the cone near the apex (see Figure 3).

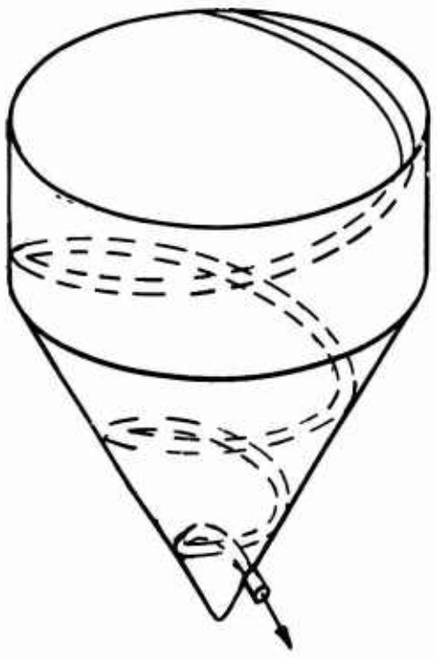

Figure 3. The Stromquist Separator

Van Dongen and ter Linden [4] in a somewhat qualitative analysis, suggest that the concial section is not always the most desirable shape due to turbulent re-entrainment of the liquid in the strong secondary gas flows. They also speculate that a smaller pressure drop would result for the separator shape indicated in Figure 4.

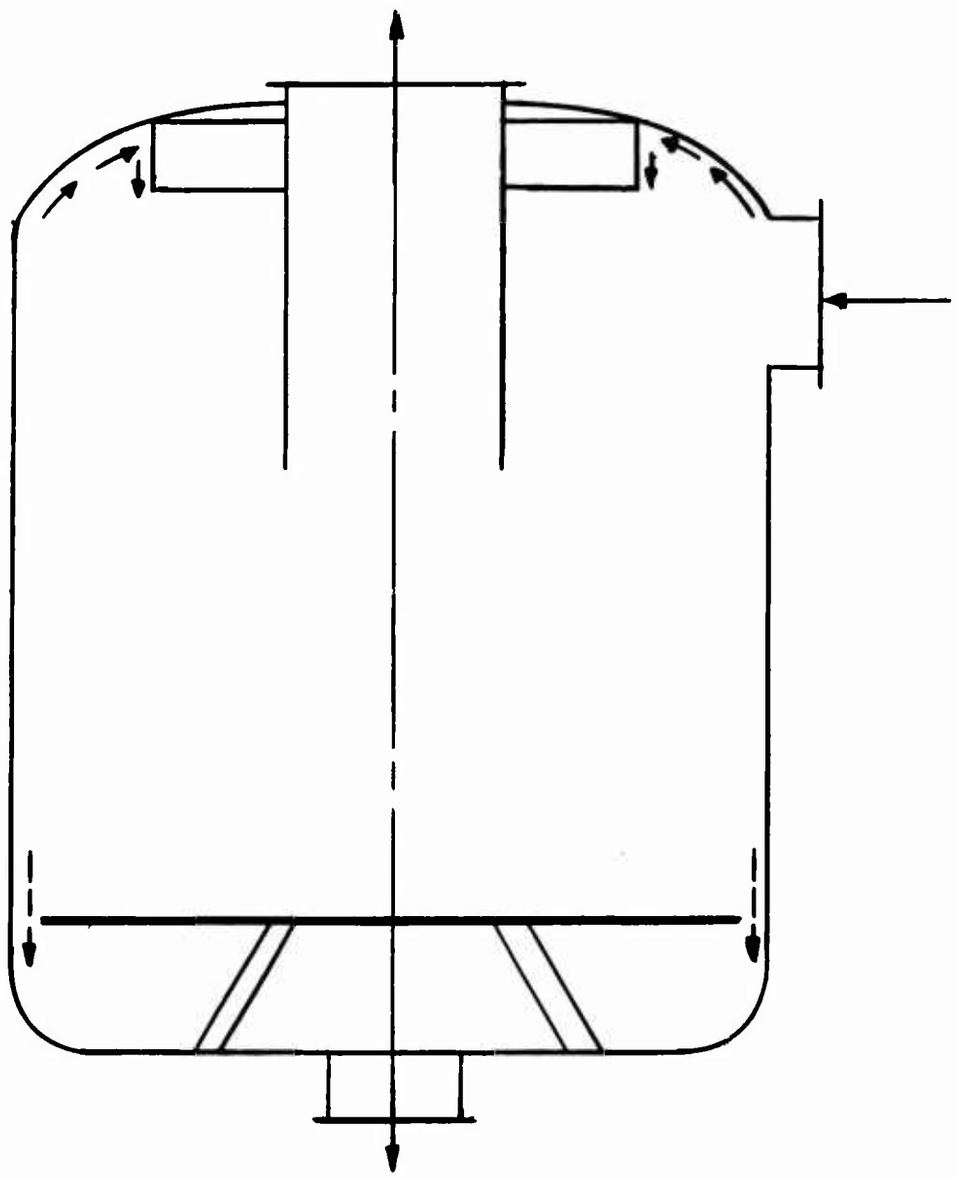

Figure 4. The ter Linden Cyclone

Lawler, with the separator configuration indicated in Figure 2, used water and air as the working fluids to obtain data on pressure drop and efficiency. However, the evaporation of the water into the air and the fact that the Reynolds number could only be varied by changing the inlet flow rate indicated the necessity of more experimental information.

I.3 Proposed Work And Relation To Previous Work

There are two primary purposes of the present study. The first is to obtain analytically a more accurate engineering approximation to the secondary flow rate. This is accomplished by an analysis similar to those of Ostrach, Taylor and Lawler, but which makes use of a cyclone boundary layer velocity profile which was experimentally determined using dust particles in a gas by ter Linden [3]. This analysis should result in more accurate secondary flow rate predictions than those obtained by Lawler since the singularity of the potential flow in the cylinder resulting from Lawler's assumption of a potential vortex has been eliminated. However, the effect of the gaseous boundary layer on the velocity of the liquid boundary layer still has not been considered. Hence, one might expect that this new secondary flow rate prediction might still be too large.

The second purpose is to obtain improved experimental results, making use of the same cyclone separator as used by Lawler. Over certain ranges of operating conditions Lawler's working fluids, air and water, may not have formed a mixture. Thus, it is desired

to improve the mixing of the two working fluids so as to have a uniform mixture entering the cylindrical chamber over all operating conditions. Also, as mentioned in the previous section, Lawler's experimental results were affected by evaporation and by the limited range of Reynolds number variation. Hence, results without the effect of evaporation and over a wide range of parameter variation are also to be obtained.

CHAPTER II

ANALYSIS

II.1 Derivation Of The Boundary Layer Equations

The tangential injection of the fluid mixture into the cyclone separator and the subsequent separation into components and secondary flow is to be considered, for the purpose of analysis, to be composed of three distinct and separate operations: (1) the establishment of the rotational flow; (2) the separation of the mixture into components; (3) the flow of the components.

A vortex-like flow is established in the cylindrical section of the separator due to the tangential injection of the fluid mixture. This has been observed experimentally by ter Linden [3] and by Lawler [6].

Assuming the separation process to be independent of the subsquent flow of the two components is not completely correct. However, if this assumption is not invoked then one must consider the mixing and separation with the flow model being one of globules of one component dispersed in the other component which acts as the carrier fluid of the mixture. As pointed out by Lawler, it is extremely difficult if not impossible, actually to solve this problem in such a manner. Hence, in order to obtain an approximate solution to the problem, it is assumed that the separation process is independent of the flow of the mixture components.

To continue this analysis the following assumptions are made:

i) The actual separation of the mixture into a lighter and a heavier component occurs only in the cylindrical section of the cyclone separator. This permits the boundary layer flow to be considered independent of the separation process.

ii) The cross-section of the separator is as indicated in Figure 2 —— The heavier component is on the surface of the conical section and the lighter component is nearer to the center of the separator, away from the surface of the cone. This assumption has been experimentally verified.

iii) There is only one component of the mixture comprising the boundary layer, namely the heavier component. This permits a one-fluid boundary layer analysis to be used.

iv) The heavier component of the mixture has a constant viscosity and is also incompressible.

v) Time-independence of the flow is also assumed, that is, steady flow.

Next, a coordinate system must be chosen. A convenient coordinate system to choose is the Geodesic Coordinate System as suggested by Moore [5]. Another assumption is now made: the surface under consideration is a surface of revolution with a principal radius of curvature which is large compared to the boundary layer thickness. This assumption permits the boundary layer equations to be easily obtained in the Geodesic Coordinate System. The reader is referred to Lawler [6] for the detailed derivation of these equations.

In the Geodesic Coordinate System, the coordinates are denoted by X, Y and Z: X is taken to be the arc length along a generator of the surface; Y is the azimuthal angle measured along the orthogonal trajectories of the generators; and Z is the normal to the surface. R, the radius of the revolution of the generators, is a function of X which is specified for each particular surface. Such a right-handed system is indicated in Figure 5.

The boundary layer and continuity equations in this coordinate system are:

$$\omega_1 \frac{\partial \omega_1}{\partial X} - \frac{\omega_2^2}{R} R' + \frac{\omega_2}{R} \frac{\partial \omega_1}{\partial Y} + \omega_3 \frac{\partial \omega_1}{\partial Z} = F_1 - \frac{1}{\rho} \frac{\partial P}{\partial X} + \nu \frac{\partial^2 \omega_1}{\partial Z^2} \qquad (2\text{-}1a)$$

$$\frac{\omega_2}{R} \frac{\partial \omega_2}{\partial Y} + \omega_3 \frac{\partial \omega_2}{\partial Z} + \omega_1 \frac{\partial \omega_2}{\partial X} + \omega_1 \omega_2 \frac{R'}{R} = F_2 - \frac{1}{\rho R} \frac{\partial P}{\partial Y} + \nu \frac{\partial^2 \omega_2}{\partial Z^2} \qquad (2\text{-}1b)$$

$$F_3 - \frac{1}{\rho} \frac{\partial P}{\partial Z} = 0 \qquad (2\text{-}1c)$$

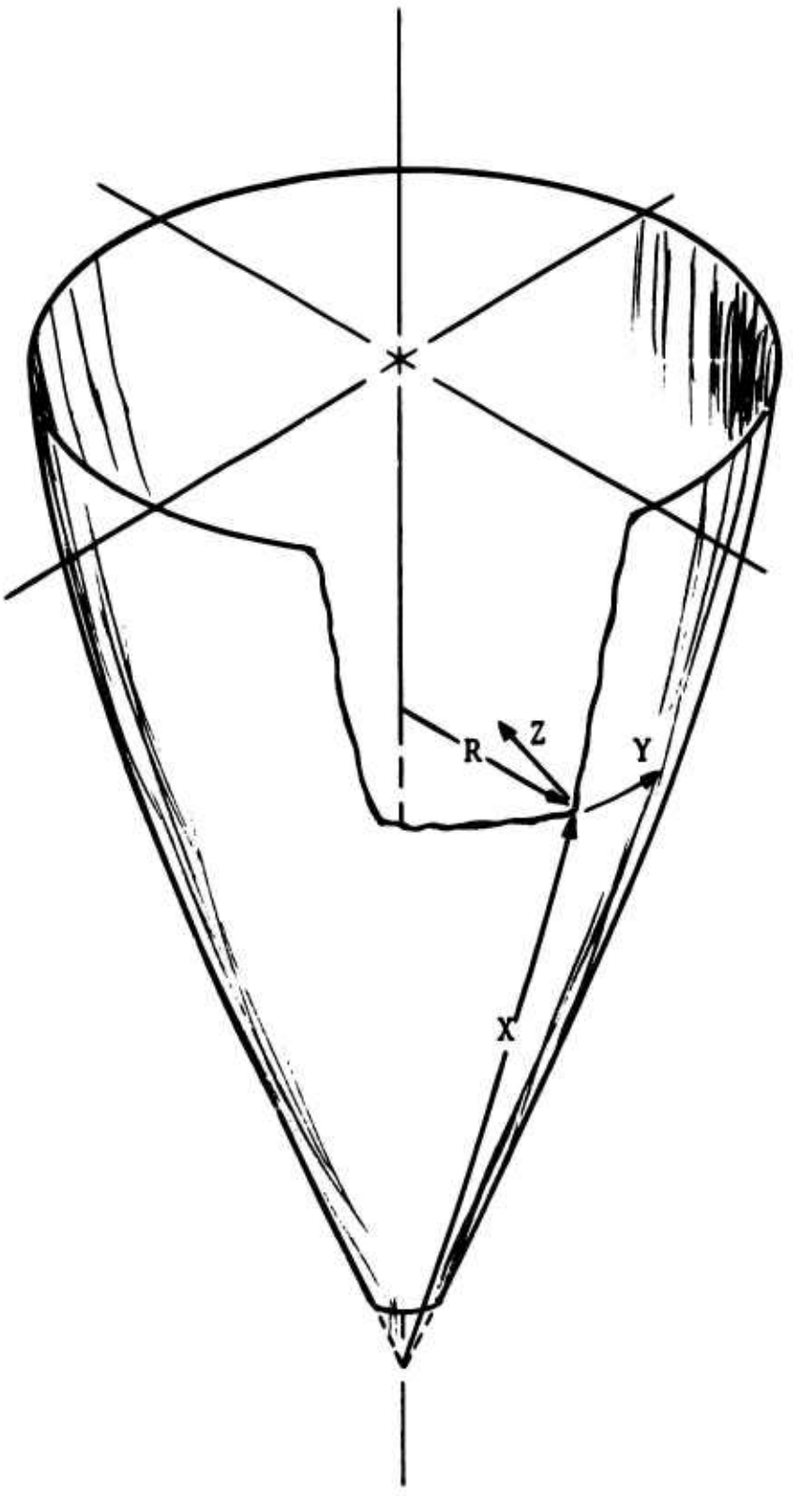

Figure 5. Geodesic Coordinate System For A Body Of Revolution

$$\frac{\partial \omega_1}{\partial X} + \frac{R'}{R}\omega_1 + \frac{1}{R}\frac{\partial \omega_2}{\partial Y} + \frac{\partial \partial \omega_3}{\partial Z} = 0 \qquad (2\text{-}1d)$$

Where $\vec{\omega}$ is the velocity field whose components in the X, Y and Z directions are respectively ω_1, ω_2 and ω_3;

F_1, F_2 and F_3 are the respective components of the body force per unit mass:

and R' denotes $\frac{dR}{dX}$.

In order to obtain non-dimensional equations, the inlet velocity of the mixture, V_o, is chosen as a characteristic velocity, and the following dimensionless quantities are defined:

$$x = \frac{X}{L}\ ;\ y = \frac{Y}{L}\ ;\ z = \frac{Z}{L}\ ;\ r = \frac{R}{L}\ ;$$

$$p = \frac{P}{\rho V_o^2}\ ;\ u = \frac{\omega_1}{V_o}\ ;\ v = \frac{\omega_2}{V_o}\ ;\ w = \frac{\omega_3}{V_o}\ ;$$

$$\gamma_i = \frac{F_i}{|\vec{g}|}\ ;\ R_e = \frac{V_o L}{\nu}\ ;\ F_r = \frac{V_o^2}{L\vec{g}} \qquad (2\text{-}2)$$

Where L is taken to be the length along the side of the cone surface;

$\vec{g}$ is the acceleration due to gravity;

R_e, the Reynolds number, is the ratio of inertia forces to viscous forces;

F_r, the Froude number, is the ratio of the inertia

forces to the body forces.

In non-dimensional form equations (2-1a)- (2-1d) are:

$$u\frac{\partial u}{\partial x} + \frac{u}{r}\frac{\partial u}{\partial y} + w\frac{\partial u}{\partial z} - \frac{v^2}{r}r' = \frac{1}{F_r}\gamma_1 - \frac{\partial p}{\partial x} + \frac{1}{R_e}\frac{\partial^2 u}{\partial z^2} \qquad (2\text{-}3a)$$

$$u\frac{\partial v}{\partial x} + \frac{v}{r}\frac{v}{y} + w\frac{\partial v}{\partial z} + \frac{uv}{r}r' = \frac{1}{F_r}\gamma_2 - \frac{1}{r}\frac{\partial p}{\partial y} + \frac{1}{R_e}\frac{\partial^2 v}{\partial z^2} \qquad (2\text{-}3b)$$

$$\frac{1}{F_r}\gamma_3 - \frac{\partial p}{\partial z} = 0 \qquad (2\text{-}3c)$$

$$\frac{1}{r}\frac{\partial}{\partial x}(ru) + \frac{1}{r}\frac{\partial v}{\partial y}\frac{\partial p}{\partial z} = 0 \qquad (2\text{-}3d)$$

Looking at these equations and recognizing that the driving force for the flow is composed of both the body force and the pressure gradient, the relative importance of the Froude number can be recognized. Since the Froude number multiplies only the body forces and not the prssure gradient, the value of the Froude number determines the relative importance of the two components of the driving force: i) a small Froude number indicates that the driving force will be primarily a result of the body force; ii) a large Froude number indicates that the body forces will be but a negligible part of the driving force. Hence, for large values of the Froude number the body force terms may be neglected.

Two more assumptions are now made:

i) The only body force acting is that of gravity. Also, the axis of revolution of the body is

parallel to the line of action of gravity. This implies that $\gamma_2 = 0$; $\gamma_1 = \pm\sqrt{1-r'^2}$; $\gamma_3 = r'$. Thus, the shape of the underportion of the separator determines the influence of the body force in the X - direction. A suitable shape could maximize or even eliminate the influence of this body force component. For a conical undersection, r' = constant and, for the special case of $R_o = L$, a flat plate, $r' = 1$ and $\gamma_1 \equiv 0$. Hence a flat plate undersection would eliminate the effect of body force in the X direction.

ii) Viscous flow theory states that the driving force across a boundary layer is zero, that is, $\gamma_3 - \frac{\partial p}{\partial z} = 0$. Hence, by a consideration of the inviscid flow outside of the boundary layer, the pressure gradients within the boundary layer can be determined.

The fact that the boundary layer flows over a surface of revolution (a cone) can now be taken into consieration:

$\frac{r'}{r} = \frac{1}{x}$ Geometry of a cone

$\frac{\partial}{\partial y} = 0$ Axial symmetry of a cone.

Thus; the final boundary layer equations are:

$$u \frac{\partial u}{\partial x} + w \frac{\partial u}{\partial z} - \frac{v^2}{x} = - \frac{\partial p}{\partial x} + \frac{1}{R_e} \frac{\partial^2 u}{\partial z^2} \tag{2-4a}$$

$$u \frac{\partial v}{\partial x} + w \frac{\partial v}{\partial z} + \frac{uv}{x} = \frac{1}{R_e} \frac{\partial^2 v}{\partial z^2} \tag{2-4b}$$

$$\frac{1}{F_r} r' - \frac{\partial p}{\partial z} = 0 \tag{2-4c}$$

$$\frac{\partial u}{\partial x} + \frac{u}{x} + \frac{\partial w}{\partial z} = 0 = \frac{\partial}{\partial x} (xu) + \frac{\partial}{\partial z} (xw) \tag{2-4d}$$

To relate the driving forces within the boundary layer to the outer inviscid flow, the Euler Equations and continuity must be considered.

Let the subscript I denote the inviscid flow. Assume that in the flow outside of the boundary layer $u_I = w_I = 0$.

Thus: $$\frac{v_I^2}{x} = \frac{\partial p}{\partial x}$$

Equation (2-4a) becomes:

$$u \frac{\partial u}{\partial x} - \frac{v^2}{x} + v \frac{\partial u}{\partial z} = - \frac{v_I^2}{x} + \frac{1}{R_e} \frac{\partial^2 u}{\partial z^2} \qquad (2\text{-}5)$$

The boundary conditions for the boundary layer equations 2-5, 2-4b, 2-4c, 2-4d are:

$$u = v = 0 \quad \text{at } z = 0 \qquad (2\text{-}6a)$$

$$u = 0 = \frac{\partial u}{\partial z} = \frac{\partial v}{\partial z} \quad v_I = K(x) \quad \text{at } z = \delta \qquad (2\text{-}6b)$$

where δ is the boundary layer thickness; and $v_I = K(x)$ is such that the inviscid flow may be said to be a vortex-like flow.

II.2 Soultion Of The Boundary Layer Equations

In solving equations similar to the boundary layer equations (2-4)- (2-6), Taylor used a momentum integral method, integrating from 0, the cone surface, to δ, the boundary layer thickness, with respect to z.

In a manner similar to that of Taylor, equations (2-5) - (2-4b,c,d) are integrated with respect to z from 0 to δ, giving two integral relationships which must satisfy the boundary conditions (2-6a) - (2-6b). The reader is referred to Appendix I for a

derivation of the integral relations. To satisfy the boundary conditions let:

$$u = E(x)\ K(x)\ F(\eta) = E(x)\ K(x)\ (\eta - 2\eta^2 + \eta^3) \qquad (2\text{-}7a)$$

and

$$v = K(x)\ \phi(\eta) = k(x)\ (2\eta - \eta^2) \qquad (2\text{-}7b)$$

where: $\eta \equiv \frac{z}{\delta}$ = a dimensionless coordinate in the direction normal to the boundary layer.

$E(x)$ is a dimensionless parameter which allows for changes in u with respect to x. $E(x)$ is to be determined.

$K(x)$ determines the velocity profile in the boundary layer and is assumed known.

These expressions, (2-7a) - (2-7b), are substituted into the integral relations, and the variable of integration is changed from z to η. The following two non-dimensional quantities are defined:

$$\delta_1 = \delta \sqrt{\frac{K(x)}{L\nu}} \qquad (2\text{-}8)$$

Finally the integral relations are reduced to two differential equations in terms of E^2 and $E\delta_1^2$ with the condition that at x=1 corresponding to the outer edge of the cone—— $E = \delta_1 = 0$.

The final two non-linear differential equations are:

$$\frac{d}{dx}(E^2) = -\frac{3E^2}{x} - 5E^2 \frac{d}{dx}(\ln K(x)) - \frac{98}{x} - \frac{330\ E^2}{E\ \delta_1^2} \qquad (2\text{-}9a)$$

$$\frac{d}{dx}(E\delta_1^2) = \frac{5}{2}\frac{E\delta_1^2}{x} + \frac{7}{2}E\delta_1^2\frac{d}{dx}(\ell n\, K(x)) + \frac{49E\delta_1^2}{xE^2} + 285 \qquad (2\text{-}9b)$$

Taylor chose his K(x) to represent a potential vortex flow; $K(x) = \Omega/R = \Omega/x\sin\Theta$ where Θ is the semi-vertex angle of the cone being considered. The corresponding dimensionless boundary layer thickness is given by $\delta_1 = \frac{\delta}{Ro}\sqrt{\frac{\Omega}{\nu\sin\Theta}}$.

ter Linden experimentally determined the velocity profile for dust particles in a cyclone separator of semi-vertex angle equal to 15°. This author has approximated ter Linden's results by $K(x) = 13.6+26.1\ [\sin(1.10x)\ e^{-0.95x}]$. See Figure 6. This approximate velocity distribution is used herein for the numerical solution of equations (2-9a) and (2-9b) in order to obtain a more realistic secondary flow rate prediction. The results of the numerical integration are presented in tabular form in Table I.

Figure 7, comparing the dimensionless boundary layer thickness for K(x) equal to a potential vortex $(Kx) = \Omega/R)$ and $K(x) = 13.6 + 26.1\ [\sin(1.10x)\ e^{-0.95x}]$, indicates that for x close to unity, the results are nearly the same whereas for the small x the results differ. This result was to be expected due to the nature of $K(x) = 13.6 + 26.1\ [\sin(1.10x)\ e^{-0.457}]$ - chosen to be finite at the origin as compared to the potential vortex which tends to infinity for small x.

It should be noted that an exact calculation of the flow characteristics in the separator would involve solving the two-fluid problem, matching velocity and shear stress at the interface. Since this is a very difficult problem, an approximate calculation was used in this paper.

A better, but more involved, approximation would be the following: first solve the single rotating fluid problem (for the lighter fluid), imposing the no-slip condition at the separator surface. Then evaluate the shear stress at the surface. Next, instead of using the condition that at the outer edge of the heavier fluid boundary layer the velocities of the two fluids are equal, use the condition that the shear stresses are equal with the velocity gradient of the lighter fluid at the interface being approximated by the velocity gradient at the wall: $\frac{\partial v_r}{\partial z}\Big|_{\zeta} = \frac{\mu_1}{\mu_2} \frac{\partial v_r}{\partial z}\Big|_{wall}$. This will yield a boundary layer thickness and velocity profile which could be considered to be the first step in an iterative scheme to obtain a good approximation to the solution of the exact two-fluid problem.

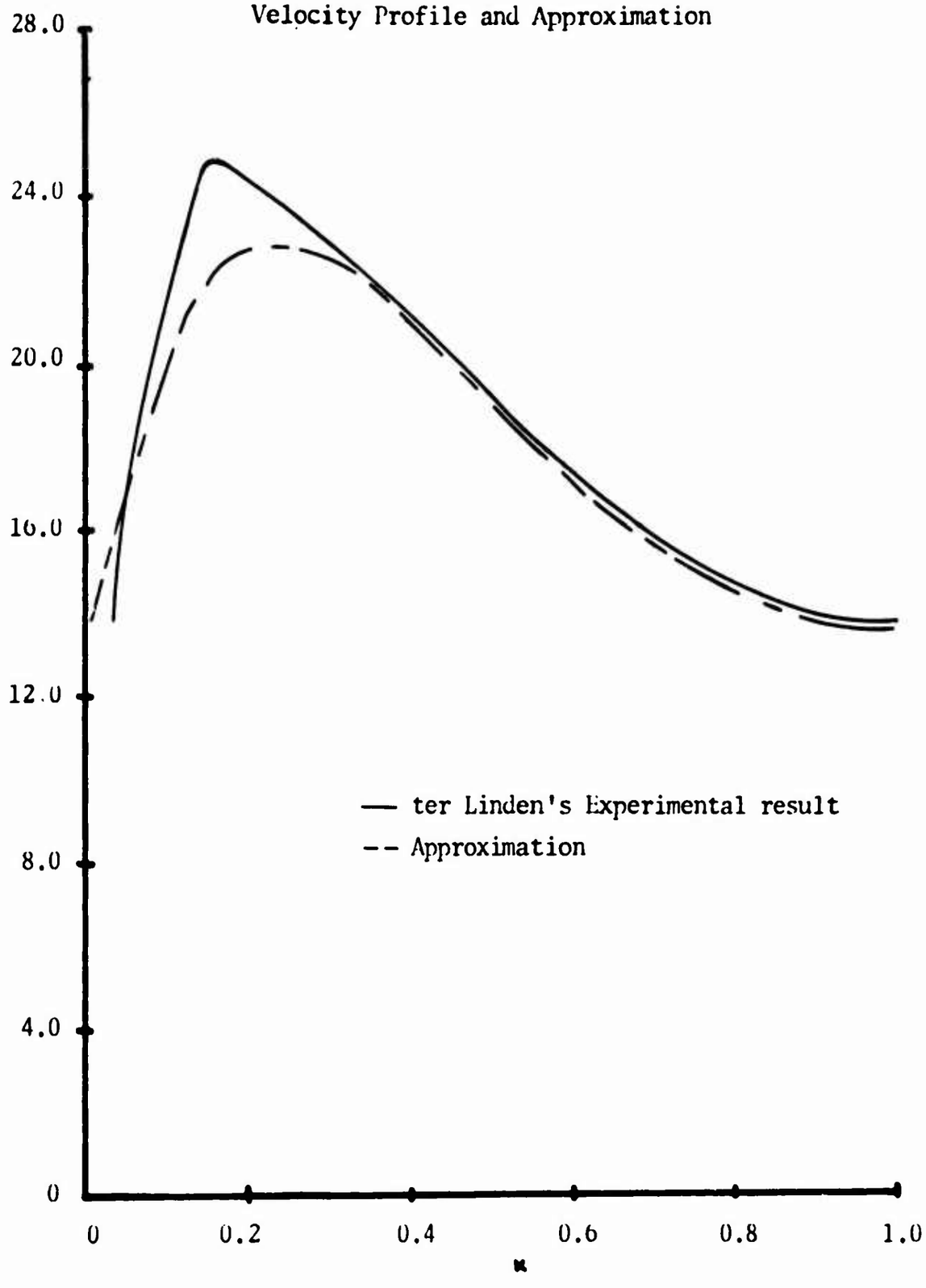
Velocity Profile and Approximation
28.0
24.0
20.0
16.0
12.0
8.0
4.0
0
0
0.2
0.4
0.6
0.8
1.0
x
— ter Linden's Experimental result
-- Approximation

Figure 6

Solution with $K(x) = 13.6 + 26.1[\sin(1.10x)e^{-0.95x}]$

x	1.000	0.975	0.950	0.925	0.900	0.875	0.850
-E	0.000	0.747	1.046	1.280	1.482	1.665	1.834
δ_1	0.000	1.714	2.011	2.197	2.335	2.444	2.534
x	0.825	0.800	0.775	0.750	0.725	0.700	0.675
-E	1.992	2.143	2.289	2.429	2.567	2.702	2.837
δ_1	2.610	2.676	2.734	2.784	2.828	2.865	2.896
x	0.650	0.600	0.550	0.500	0.450	0.400	0.350
-E	2.973	3.251	3.549	3.884	4.275	4.751	5.353
δ_1	2.921	2.948	2.941	2.895	2.804	2.661	2.465
x	0.300	0.250	0.200	0.150	0.100	0.05	0.02
-E	6.150	7.254	8.88	11.48	16.22	27.81	54.17
δ_1	2.215	1.915	1.575	1.210	0.835	0.462	0.221

Table I

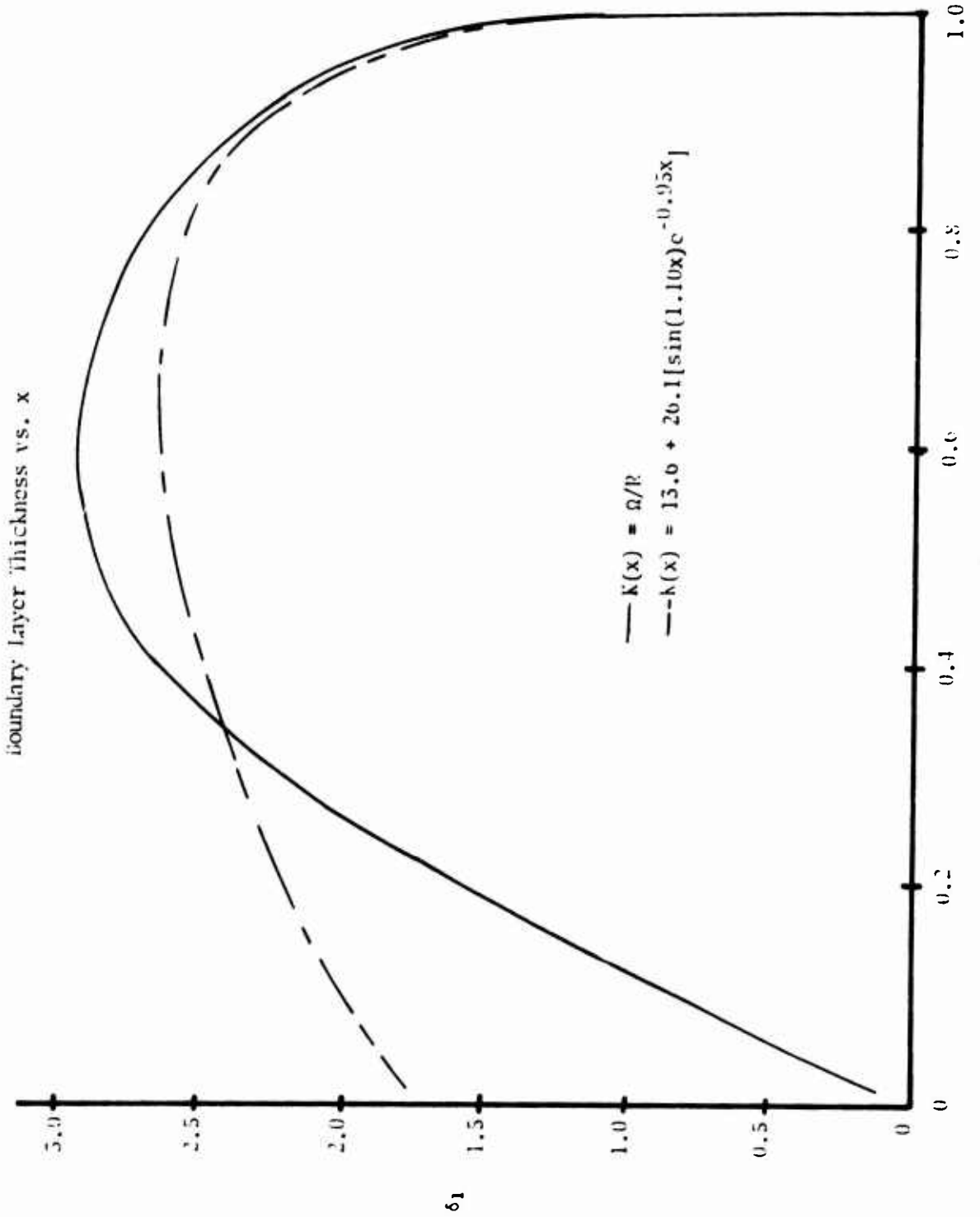
Boundary Layer Thickness vs. x
δ_1
3.0
2.5
2.0
1.5
1.0
0.5
0
0
0.2
0.4
0.6
0.8
1.0
x
K(x) = Ω/R
k(x) = 13.6 + 26.1[sin(1.10x)e^-0.95x]

Figure 7

II.3 Boundary Layer Flow Rate

For this section it is to be assumed that the boundary layers meet at the apex of the cone. This means that only the boundary layer flow consisting of the heavier component of the mixture will be exiting through the cone apex. The reason for considering this case is that the requirement of the meeting of the boundary layers is one of the experimental operating criterion. The other possibility — that of the boundary layers not meeting is discussed in Lawler's paper [6].

For the ensuing discussion, which is still only concerned with the flow in the conical portion of the separator, θ is taken as the semi-vertex angle of the cone, R_o is the radius of the cone taken at its base, r_1, is the exit radius and L, the characteristic height is taken as the slant height of the cone.

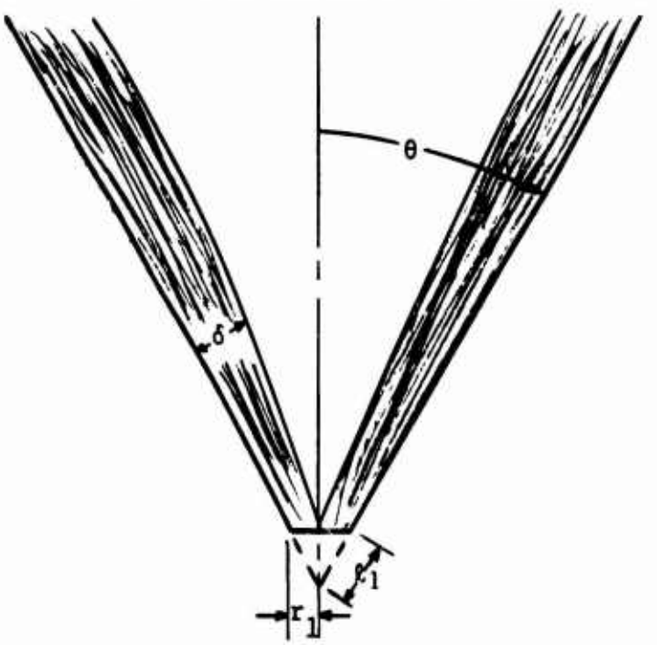

Figure 8

As can be seen from Table I, the boundary layer equations have been solved for small values of x. Physically, however, small values of x correspond to the region near the cone apex, a region in which the boundary layer may not be thin as compared to the radius of curvature. Hence, the following assumption is necessary:

assume the results of the boundary layer analysis as previously determined give a reasonable approximation to the flow for the region of small x.

The geometrical condition for the boundary layers to meet is:

$$\delta = r_1 \cos\theta = \ell_1 \sin\theta \cos\theta \qquad (2\text{-}10)$$

The volume flow rate in the boundary layer, $\dot{q}_H$ is given by:

$$\dot{q}_H = \int_{r_1 - \delta/\cos\theta}^{r_1} 2\pi r\, u\, dr \cos\theta \qquad (2\text{-}11)$$

In order to use ter Linden's experimental results, equation (2-7a) is used here to define u:

$$u = E(x)F(\eta)K(x) = E(x)K(x)(\eta - 2\eta^2 + \eta^3)$$

$$\text{where } \eta = \frac{z}{\delta} \qquad (2\text{-}12)$$

$$\text{and} \quad K(x) = 13.6 + 26.1\,[\sin(1.10x)\, e^{-0.95x}]$$

Note that the range of n is from 0 to 1, where $\eta = 0$ corresponds to the surface of the cone ($r = r_1$) and $\eta = 1$ represents the outer edge of the boundary layer ($r = r_1 - \delta/\cos\theta$).

$$\eta \equiv \frac{z}{\delta} = \frac{(r_1 - r)\cos\theta}{\delta}$$

or $$-r = \frac{\eta\delta}{\cos\theta} - r_1$$

Thus $$-dr = \frac{\delta}{\cos\theta}\, d\eta$$

Rewriting equation (2-11) in terms of η:

$$\dot{q}_H = -2\pi K E \delta r_1 \int_1^0 (\eta - 2\eta^2 + \eta^3)\left[\frac{\eta\delta}{r_1\cos\theta} - 1\ d\eta\right] \qquad (2\text{-}13)$$

Integrating and evaluating equation (2-13) gives the boundary layer flow rate:

$$\dot{q}_H = \frac{-\pi K(x) E(x) \delta r_1}{30}\left[5 - \frac{2\delta}{r_1\cos\theta}\right] \qquad (2\text{-}14)$$

From the physical criterion of the boundary layers being required to meet at the exit, $\frac{\delta}{r_1\cos\theta} = 1$:

$$\dot{q}_H = -0.314\ K(x)\ E(x)\ \delta(x)\ r_1 \qquad (2\text{-}15)$$

δ can be replaced by $\ell_1 \sin\theta \cos\theta$ and r_1 by $\ell_1 \sin\theta$.

Also let $\ell_1 = L\ L_1$ where L_1 is the dimensionless X coordinate.

Note that $L_1 = \frac{\ell_1}{L} = \frac{r_1}{R_o} = \frac{2r_1}{2R_o}$. Hence L_1 can also be interpreted as the ratio of the cone exit diameter to the maximum cone diameter, as well as being the dimensionless X coordinate.

Then:

$$\dot{q}_H = -0.314\ K(\ell_1)\ E(\ell_1)\ L^2 L_1^{\,2}\ \sin^2\theta\ \cos\theta$$

Defining the Reynolds Number as $R_e \equiv \frac{K(\ell_1)L}{\nu}$:

$$\dot{q}_H = -0.314\ \nu\ R_e E L_1^{\,2}\ L\ \sin^2\theta\ \cos\theta \qquad (2\text{-}16)$$

Note that R_e, L_1, and θ are all inter-related from the requirement of having the boundary layers meet at the cone exit — equation (2-10). From this equation and the expression for the dimensionless boundary layer thickness, δ_1:

$$\delta = \ell_1 \sin\theta \cos\theta = \sqrt{L}\ \delta_1 \sqrt{\frac{\nu}{K}}$$

$$\text{or} \quad \delta = \ell_1 \sin\theta \cos\theta = \frac{L\delta_1}{\sqrt{R_e}} \sqrt{\sin\theta}$$

$$\sqrt{\sin\theta}\ \cos\theta = \frac{1}{\sqrt{R_e}}\ \frac{\delta_1 L}{\ell_1} \qquad (2\text{-}17)$$

$$\text{or} \quad \sqrt{\sin\theta}\ \cos\theta = \frac{1}{\sqrt{R_e}}\ \frac{\delta_1}{L_1} \qquad (2\text{-}18)$$

To make use of equation (2-18), $\frac{\delta_1}{\ell_1}$ is a function of L_1, which has already been numerically determined from the boundary layer solutions. Hence equation (2-18) is actually a relationship between L_1, θ and R_e which must be satisfied for the boundary layers to meet. Since the left hand side of equation (2-18) has a maximum value of one, then $\frac{\delta_1}{L_1} > \frac{1}{2} (R_e)^{1/2}$ means that it is impossible for the boundary layers to meet. To obtain the heavy fluid flow rate, $\dot{q}_H$, equation (2-18) must be used in conjunction with equation (2-18).

To facilitate the calculations of the boundary layer flow rate, $\dot{q}_H$, the values of δ_1/L_1 and $L_1^2 E(\ell_1)$ as functions of L_1 are tabulated in Table II.

Figure 11 compares the heavy fluid flow rate as a function of the dimensionless X coordinate, L_1, for K(x) = a potential vortex, and $K(x) = 13.6 + 26.1 [\sin(1.10x)e^{-.95x}]$. The secondary flow rate predicted by means of a potential vortex appears to be physically unrealistic since as L_1 tends to zero, the flow rate goes toward infinity. This implies that as the cone exit diameter decreases (L_1 can be expressed as the ratio of cone exit diameter to maximum cone diameter) the flow rate increases.

Physically one might expect that as the exit diameter decreased to zero, the out flow would also approach zero and, since for the case of no cone ($L_1 = 1$) there would be no pressure gradient driving the flow, there should also be no flow. This implies that there

could exist a maximum flow rate.

Qualitatively the prediction presented herein based upon $K(x) = 13.6 + 26.1\ [\sin(1.10x)\ e^{-0.95x}]$ appears to be physically realistic: as the exit diameter, L_1, tends toward zero, so does the flow; at $L_1 = 1$ (the case of no cone) the flow is zero; there is a maximum secondary flow rate; a lower flow rate is predicted than for the case of a potential vortex.

It is important that the reader be aware of the limitations of these secondary flow rate equations. The equations cannot distinguish the quantity of mixture entering the separator. Hence, whether a large or a small quantity of mixture is introduced into the cyclone separator, the same secondary flow rate will be predicted. Thus, in predicting the flow rate, not only must the conditions of equations (2-16) and (2-18) be met, but also the predicted outflow rate must not be greater than the inflow rate.

For the case of very small exit diameters (very small L_1) it would seem that the secondary flow rate should not be much affected by the amount of fluid entering the separator. A very small exit should imply that only a small quantity of liquid can be removed. Figure 11 indicates the experimental points which appear at lower outflow values than those predicted. This seems reasonable when one recalls the assumption made in the analysis; the velocity at the outer edge of the liquid boundary layer is the same as that of the inner rotating gas core.

$-L_1^2E(L_1)$ vs. L_1

$L_1 = \frac{\ell_1}{L}$	1.00	0.9	0.8	0.7	0.6	0.5
$-E(L_1)$	0	1.48	2.14	2.70	3.25	3.88
$\delta_1(L_1)$	0	2.33	2.68	2.87	2.95	2.90
δ_1/L_1	0	2.59	3.35	4.10	4.92	5.80
$-L_1^2E(L_1)$	0	1.20	1.37	1.32	1.17	0.97
$L_1 = \frac{\ell_1}{L}$	0.45	0.40	0.35	0.30	0.25	0.20
$-E(L_1)$	4.28	4.75	5.35	6.15	7.25	8.88
$\delta_1(L_1)$	2.80	2.66	2.47	2.22	1.92	1.58
δ_1/L_1	6.22	6.65	7.06	7.40	7.68	7.90
$-L_1^2E(L_1)$	0.88	0.76	0.65	0.55	0.45	0.36
$L_1 = \frac{\ell_1}{L}$	0.15	0.10	0.05	0.03	0.02	0.01
$-E(L_1)$	11.48	16.22	27.81	40.28	54.17	95.78
$\delta_1(L_1)$	1.21	0.84	0.46	0.31	0.22	0.12
δ_1/L_1	8.08	8.40	9.20	10.30	11.00	12.00
$-L_1^2E(L_1)$	0.26	0.16	0.070	0.036	0.022	0.010

Table II

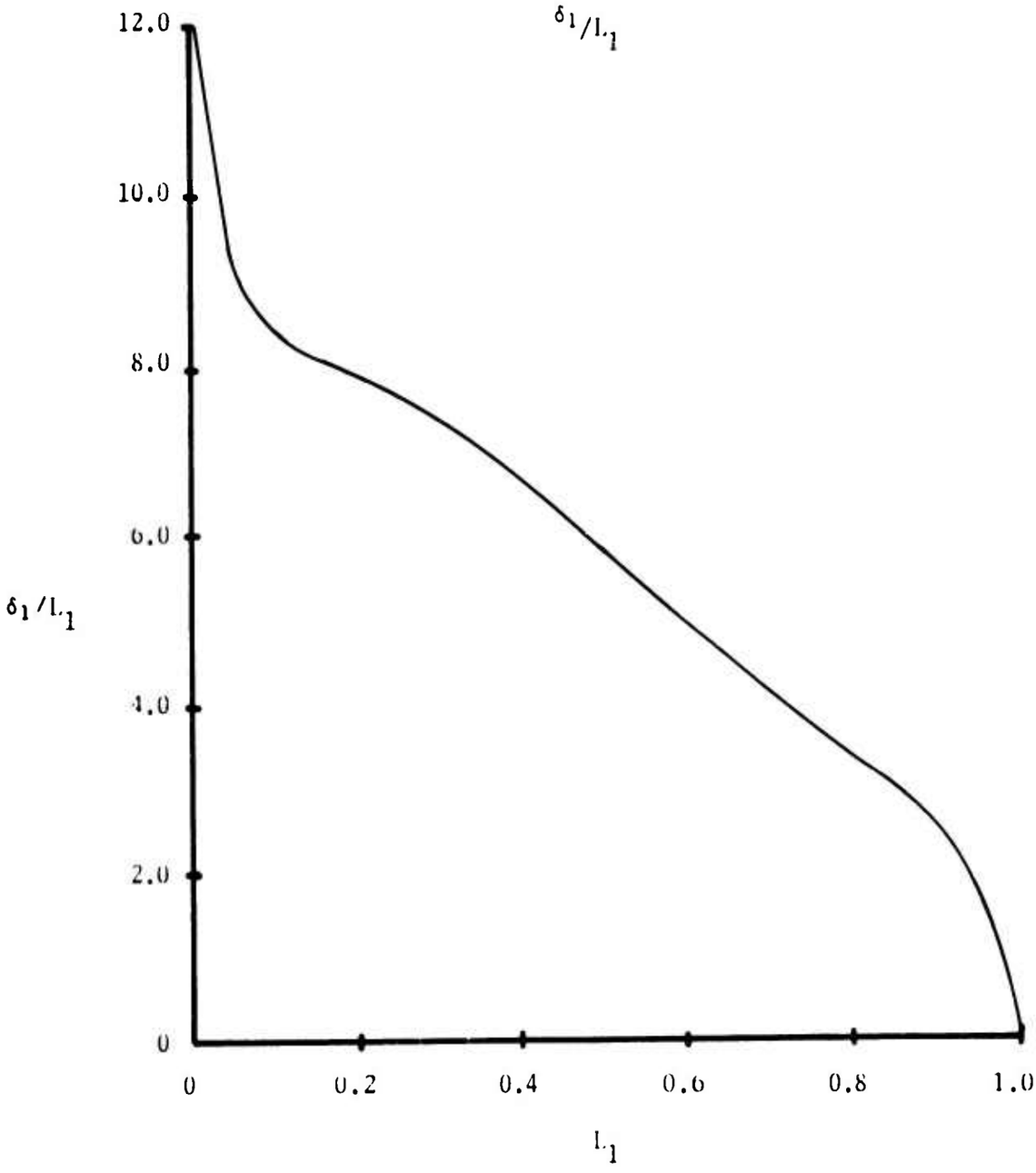

Figure 9

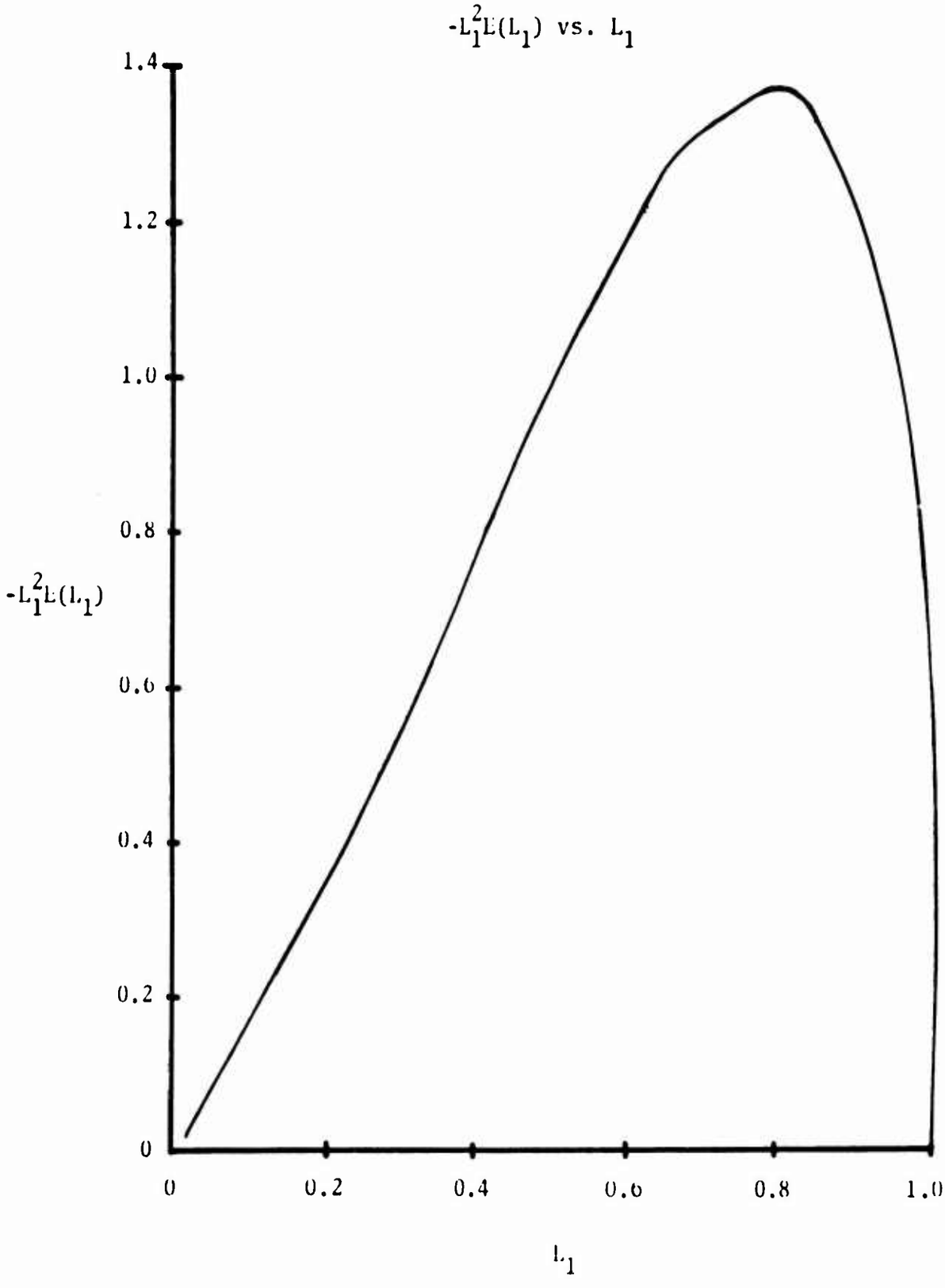

Figure 10

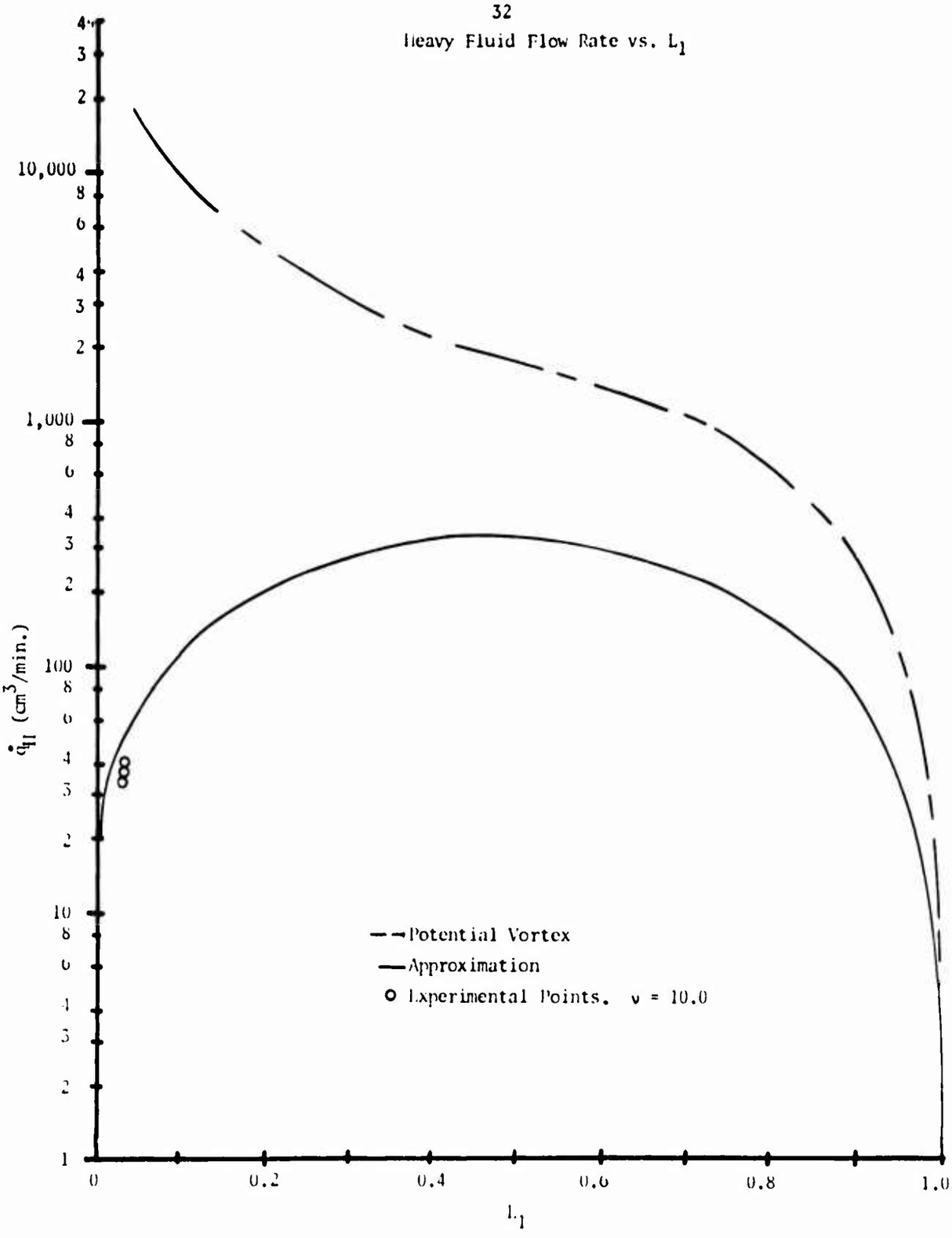
Heavy Fluid Flow Rate vs. L_1
$\dot{q}_{H}$ (cm^3/min.)
10,000
1,000
100
10
1
0
0.2
0.4
0.6
0.8
1.0
L_1
Potential Vortex
Approximation
Experimental Points, ν = 10.0

Figure 11

CHAPTER III

EXPERIMENT

III.1 Experimental Objectives

In Lawler's experiments a water-air mixture was injected into the separator. This use of water and air as the working fluids leads to the following three comments pertaining to his results:

1) To form a water-air mixture, water was sprayed into a moving stream of air. However, over certain operating ranges, it appeared as though the water spray simply traveled down the inlet tube as a jet, without mixing with the air, and impinged upon the back-plate of the cylinder. This was due, to a large extent, to the fact that the surface tension of water is relatively high, 72 dynes/cm.
2) His results pointed out the necessity of obtaining data without the effect of evaporation.
3) The Reynolds number could be varied only by varying the inlet velocity of the mixture.

Air was still used as a working fluid due to its availability but, to overcome the above limitations, silicone oils of different viscosities were used in place of water. These oils were chosen for the following reasons:

1) It was believed that they would not evaporate in air;

2) Their surface tension was much lower than that of water, approximately 20 dynes/cm. as compared to 72 dynes/cm. Hence, there should be a finer, more uniform, oil spray which should mix easily with the air stream and result in a more uniform mixture over all operating ranges, eliminating impingement on the back-plate.

3) Since a large number of silicone oils are readily available with different values of kinematic viscosities (but approximately the same value of surface tension) the Reynolds number could be varied independent of the inlet air flow rate.

Thus, for this study, air and silicone oils are used to determine the effects of varying the operating conditions and geometric dimensions for the process of cyclone separation over a relatively wide range of Reynolds number.

III.2 The Experimental Apparatus

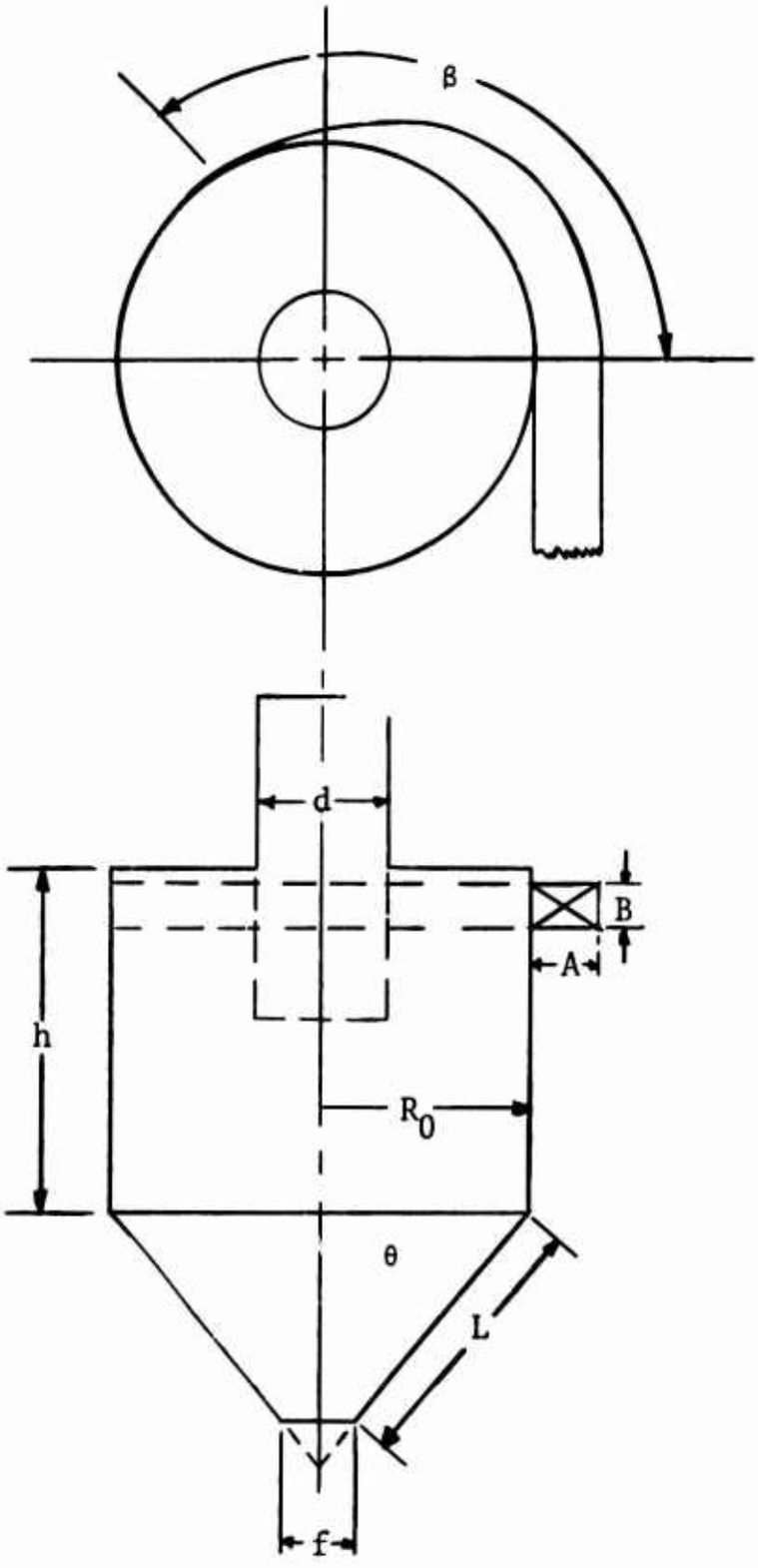

Figure 12

The dimensions of the separator used in this investigation, the same separator as was used by Lawler, are indicated in Figure 12. It is made of cast acrylic and consists of a square cross-section entrance section (A = B = 1.75 in.), an inlet angle β equal to 180°, a height, h, of 4.75 in. and a diameter, ($2R_o$), of 4.5 in. The dimensions of this section are fixed throughout the experiments, thus fixing the diameter of the cyclone. To this basic unit of the separator, various overflow and underflow sections can be attached.

The overflow section consists of a flat circular plate which holds a cast acrylic overflow tube of diameter, d, of 1.75 in. and overflow height, s, of 3.5 in. Because Lawler found that no effect was produced by varying either d or s, these two conditions were fixed during these experiments.

To the other end of the basic section it is possible to attach either the underflow sections to be studied, or additional cylindrical sections of diameter 4.5 in. also made of cast acrylic. These additional sections make it possible to vary both the cylindrical height, h, and the overall separator height H. The range of variation of h was from 4.75 in. to 15.0 in.

The underflow section was chosen to be a cone so that the theory might be verified. Two cone angles, θ, were used: $\theta = 15°$ and $\theta = 45°$. The apex of each of these acrylic cones was removed so that various values of, f, the boundary layer flow exit diameter, could be tested. For these experiments f varied from 0.052 in.

to 0.228 in. which correspond to ratios of exit diameter to cyclone diameter (f/D) = ℓ_1 from 0.015 to 0.051. For a cone, these ratios represent the dimensionless x-coordinate of the boundary layer fluid ℓ_1.

A schematic diagram of the experimental apparatus is shown in Figure 13, while photographs of the system are shown in Figures 14 through 17.

The air flow was supplied by a Roots blower, varied by means of a system of two bleed-off values, and measured by means of an orifice meter. The volume flow rate of air was able to be varied from 0 to 138 cfm, corresponding to an inlet air flow rate of from 0 to 100 fps.

The oil flow was obtained by using an oil accumulator, charged with air pressure, to supply oil to calibrated spray nozzles. The nozzles had to be re-calibrated for each of the three silicone oils used (kinematic viscosities of 1, 10 and 100 centistokes).

The rate at which the boundary layer fluid left the separater, the underflow rate, was determined from a measurement of the time required for a certain volume of the fluid to accumulate.

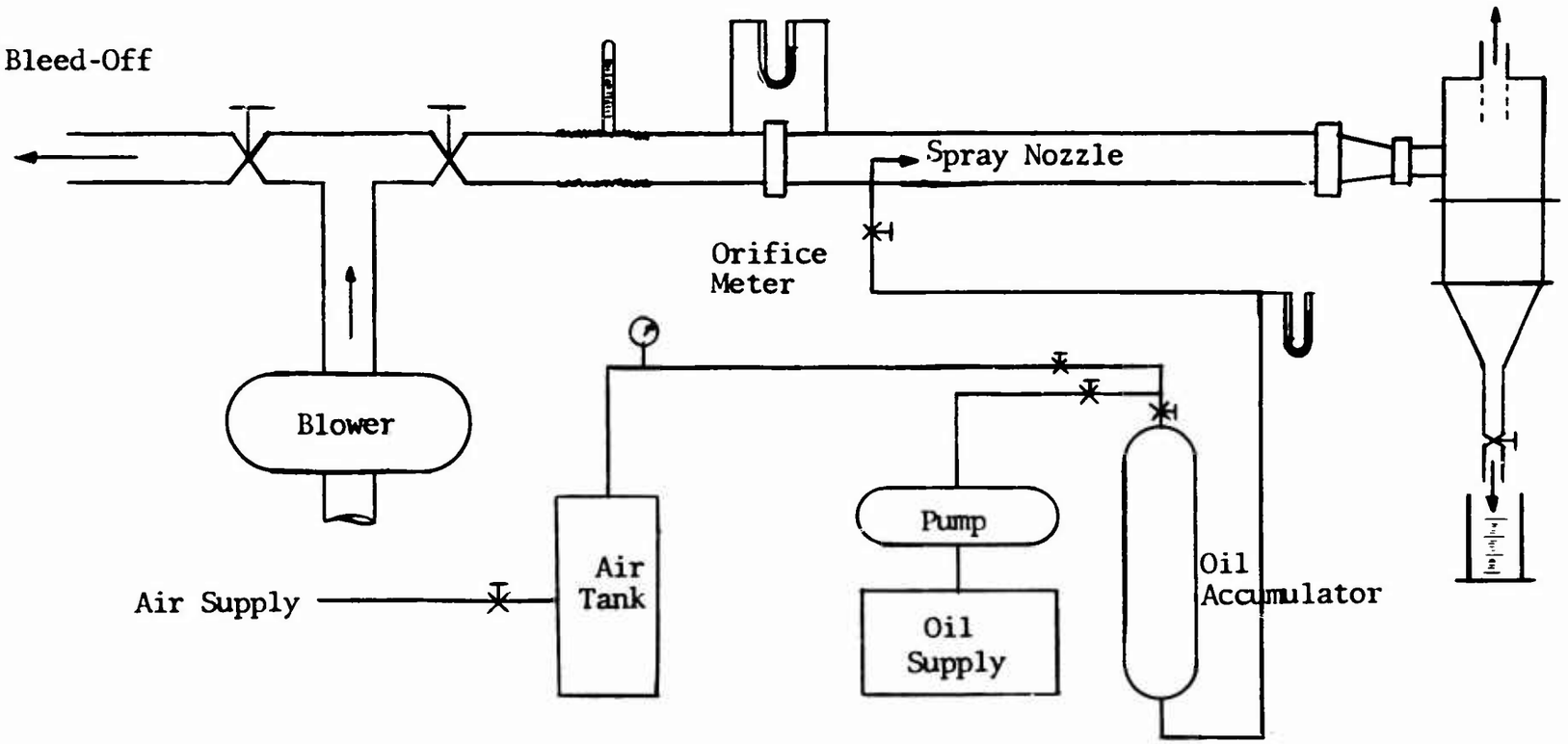
Bleed-Off
Spray Nozzle
Orifice
Meter
Blower
Air Supply
Air
Tank
Pump
Oil
Supply
Oil
Accumulator

Figure 13

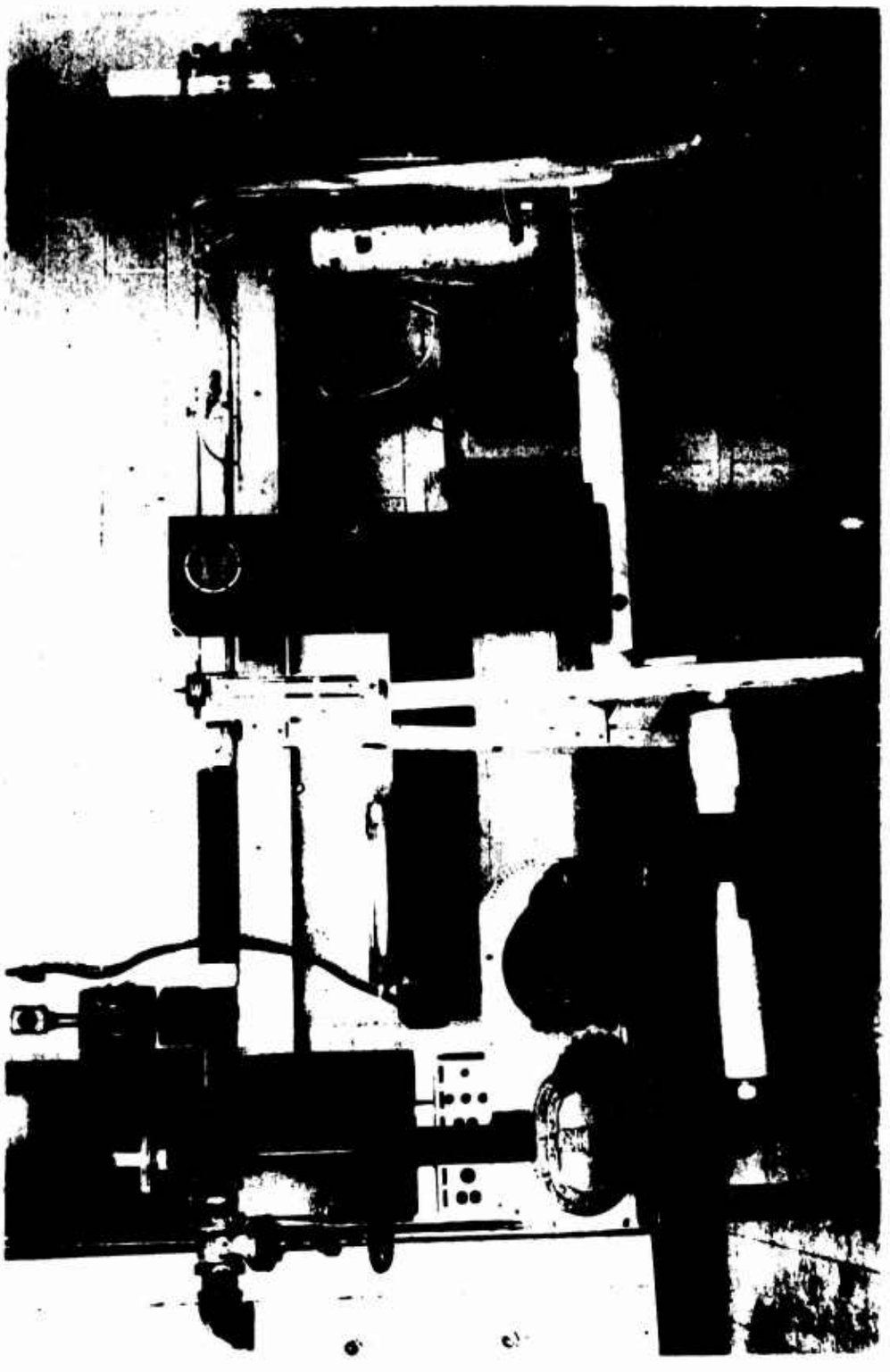

Figure 14. Experimental Apparatus

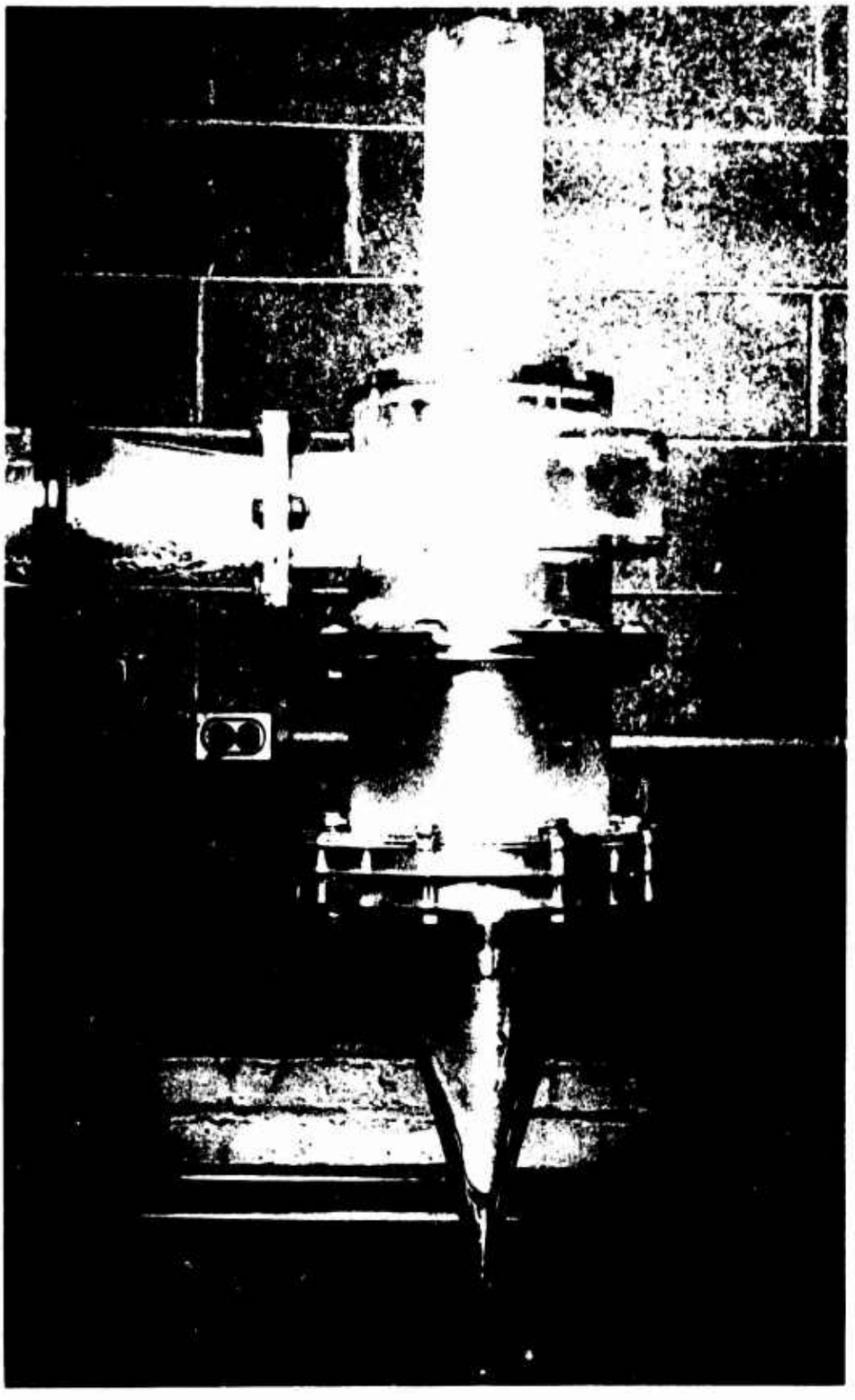

Figure 15. Cyclone Separator h = 8.25 in. θ = 15°

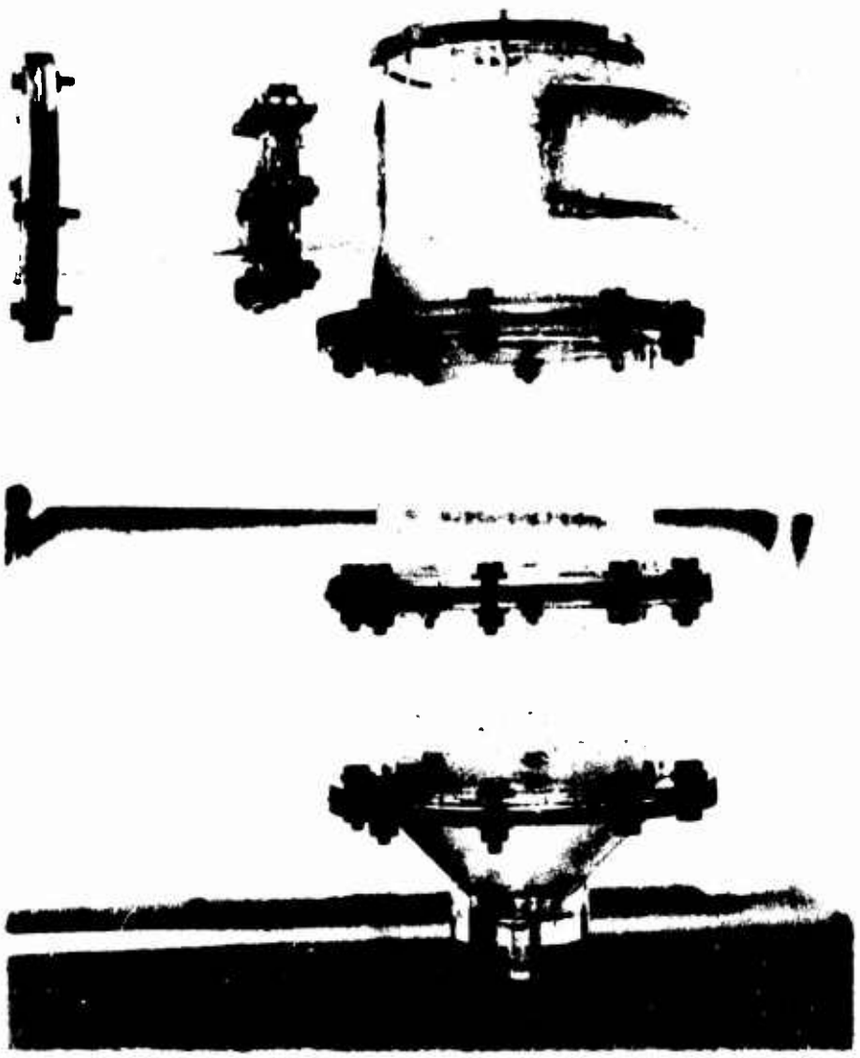

Figure 16. Cyclone Separator h = 12.25 in.

Figure 17. 15° Cone Tips

III.3 Parameters

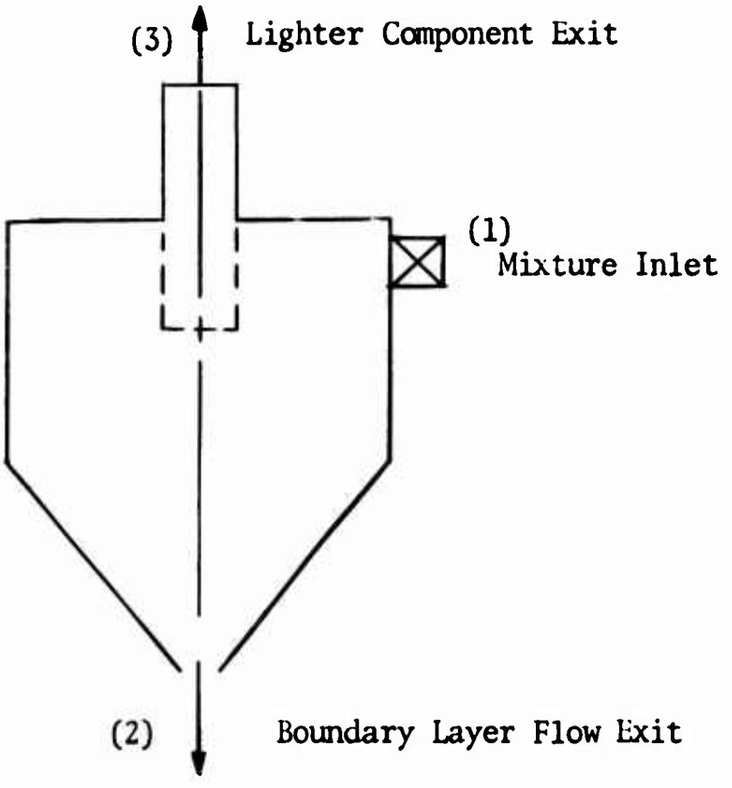

Figure 18

The following parameters are used to evaluate the performance of the cyclone separator.

i) The efficiency of removal, η_{RL}, is defined as the ratio of the mass flow of the boundary layer liquid at the underflow, W_{L2}, (Note: 1,2, and 3 refer to Figure 18) to the mass flow rate of this fluid at the inlet, W_{L1}.

$$\eta_{RL} \equiv \frac{W_{L2}}{W_{L1}}$$

When all of the heavier component is separated from the mixture, the efficiency of removal will have the value of unity.

ii) The pressure drop is another, always important, parameter which is considered.

iii) There are three similarity parameters considered: Reynolds number, Froude number and Weber number. The Reynolds and Froude numbers were discussed in Chapter II and are given by equation (2-2). The Weber number is defined as the ratio of the inertia forces to the cohesive forces, or surface tension, and is given by

$$W_e = \frac{\rho V_o^2 L}{2\sigma}$$

where σ is the surface tension of the boundary layer fluid.

Two criteria were established for the operation of this separator: 1) there was no oil in the overflow (point 3 of Figure 18) and 2) there was 100% oil in the underflow (point 2 of Figure 18). These two criteria are equivalent to demanding 100% purity of the air at the lighter component exit and 100% purity of the oil at the heavier component exit.

For operation of the separator with the aid of gravity criterion 2) was accomplished by placing a throttling valve at the heavier component exit, while the violation of criterion 1) was used to determine the end of a test run.

III.4 Results

The experimental results presented in the following graphs indicate data points which have been averaged over three runs at a given condition in which the variation was less than 2%. Samples of this data are presented in Appendix II.

The Weber number is varied only by changing the reference or inlet, velocity. This is due to the surface tensions of all three oils used, ν = 1.0, 10.0, 100.0 centistokes, being approximately the same, 17.4, 20.1, 20.9 dynes/cm. respectively. The advantage of having a nearly constant value of the surface tension is that the spray characteristics and, hence, the mixing is very nearly the same for each oil.

The Reynolds number for each individual oil is varied by changing the inlet velocity. However, the Reynolds number can also be varied independently of the inlet velocity by changing the value of the viscosity, i.e., using a different oil.

Figures 19 and 20 indicate the variation in efficiency, as functions of the Reynolds number and the Weber number respectively, for oil with ν = 1.0 centistoke and water (ν = 1.0 centistoke). From these graphs it appears as though the oil may be evaporating into the air stream at an even faster rate than for the water, and in fact, that is what has happened. Placing equal masses (33.4 grams) of water and oils with ν = 1.0, 10.0, 100.0 centistokes into an air stream for a short interval of time, it was found that 1.0 grams of water, 2.2 grams of ν = 1.0 oil, 0.2 grams of ν = 10.0 oil and 0.0

grams of $\nu = 100.0$ oil, had evaporated. It should also be noted that this test air stream was traveling with a velocity much lower than that found in the separator. Hence, it is expected that these evaporation effects would be even more pronounced in the cyclone separator.

Efficiency vs. Reynolds Number For Oil (ν = 1.0 Centistoke)
And Water For 15° Cone

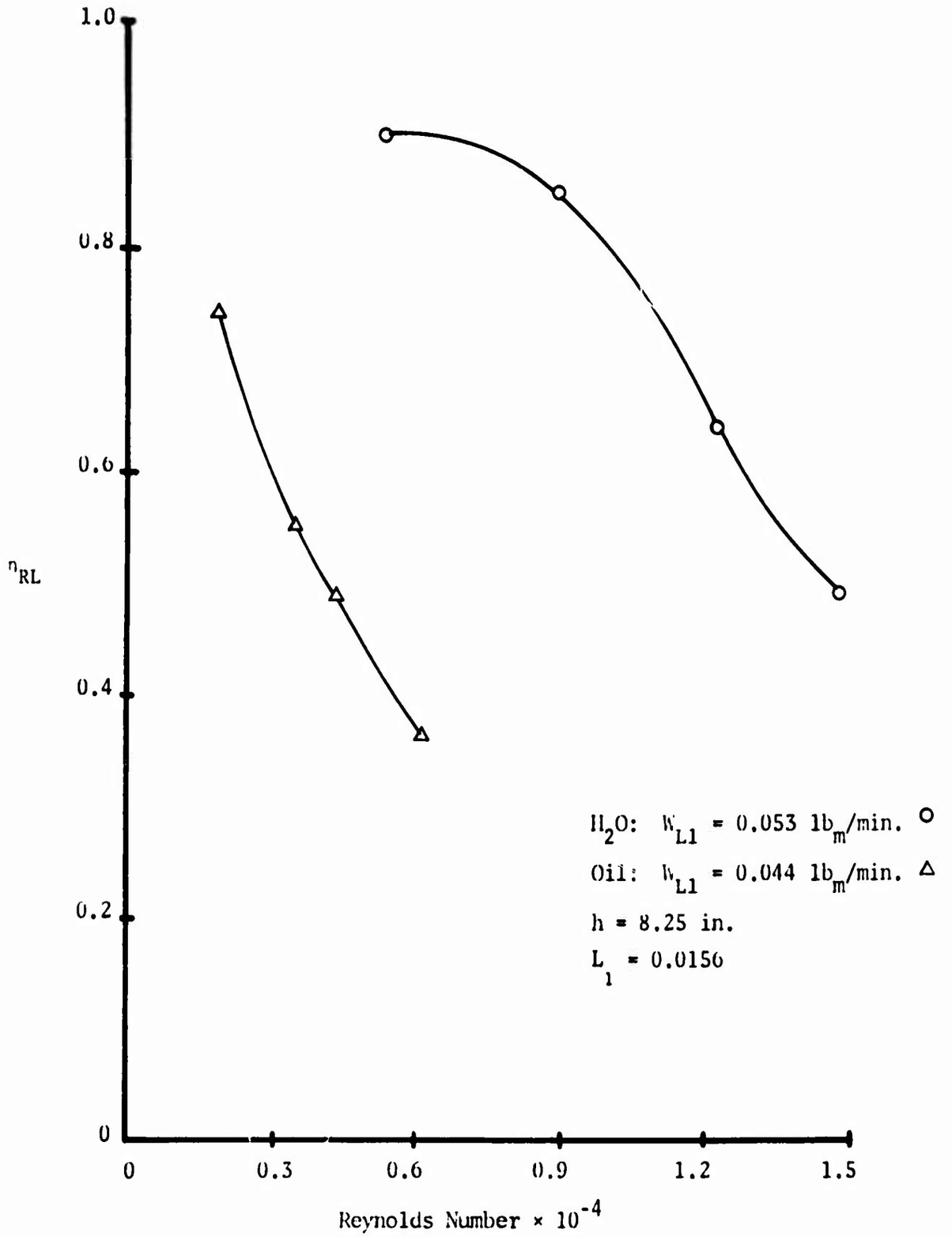

Figure 19

Efficiency vs. Weber Number For Oil (ν = 1.0 Centistoke) And Water For 15° Cone

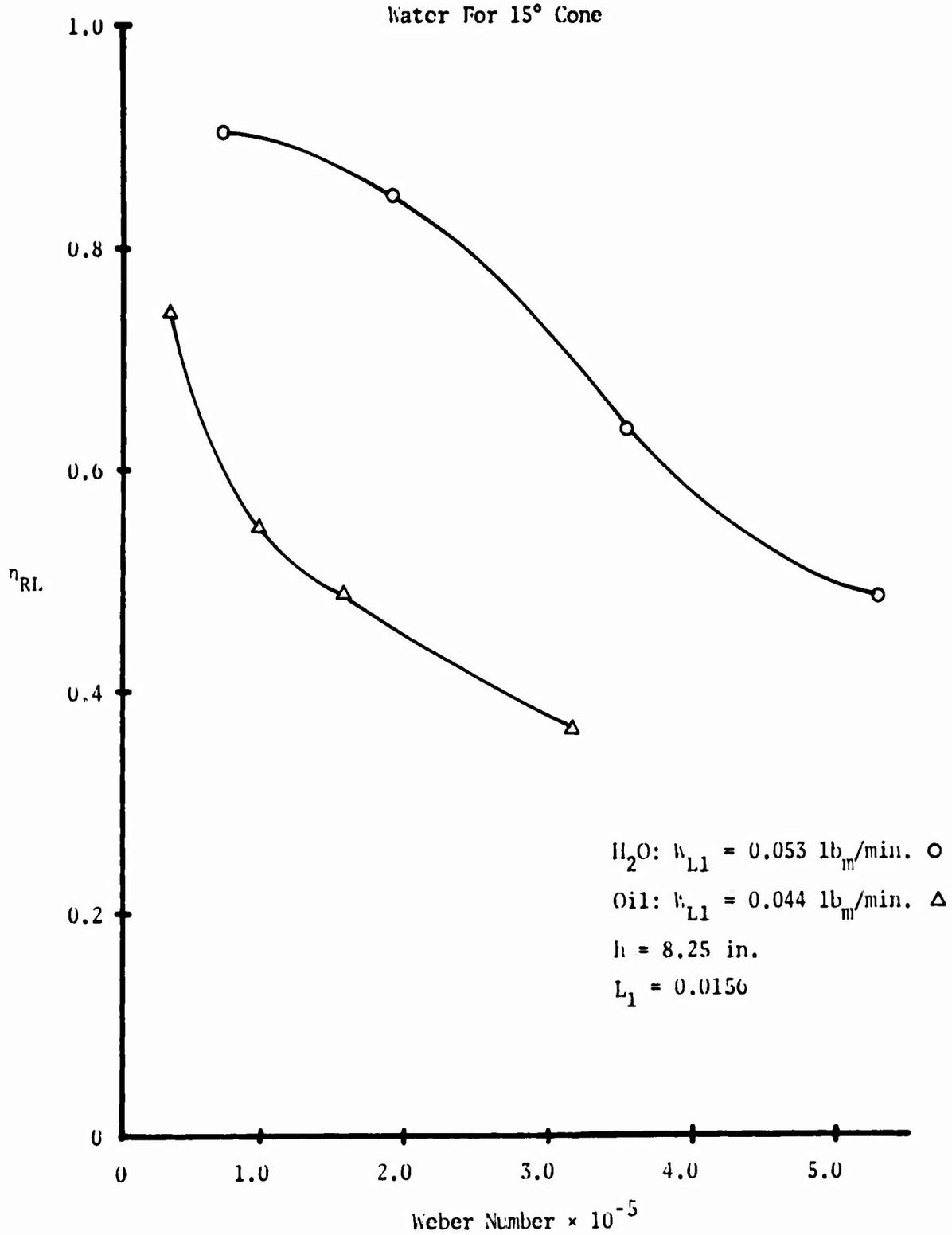

Figure 20

Pressure Drop vs. Reynolds Number For Oil (ν = 1.0 Centistoke)
And Water For 15° Cone

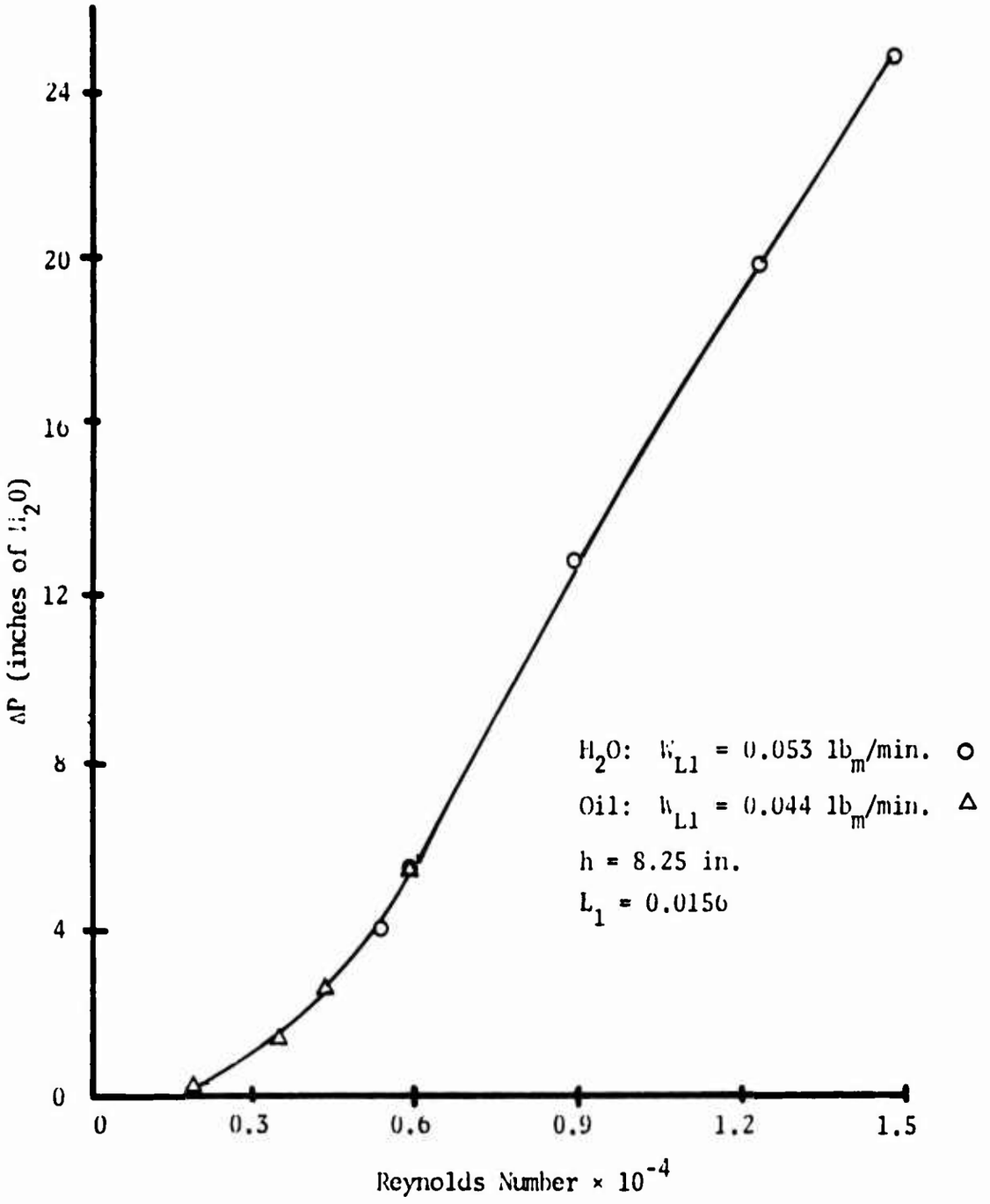

Figure 21

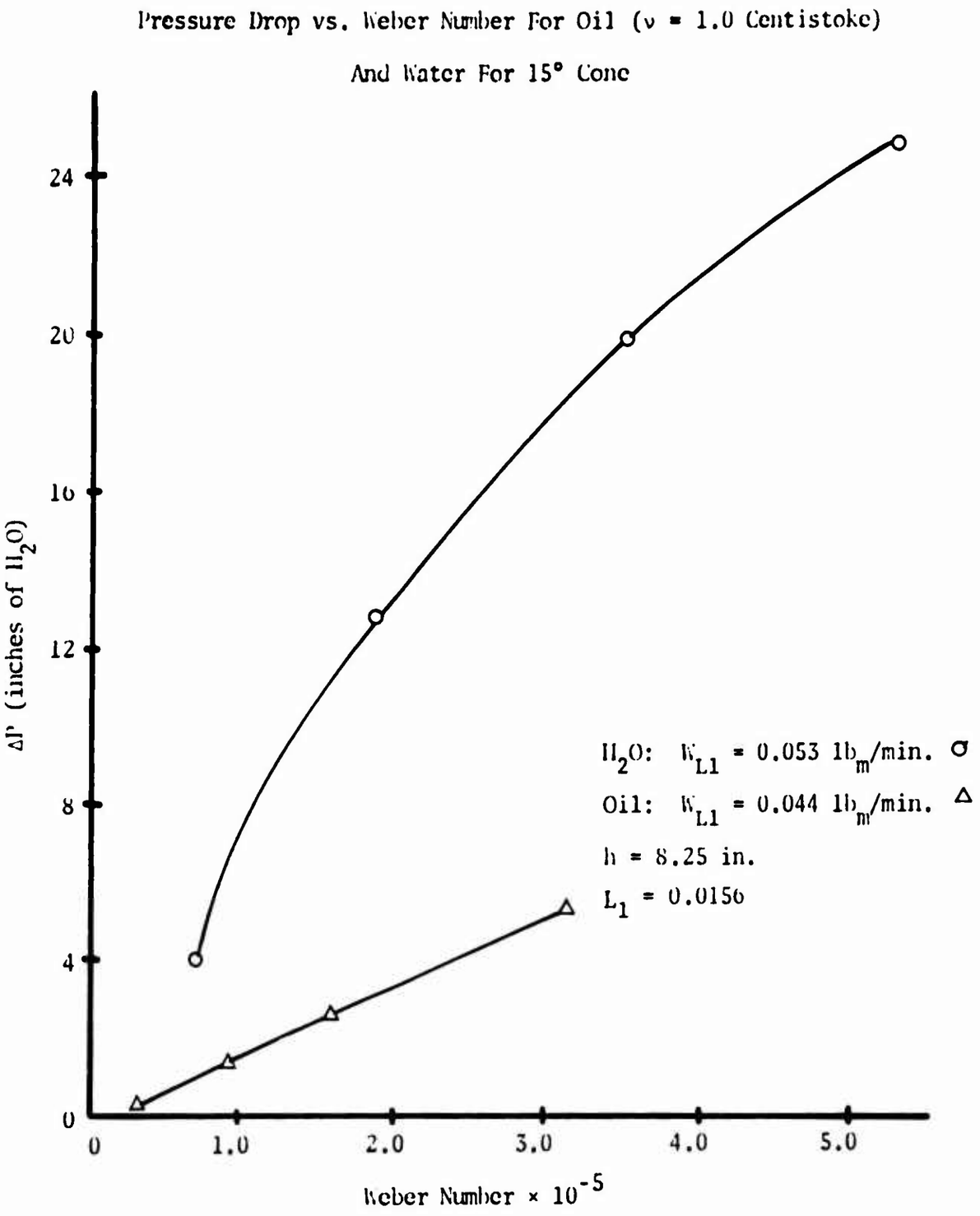
Pressure Drop vs. Weber Number For Oil (ν = 1.0 Centistoke)
And Water For 15° Cone
ΔP (inches of H2O)
24
20
16
12
8
4
0
0
1.0
2.0
3.0
4.0
5.0
Weber Number × 10-5
H2O: WL1 = 0.053 lbm/min.
Oil: WL1 = 0.044 lbm/min.
h = 8.25 in.
L1 = 0.0156

Figure 22

First, the cone with semi-vertex angle equal to 15° will be discussed.

Figure 23 through 34 indicate the effect of the separator height, h, on the efficiency of removal and the pressure drop across the separator as functions of the Reynolds number and the Weber number. The effect of the high evaporation rate of the $\nu = 1.0$ oil as compared to the other oils is easily seen by comparing Figures 28 and 29 with Figures 30 through 34. For $\nu = 1.0$ oil, the efficiency decreases with increasing inlet velocity, while for $\nu = 10.0$ and $\nu = 100.0$ oils the efficiency remains nearly constant, at nearly 100% efficiency. It should be noted that the results of Lawler's experiments exhibit the same effect as the $\nu = 1.0$ oil, efficiency decreasing with increasing inlet velocity. Hence, Lawler's conclusion that evaporation had a large effect upon his results appears to be correct.

Increasing the separator height decreases the pressure drop across the separator as can be seen from Figures 29 through 34. This result agrees with that of Lawler. It can be explained by realizing that at steady-state, the rate of energy input at a given inlet velocity is constant, equal to the rate of dissipation. Thus, increasing the height reduces the fluid's rotational speed so as to maintain constant dissipation, and along with this reduced speed goes the fact that it requires less of a pressure drop to support the flow.

Due to the high evaporation rate, the oil with viscosity $\nu = 1.0$ centistoke will not be considered in the remainder of this paper.

Efficiency vs. Reynolds Number For Oil With ν = 1.0 Centistoke At Various Heights For 15° Cone

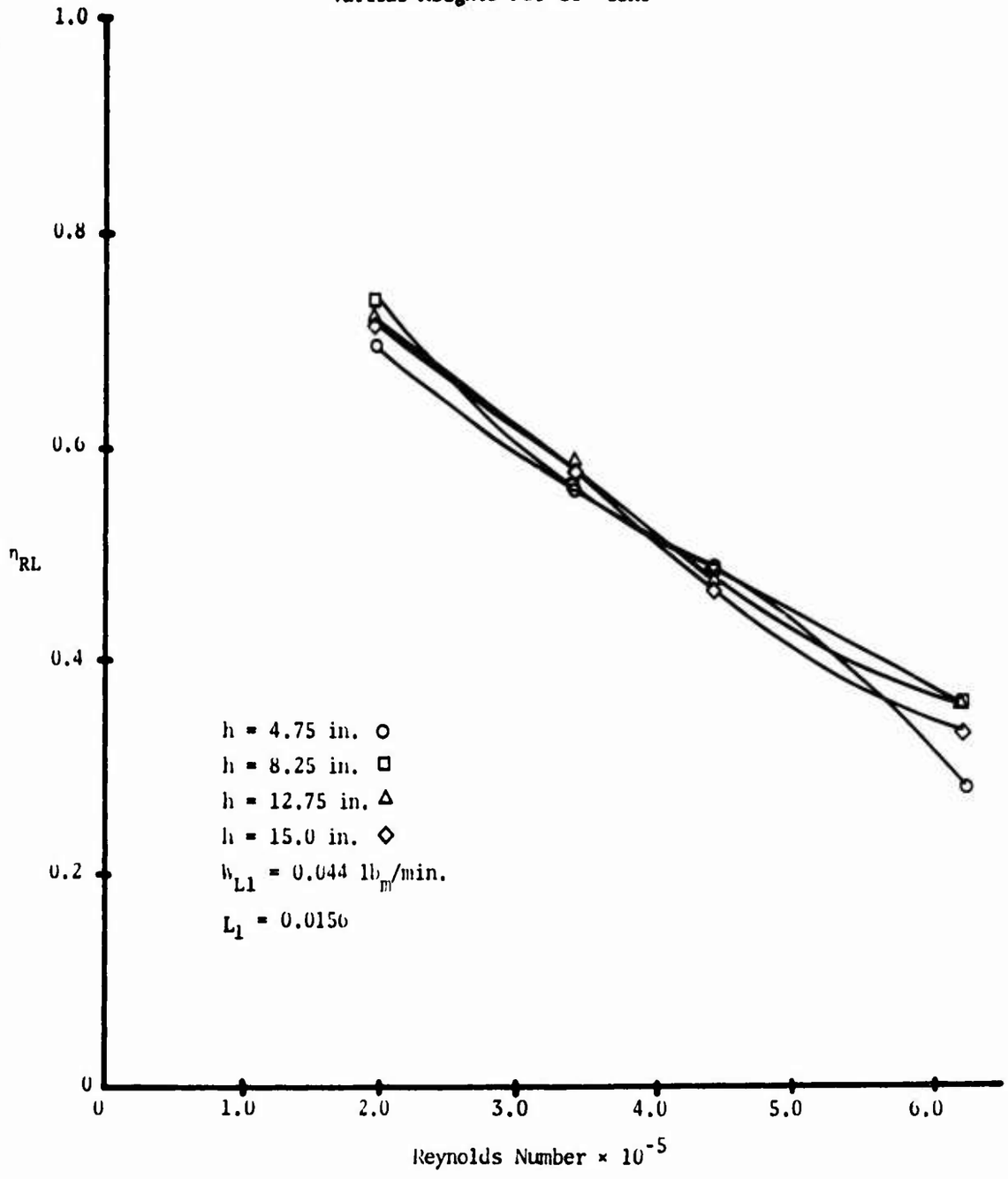

Figure 23

Efficiency vs. Weber Number For Oil With ν = 1.0 Centistoke

At Various Heights for 15° Cone

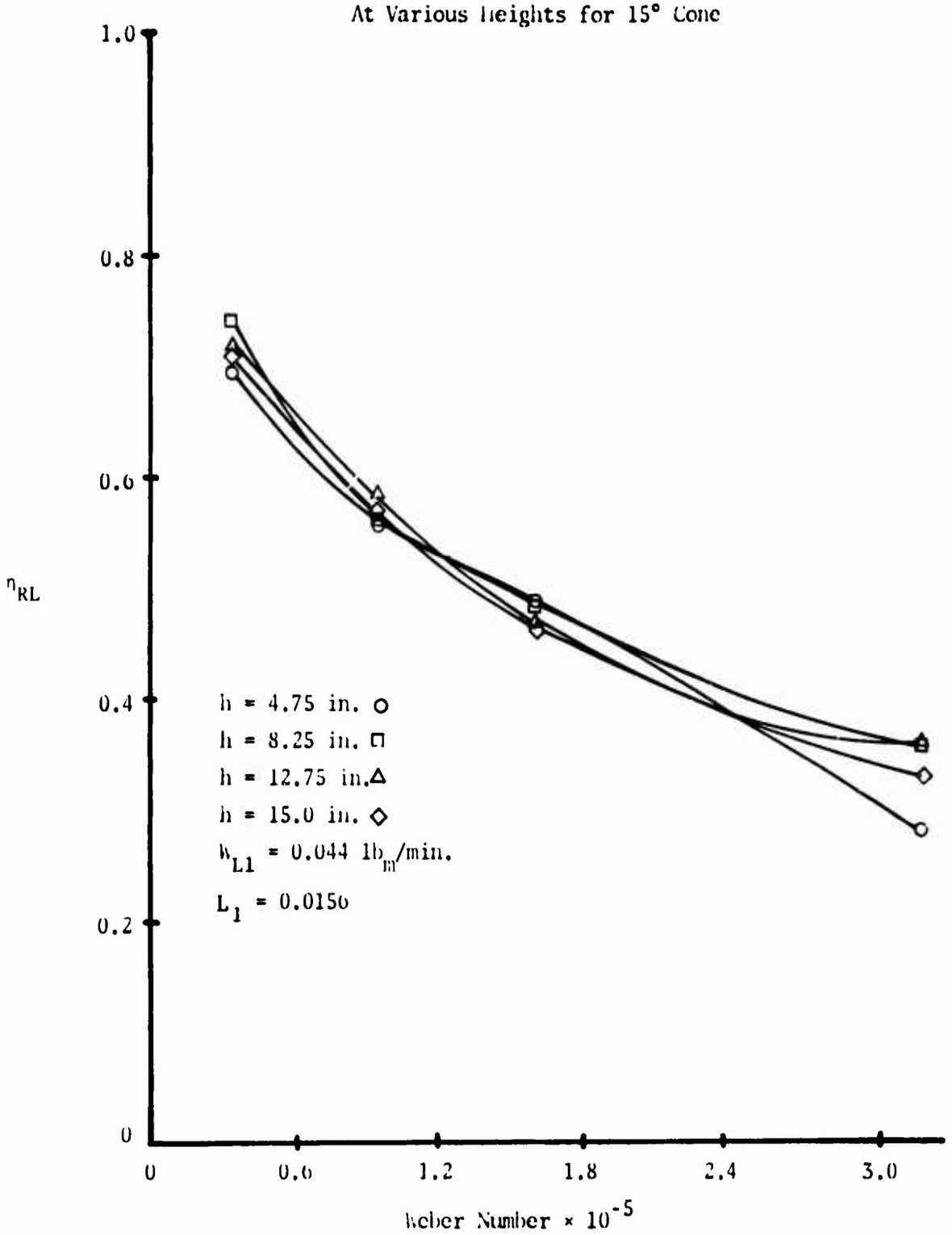

Figure 24

Efficiency vs. Reynolds Number For Oil With ν = 10.0 Centistokes

At Various Heights For 15° Cone

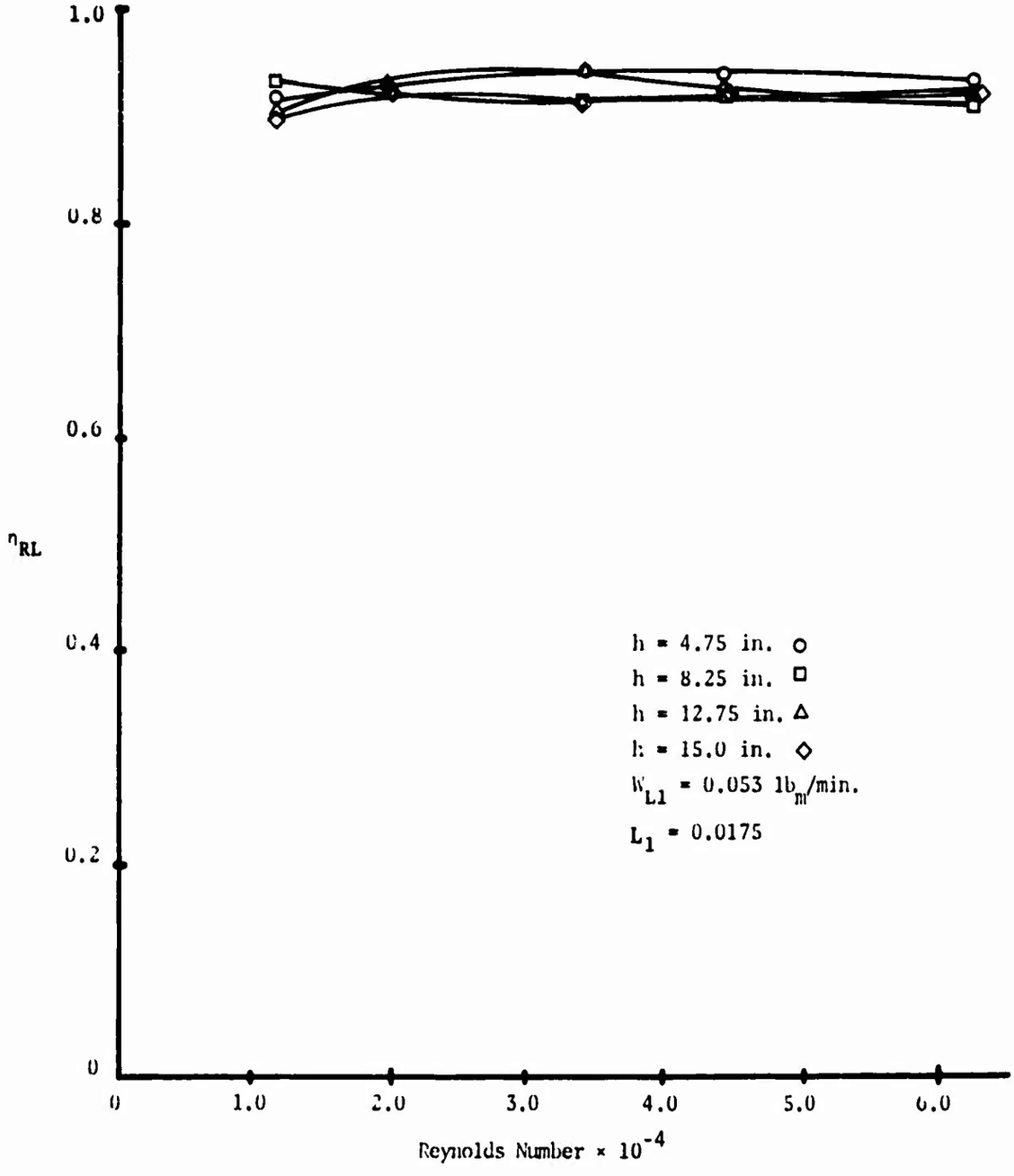

Figure 25

Efficiency vs. Weber Number For Oil With ν = 10.0 Centistokes

At Various Heights For 15° Cone

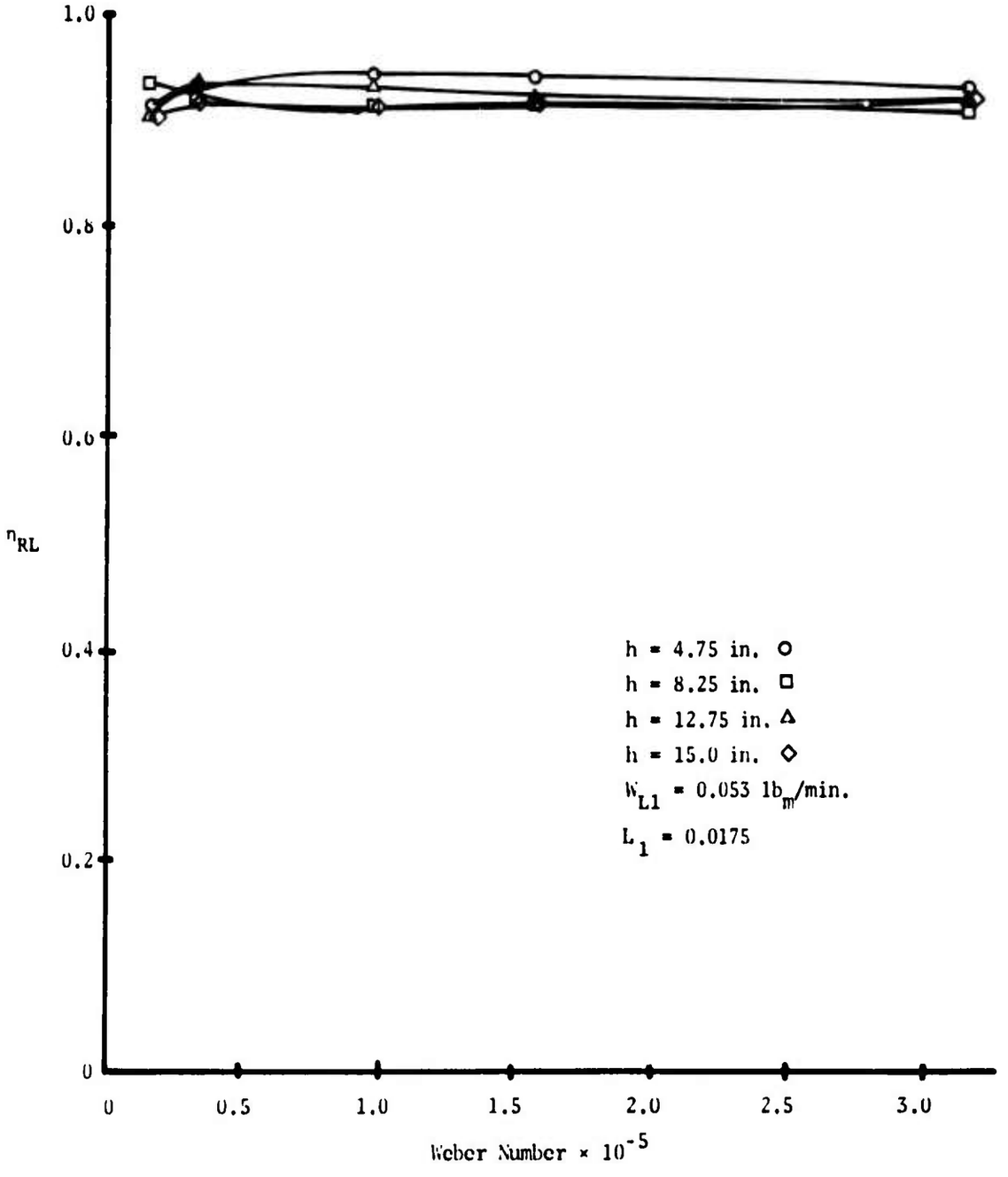

Figure 26

Efficiency vs. Reynolds Number For Oil With ν = 100.0 Centistokes

At Various Heights For 15° Cone

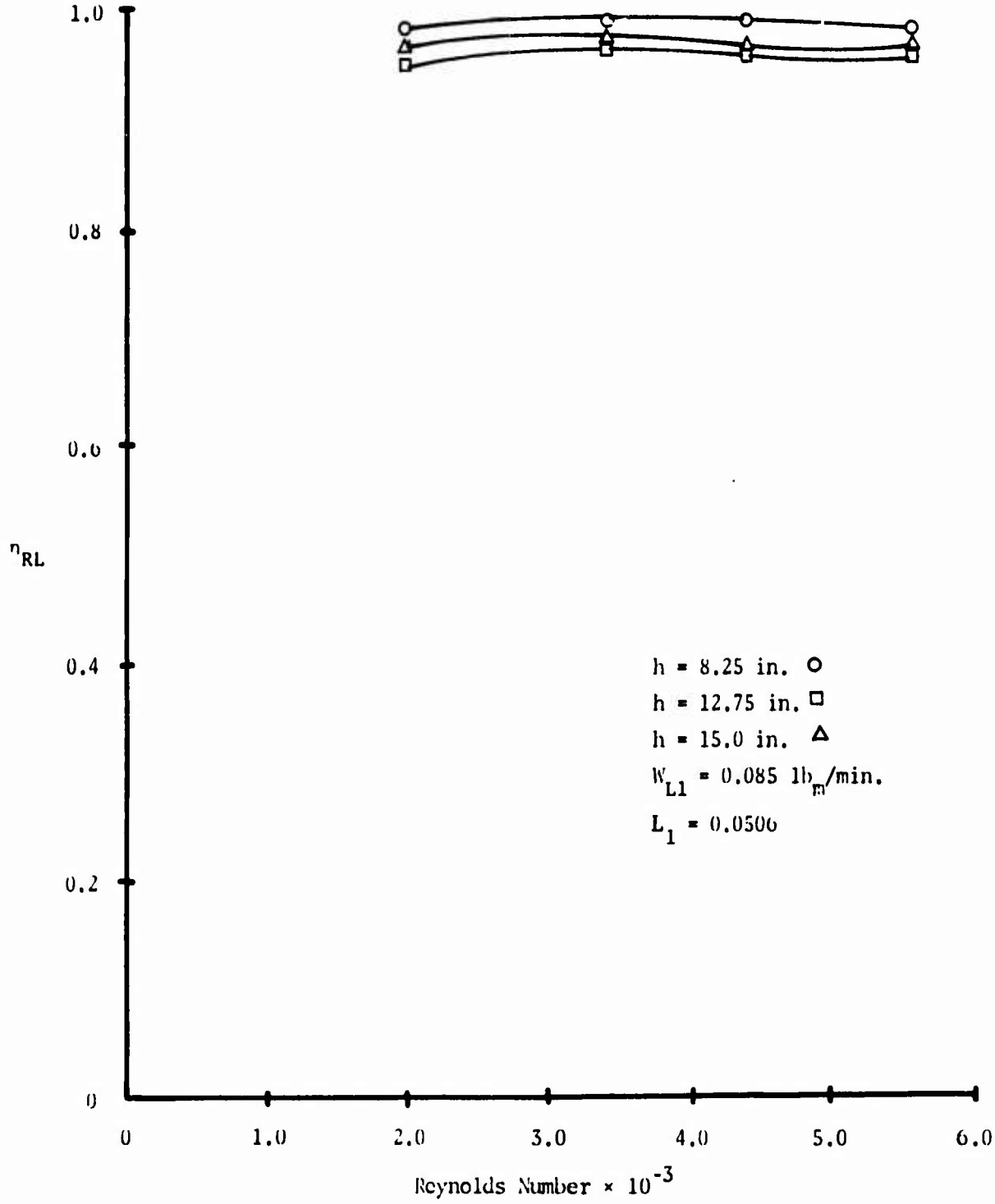

Figure 27

Efficiency vs. Weber Number For Oil With ν = 100.0 Centistokes At Various Heights For 15° Cone

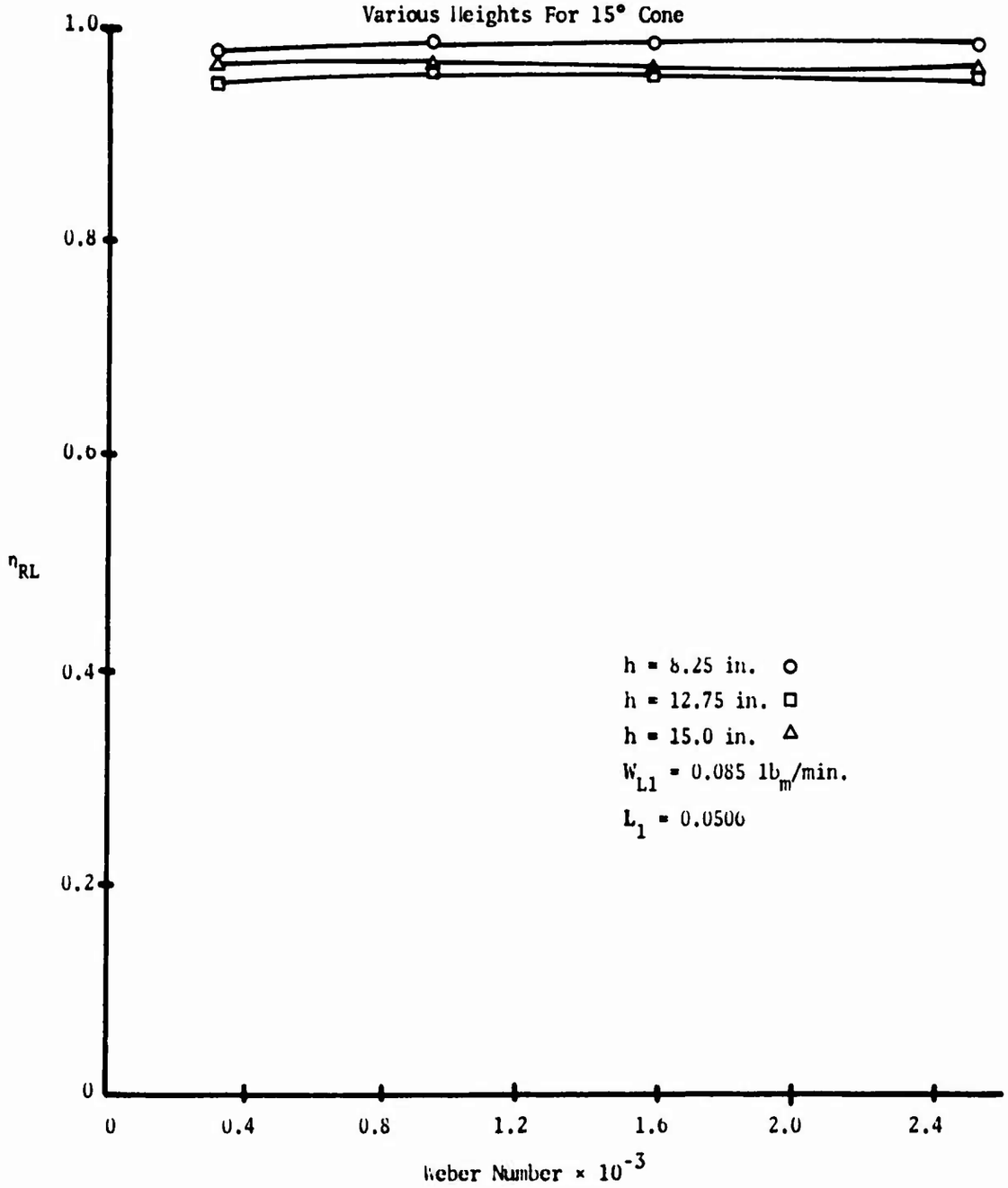

Figure 28

Pressure Drop vs. Reynolds Number For Oil With ν = 1.0 Centistoke

At Various Heights For 15° Cone

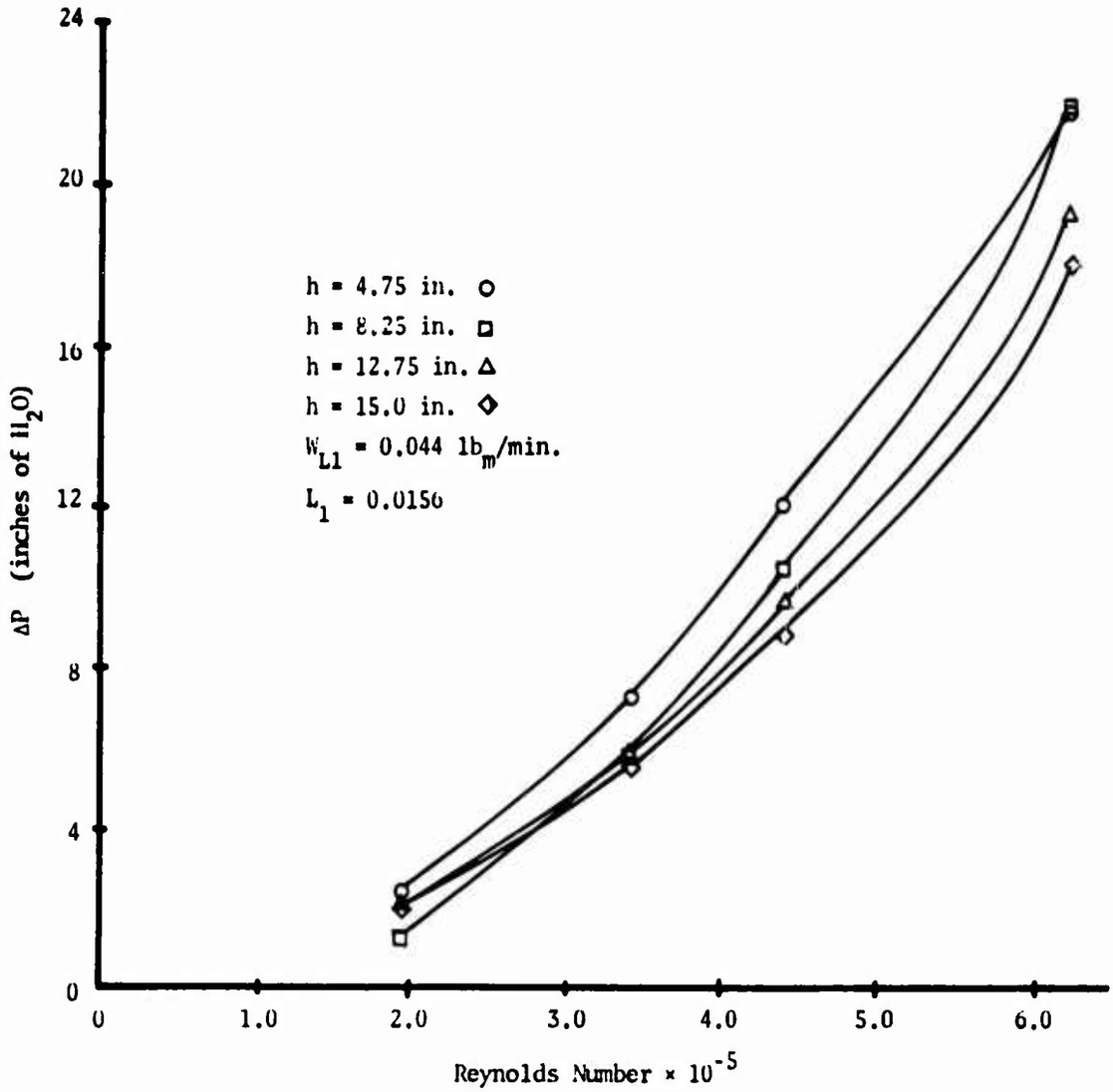

Figure 29

Pressure Drop vs. Weber Number For Oil With ν = 1.0 Centistoke

At Various Heights For 15° Cone

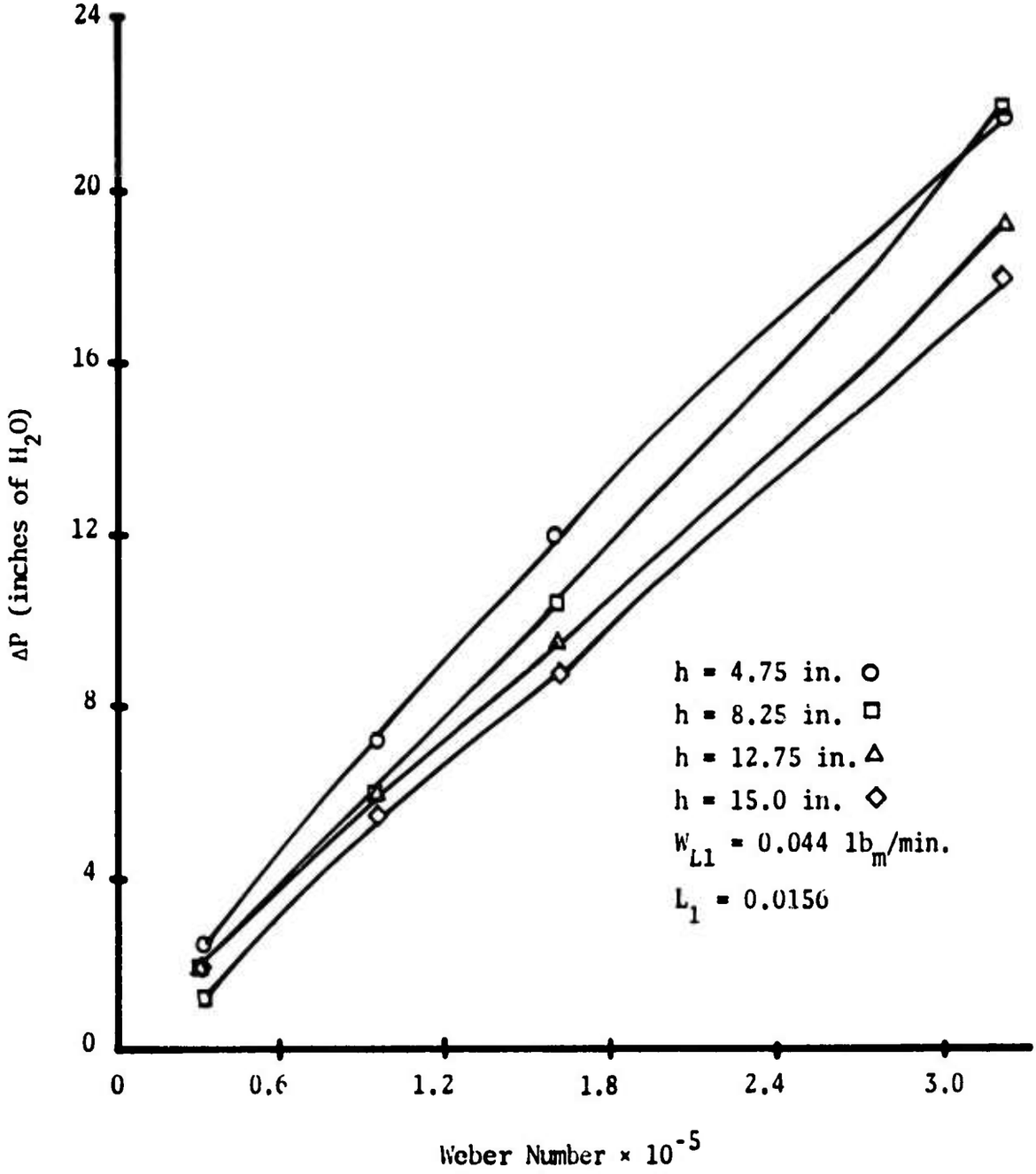

Figure 30

Pressure Drop vs. Reynolds Number For Oil With ν = 10.0 Centistokes

At Various Heights For 15° Cone

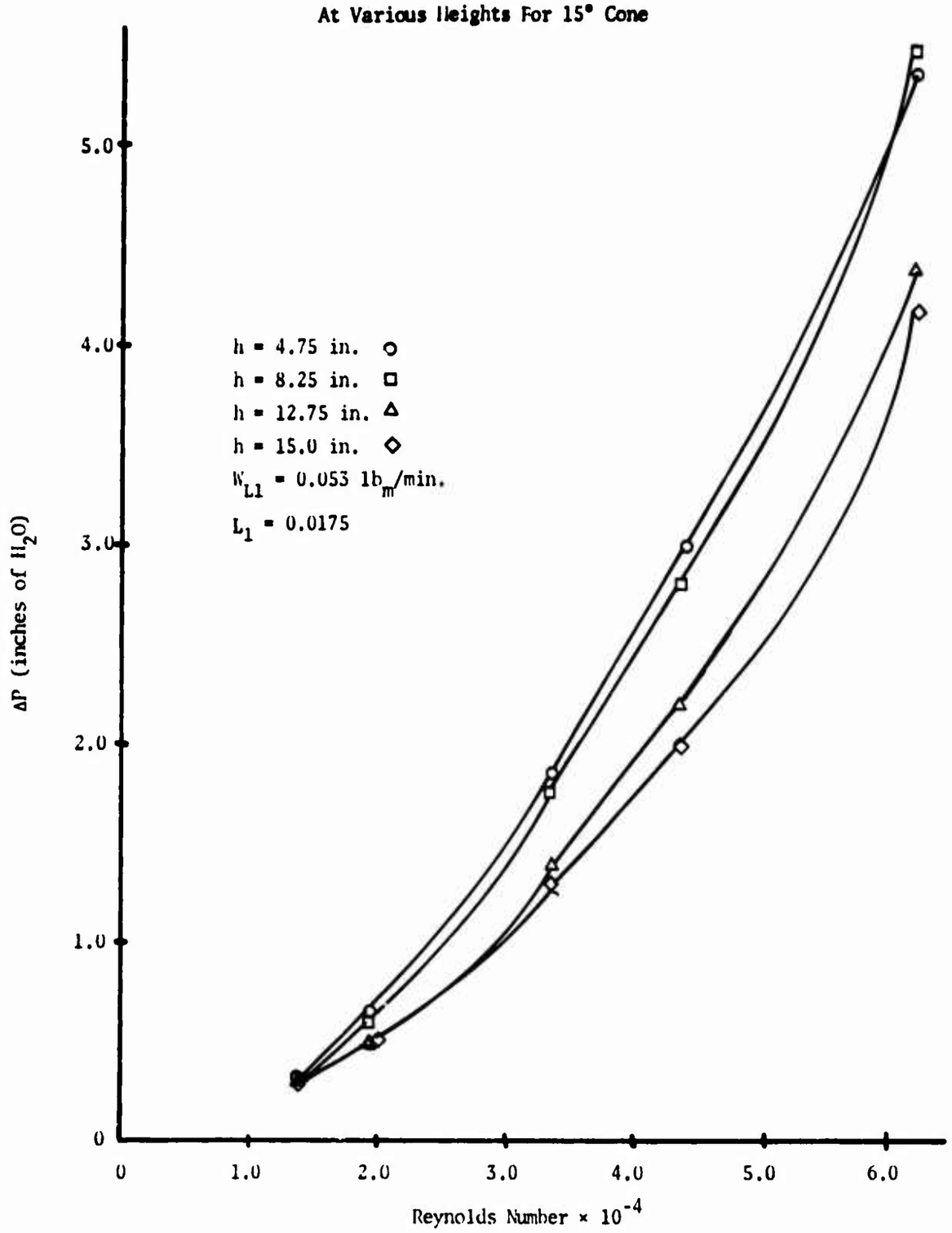

Figure 31

Pressure Drop vs. Weber Number For Oil With ν = 10.0 Centistokes

At Various Heights For 15° Cone

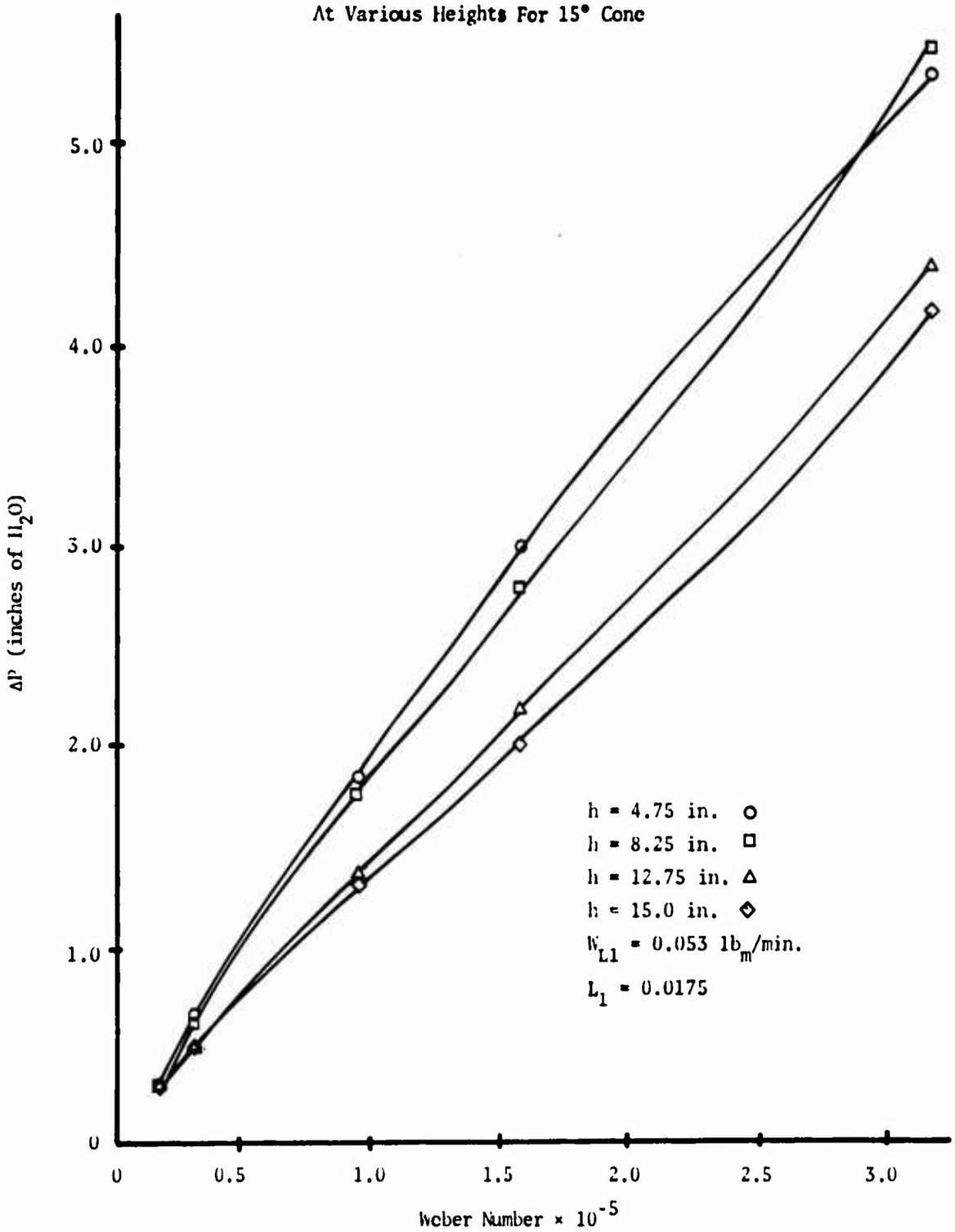

Figure 32

Pressure Drop vs. Reynolds Number For Oil With ν = 100.0 At Various Heights For 15° Cone

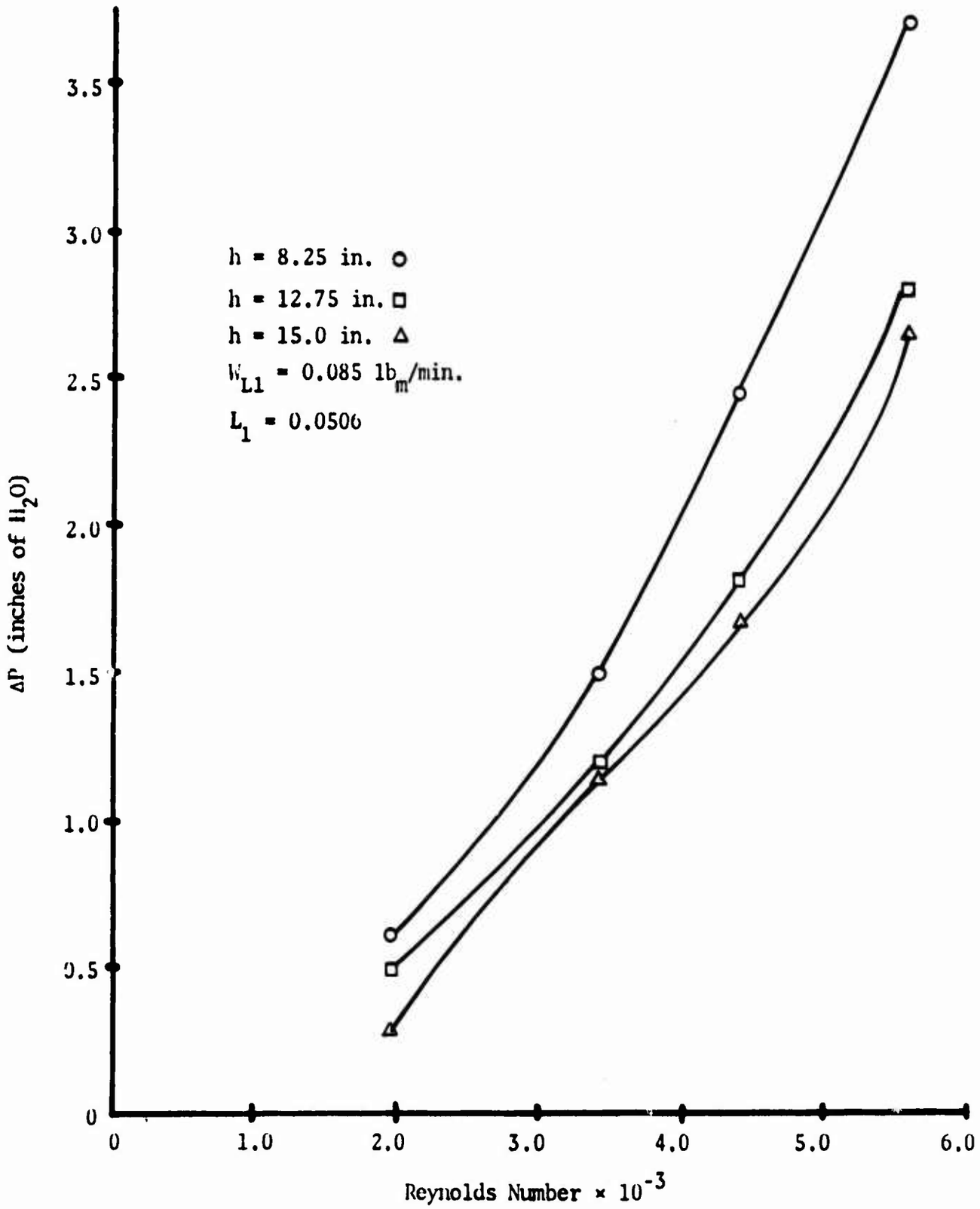

Figure 33

Pressure Drop vs. Weber Number For Oil With ν = 100.0 Centistokes

At Various Heights For 15° Cone

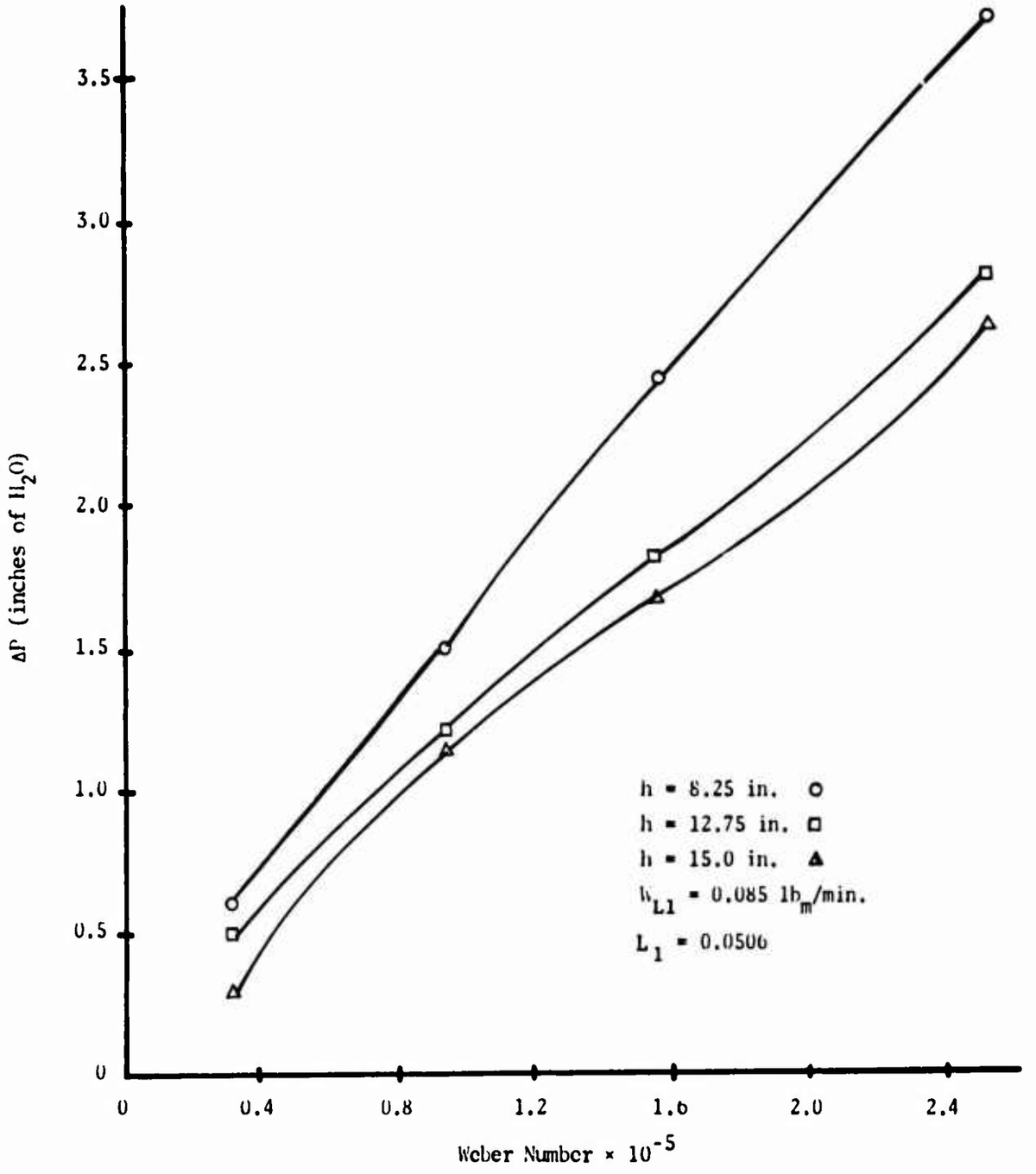

Figure 34

The effect of varying the oil inlet flow rate on efficiency and pressure drop is indicated in Figures 35-38. The efficiency of removal increases with increasing oil flow rates, approaching close to 100% efficiency at the higher flow rates. This may be due to the fact that at a given air inlet velocity (indicated on the graphs by a particular Reynolds or Weber number), the evaporation rate is nearly constant, (a very small constant). Thus, by increasing the oil flow rate, the fraction of oil which is evaporated decreases, and the efficiency increases.

The pressure drop across the separator decreases slightly with increasing oil flow rates at a particular Reynolds or Weber number. This is seen in Figures 37 and 38. Lawler found this same result which he felt was due to the speed of rotation of the cyclone being reduced by the increased mass of oil in the separator at the higher oil flow rates. The effect of the decrease of rotational speed on the pressure drop was discussed earlier in this paper.

Efficiency vs. Reynolds Number For Oil With ν = 10.0 Centistokes

At Various Oil Flow Rates For 15° Cone

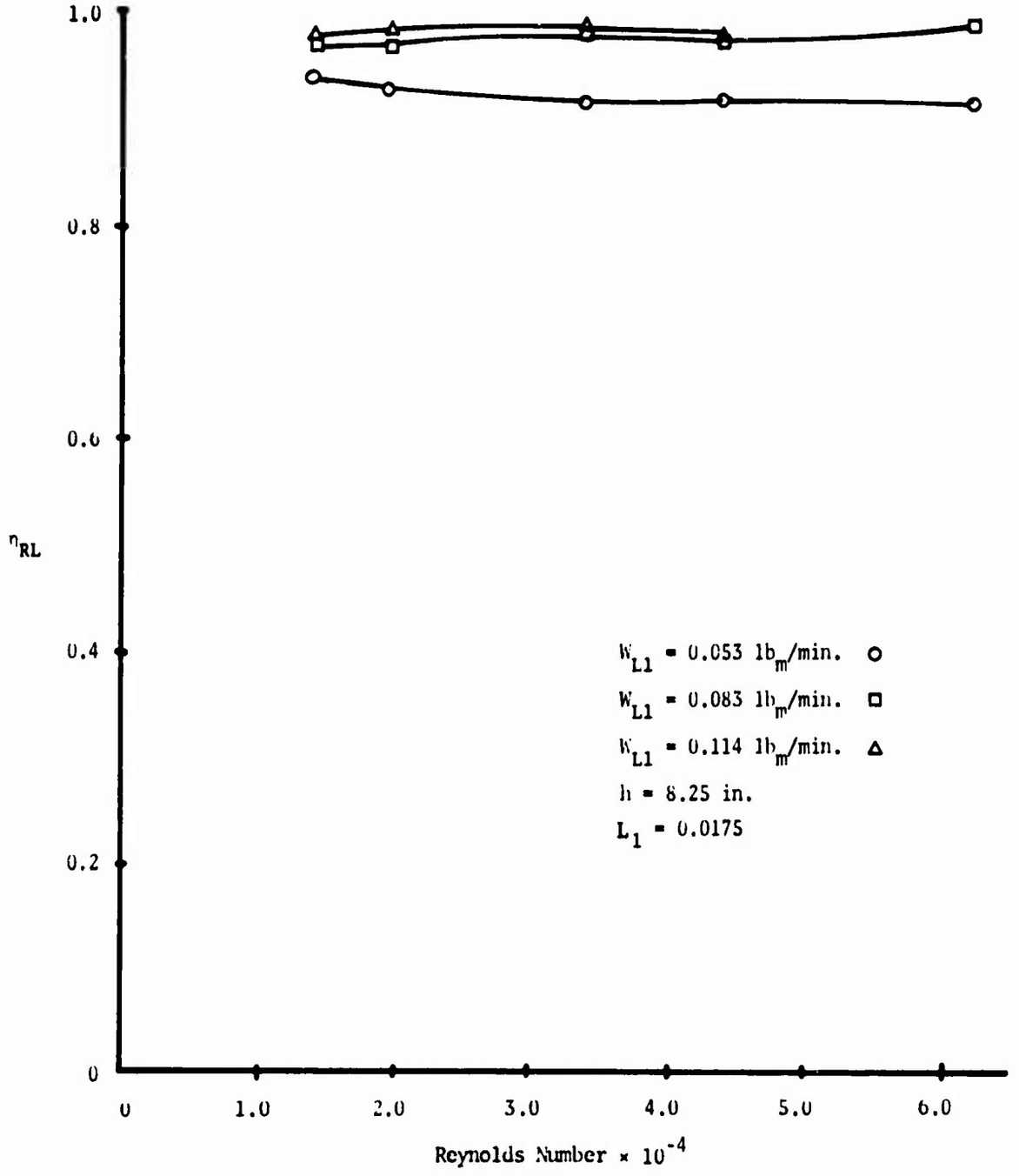

Figure 35

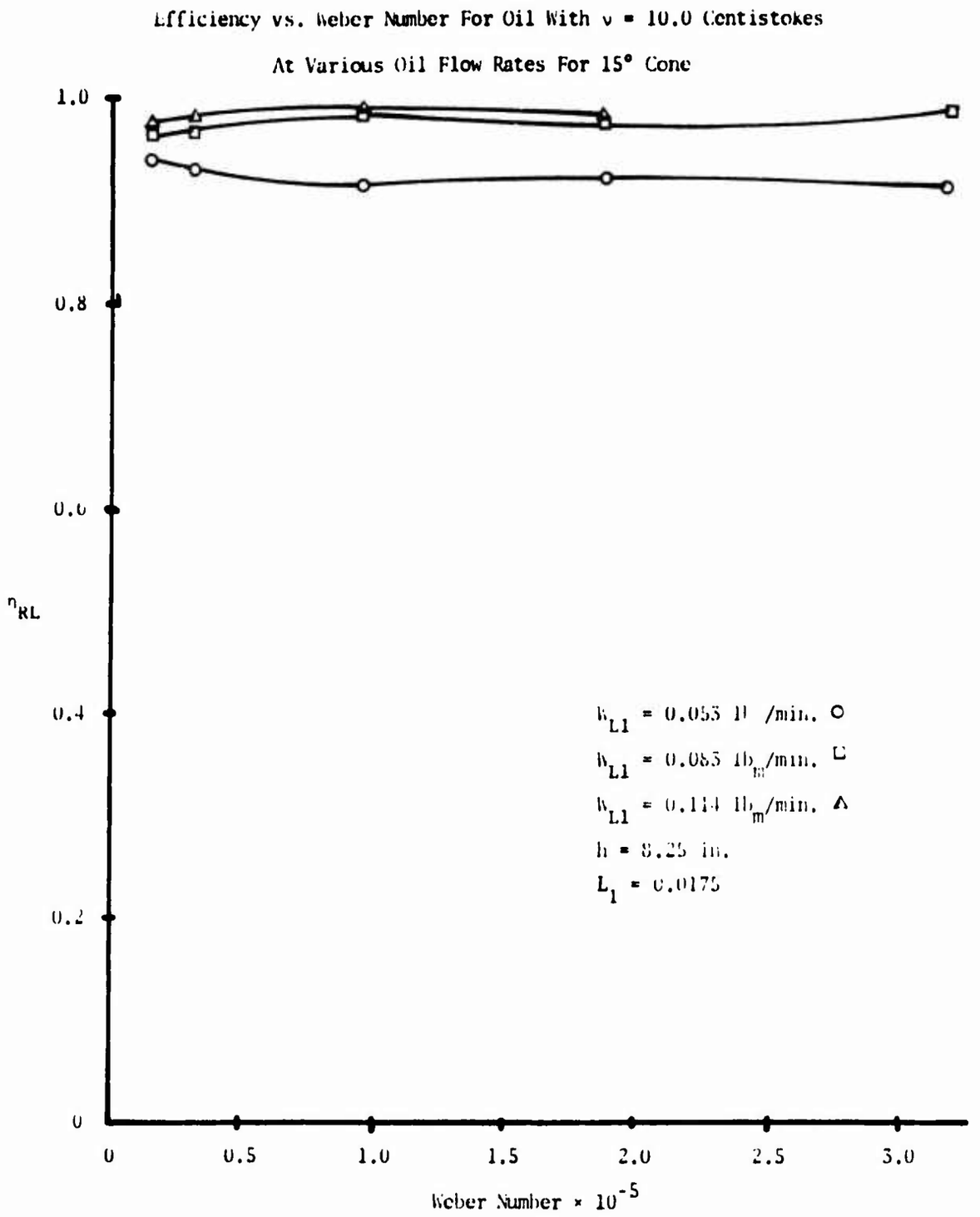
Efficiency vs. Weber Number For Oil With ν = 10.0 Centistokes
At Various Oil Flow Rates For 15° Cone
1.0
0.8
0.6
0.4
0.2
0
η_{RL}
W_{L1} = 0.053 lb /min. ○
W_{L1} = 0.083 lb$_m$/min. □
W_{L1} = 0.114 lb$_m$/min. △
h = 0.25 in.
L_1 = 0.0175
0
0.5
1.0
1.5
2.0
2.5
3.0
Weber Number × 10^{-5}

Figure 36

Pressure Drop vs. Reynolds Number For Oil With ν = 10.0 Centistokes

At Various Oil Flow Rates For 15° Cone

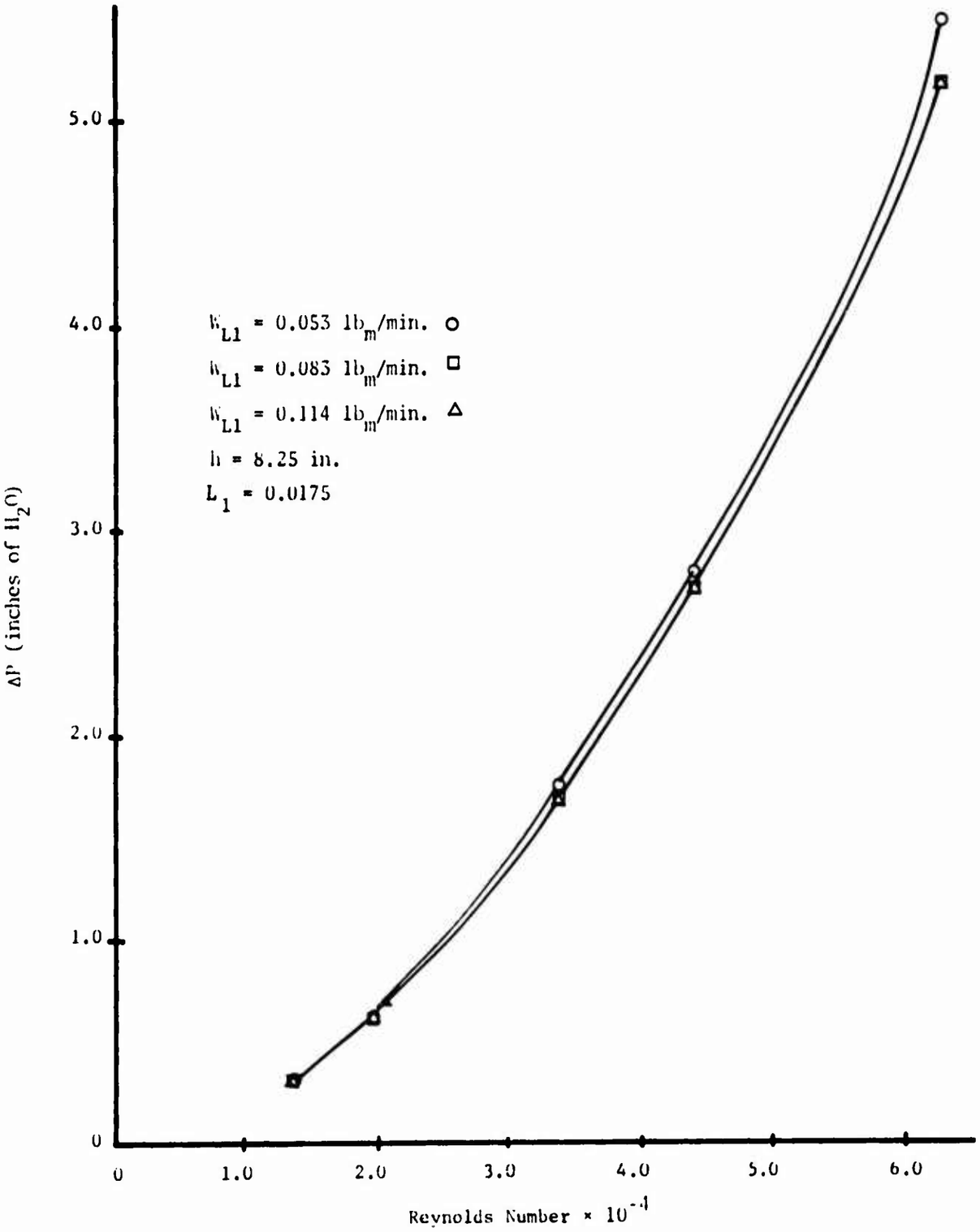

Figure 37

Pressure Drop vs. Weber Number For Oil With ν = 10.0 Centistokes

At Various Oil Flow Rates For 15° Cone

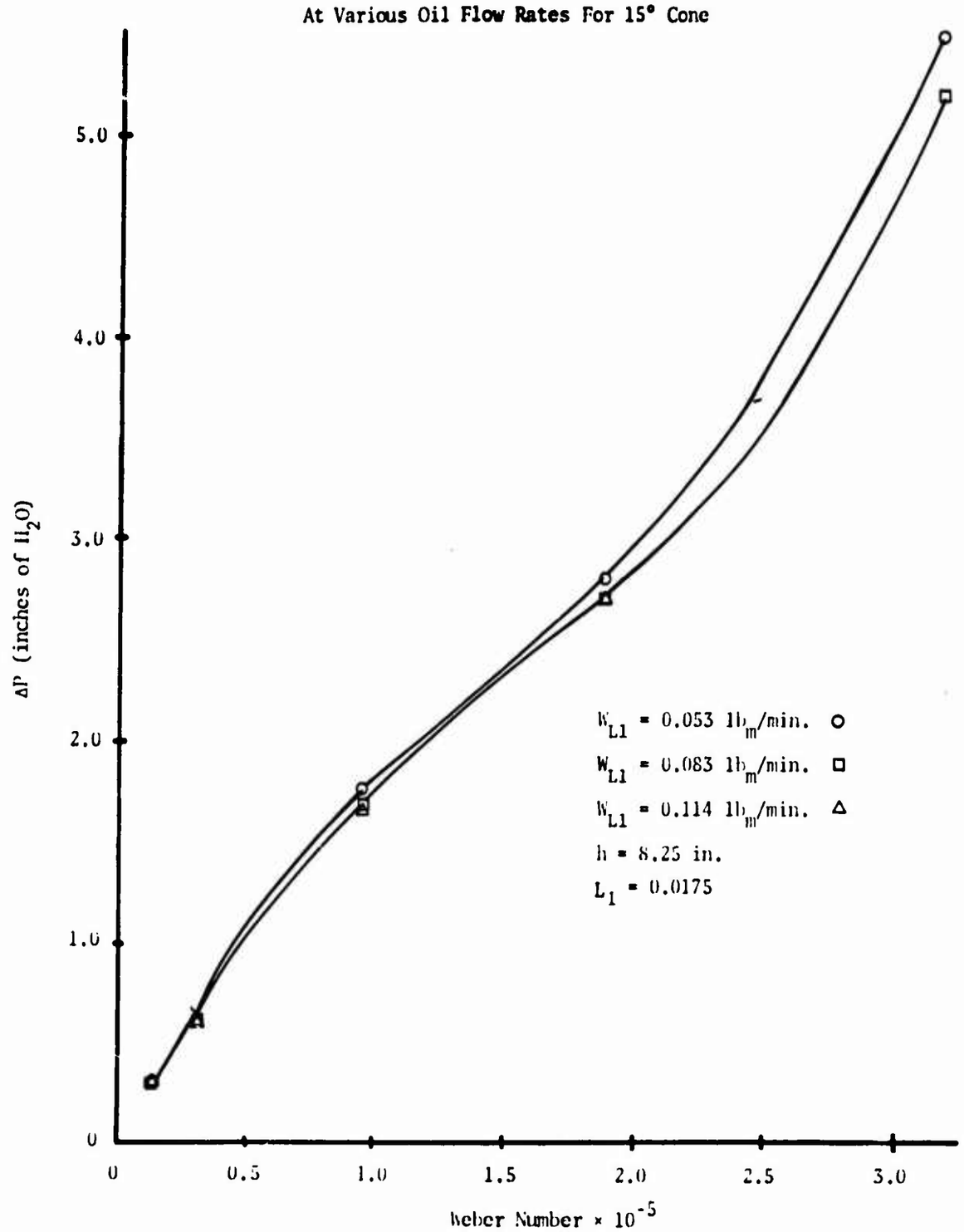

Figure 38

Figures 39 through 42 indicate the effect of the underflow diameter (ℓ_1 = fld) on efficiency and pressure drop. The efficiency decreases as the underflow diameter increases. The pressure drop across the separator is decreased slightly at high Reynolds number as the underflow diameter is increased. This is to be expected as an expansion of the underflow would decrease the pressure drop. This agrees with Lawler's results.

This completes the presentation of the results of experiments run on the 15° cone. Next consider the effect of varying operating conditions and the Reynolds and Weber numbers on a cone of semi-vertex angle of 45°. Only the oil with viscosity ν = 10.0 centistokes was used for these tests as the primary interest in these results is as a comparison with the results for the 15°cone.

Figures 43 and 44 indicate the effect of separator height variation on the efficiency and pressure drop. It can be seen that the efficiency decreases as the separator height increases, as for the 15° cone. Comparing Figures 25 and 43 it appears as though the efficiency is not much affected by the change in cone angles. The 45° cone results do exhibit a very slight increase in efficiency over the 15° cone as can be seen by comparing Figures 25 and 43. This increase agrees qualitatively with the theory which indicates that $\dot{q}_H$ should be proportional to $\sin^2\theta \cos\theta$ with all of the other variables fixed. A more physical interpretation is that the driving force, the pressure gradient toward the cone apex, increases as the cone angle increases. Hence, the cone with the larger semi-

vertex angle is more efficient. Lawler found a marked increase in the efficiency of the 45° cone as compared to the 15° cone. However, he attributed this to the fact that the fluid's residency time in the 45° cone was less than in the 15° cone, and therefore, evaporation had less of an effect. Using oil with $\nu = 10.0$ centistokes, there is not very much evaporation and, therefore, there is less charge in efficiencies caused by using cones of different angles. For the 45° cone, as for the 15° cone, the pressure drop decreases with increasing height. This decrease, at a particular Reynolds number, is much greater for the 45° cone than for the 15° cone as can be seen by comparing Figures 31 and 44. This last result agrees with that found by Lawler.

Lfficiency vs. Reynolds Number For Oil With ν = 10.0 Centistokes

At Various Underflow Diameters For 15° Cone

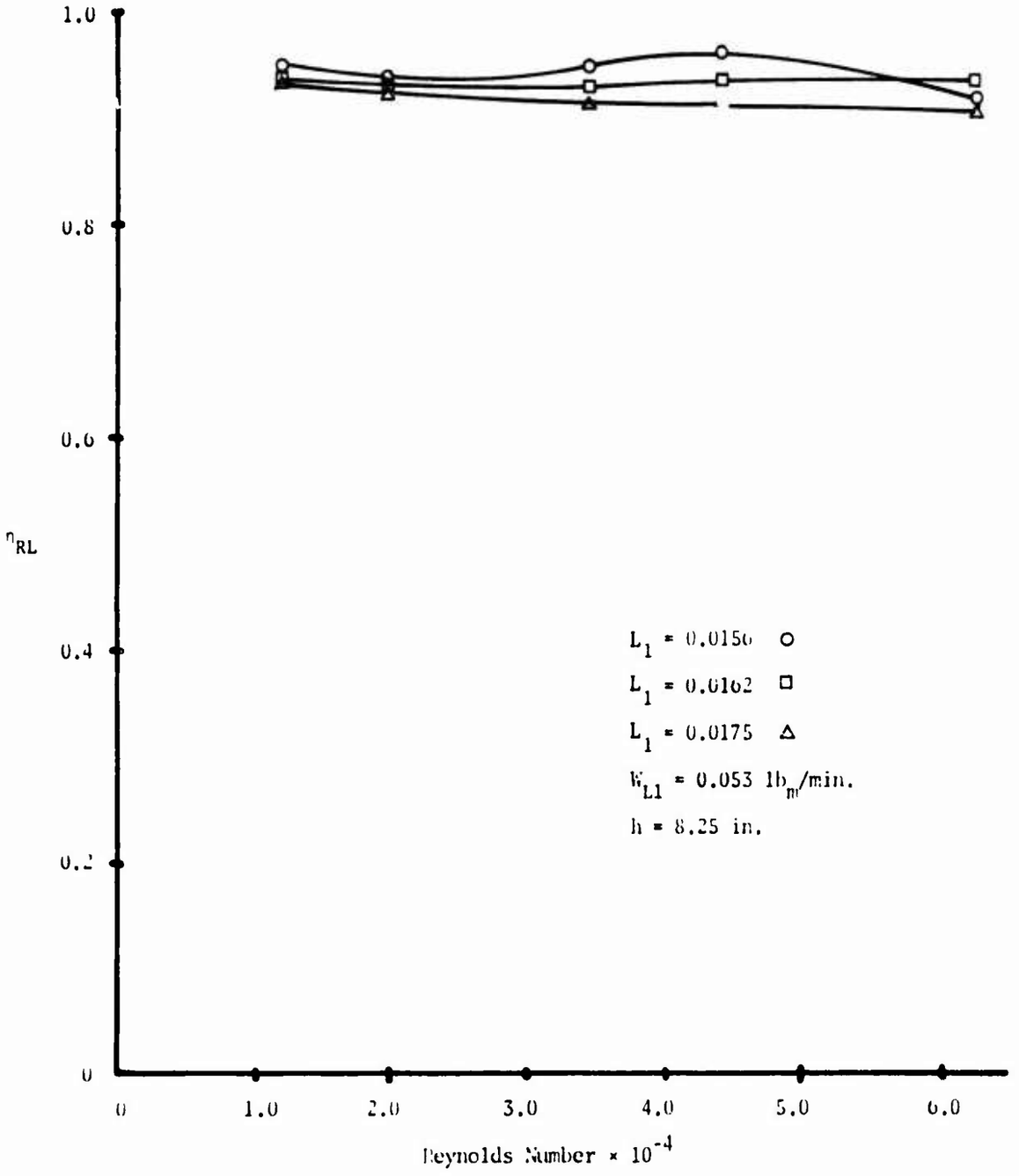

Figure 39

Efficiency vs. Weber Number For Oil With ν = 10.0 Centistokes At Various Underflow Diametes For 15° Cone

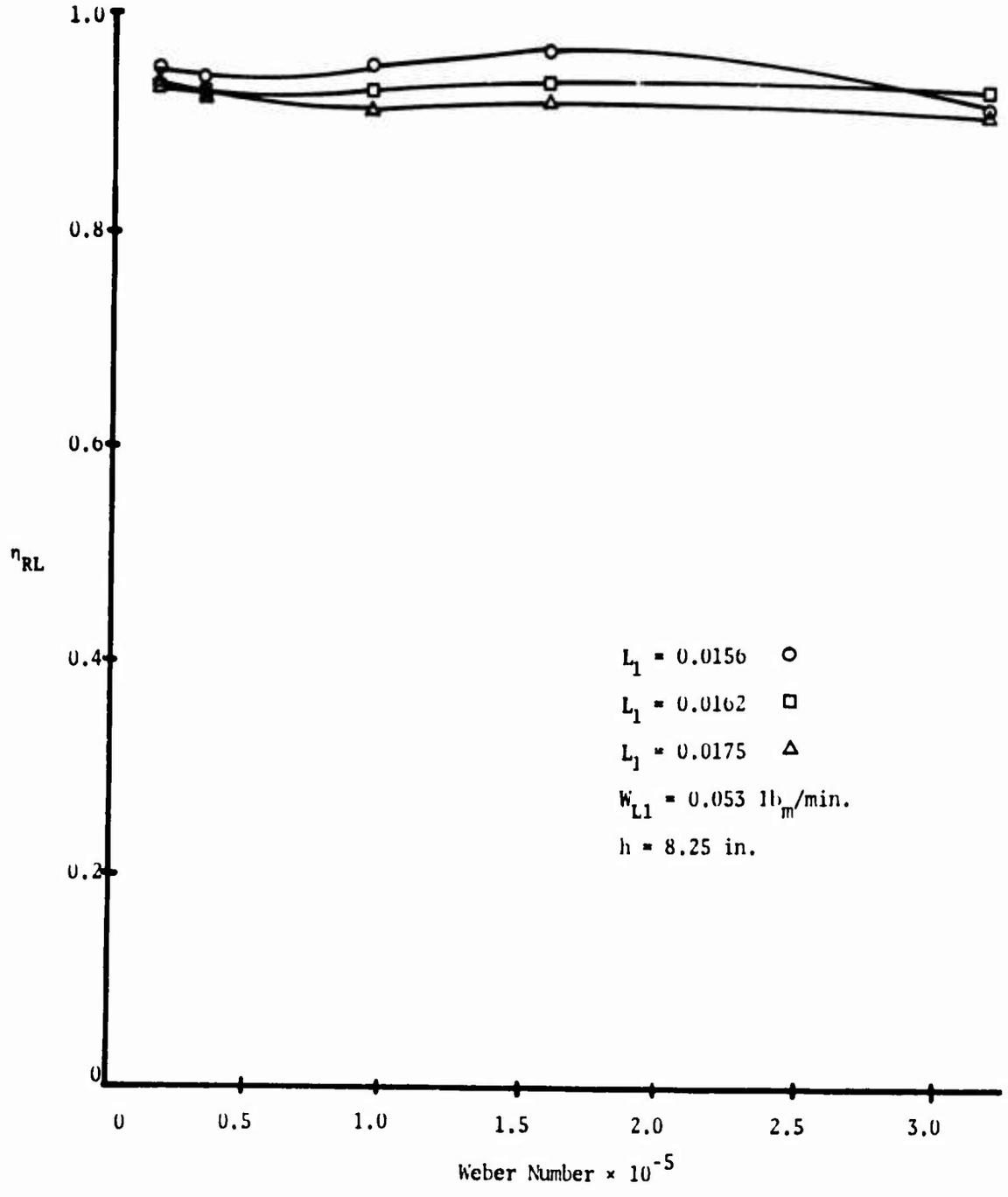

Figure 40

Pressure Drop vs. Reynolds Number For Oil With ν = 10.0 Centistokes

At Various Underflow Diameters For 15° Cone

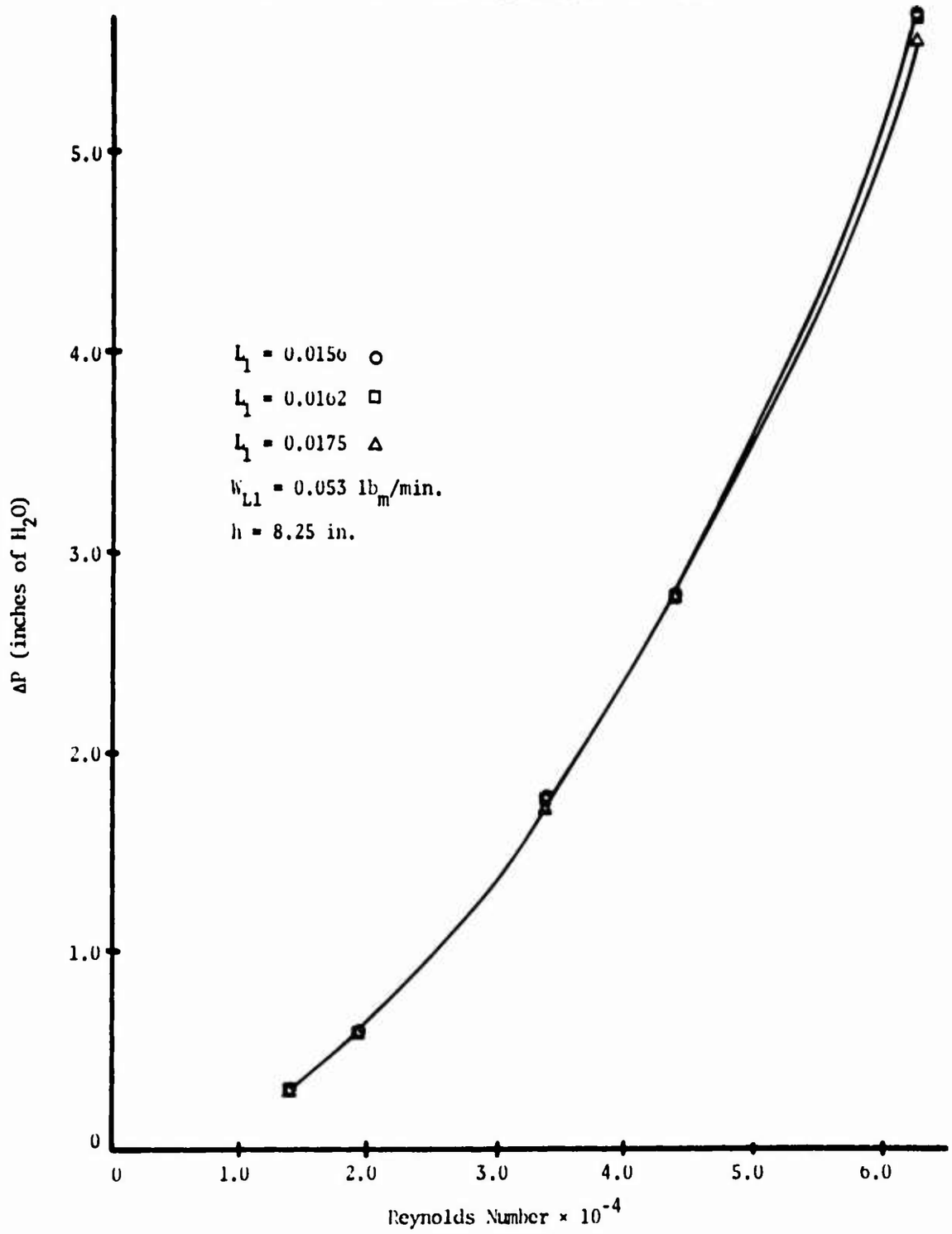

Figure 41

Pressure Drop vs. Weber Number For Oil With ν = 10.0 Centistokes

At Various Underflow Diameters For 15° Cone

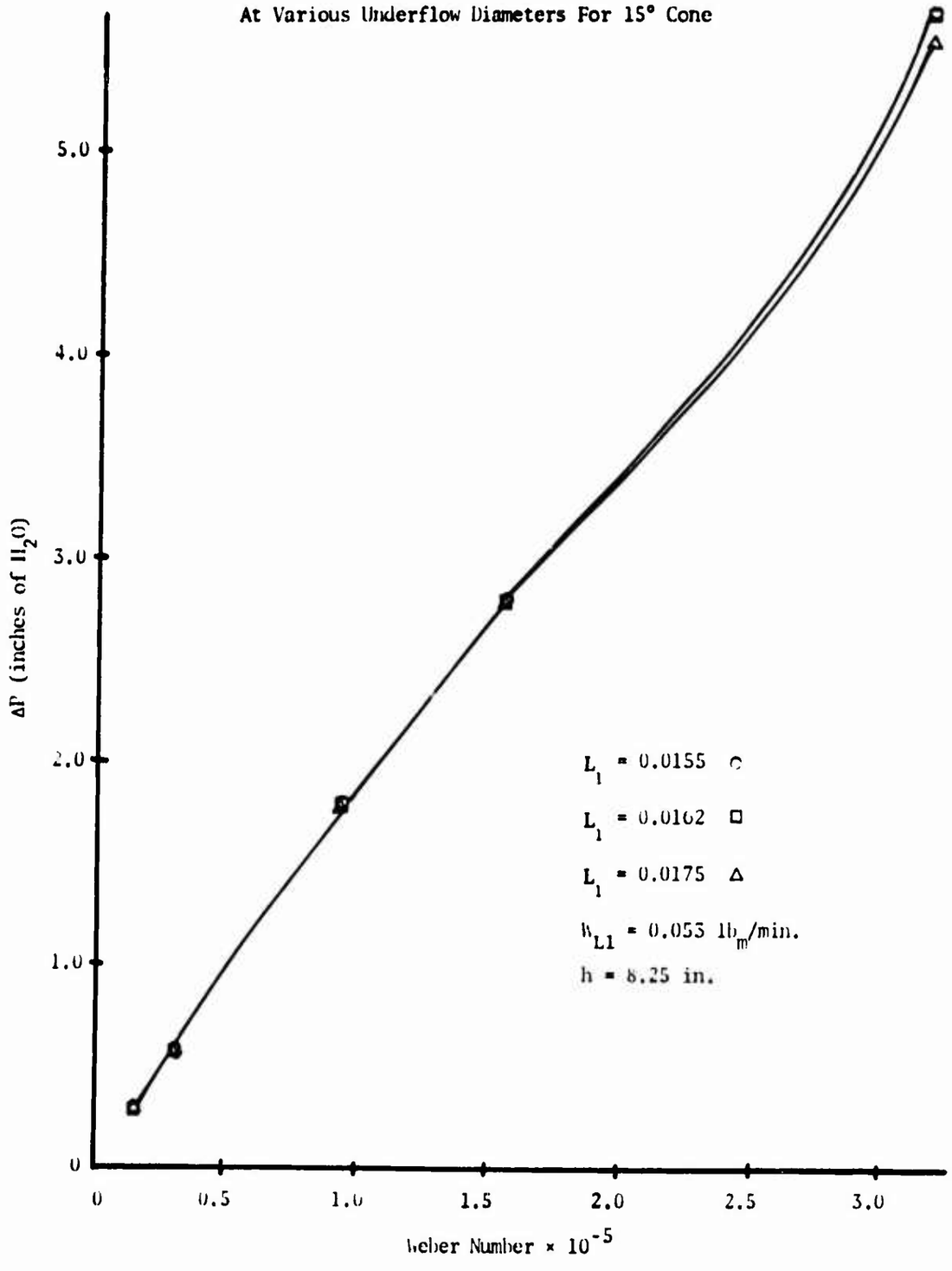

Figure 42

Efficiency vs. Reynolds Number For Oil With ν = 10.0 Centistokes

At Various Heights For 45° Cone

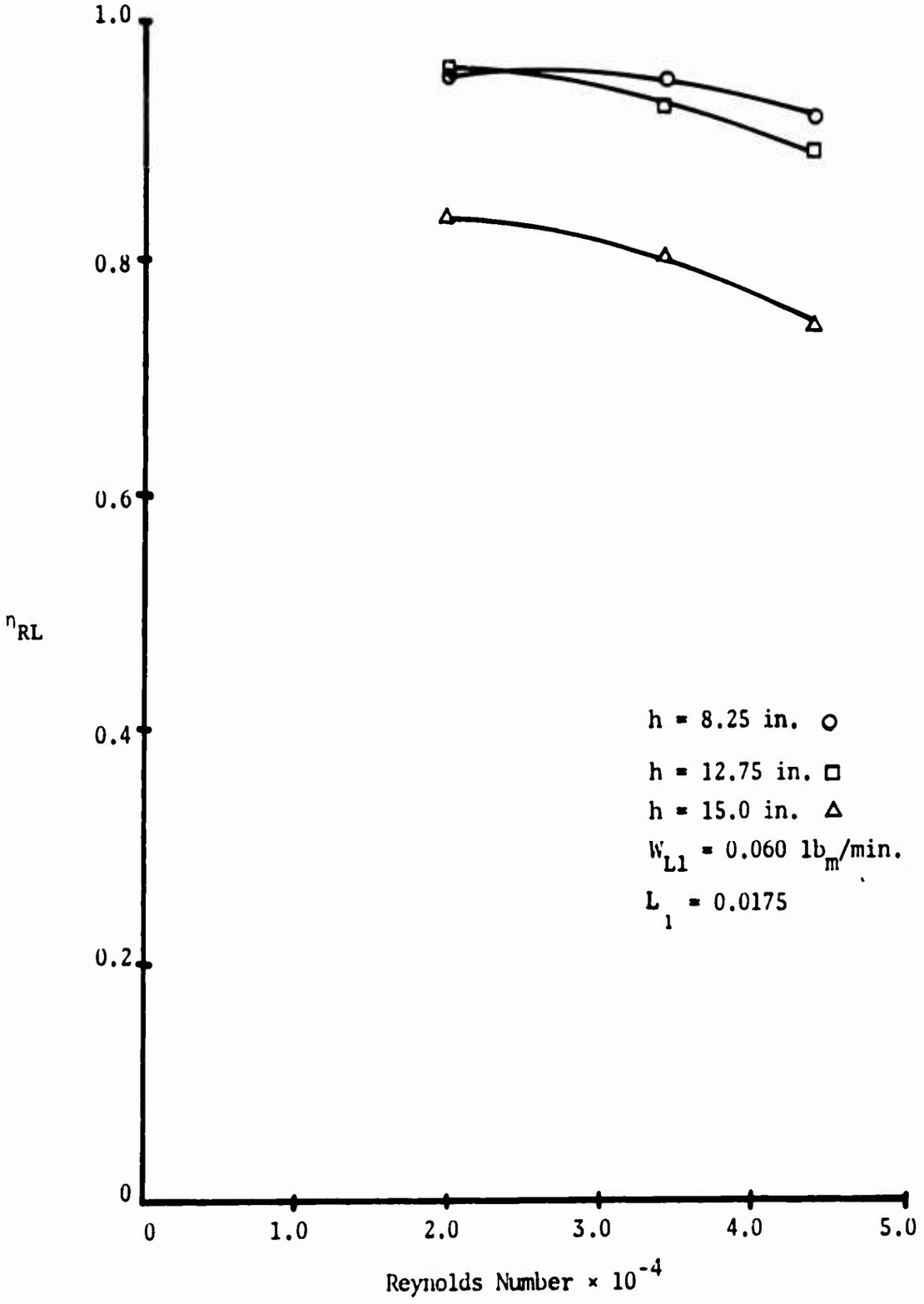

Figure 43

Pressure Drop vs. Reynolds Number For Oil With ν = 10.0 Centistokes At Various Heights For 45° Cone

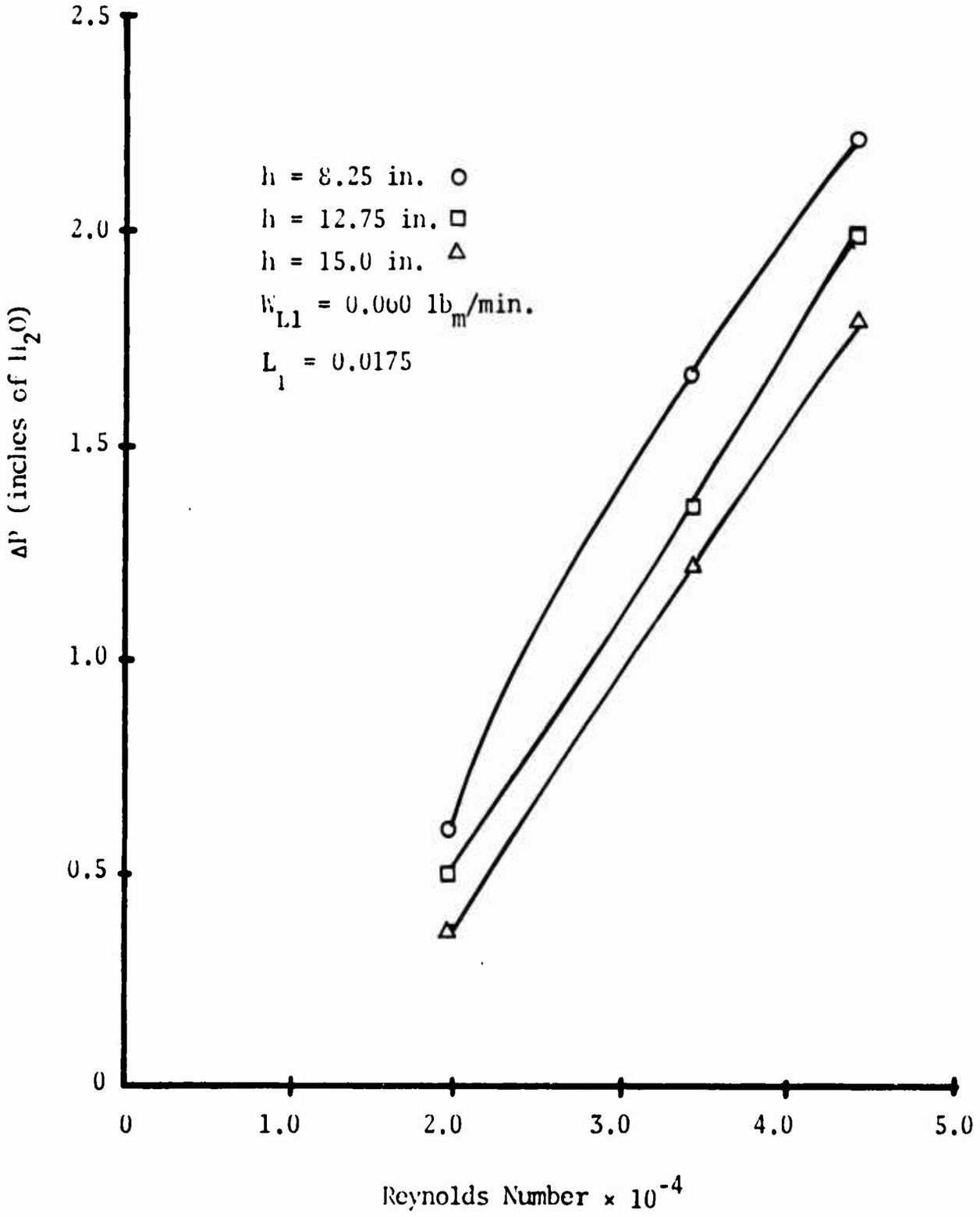

Figure 44

Figures 45 and 46 show that, for the 45° cone, the higher the oil flow rate, the greater the efficiency and the smaller the pressure drop. These are the same type of results as found for the 15° cone. However, the curvatures of the pressure drop versus the Reynolds number are different for the two cones: the 45° cone results indicate that may be some maximal pressure drop, that is, some Reynolds number beyond which the pressure drop across the separator is constant, whereas the 15° cone results do not indicate the possibility of such a maximum. See Figures 36 and 46.

Figures 47 and 48 present the effect of underflow diameter on efficiency and pressure drop. The efficiency tends to decrease as the underflow diameter increases, as for the 15° cone. The pressure drop, while large for the 45° cone also exhibits the same trend as the 15° cone, decreasing as the underflow diameter increases.

Efficiency vs. Reynolds Number For Oil With ν = 10.0 Centistokes

At Various Oil Flow Rates For 45° Cone

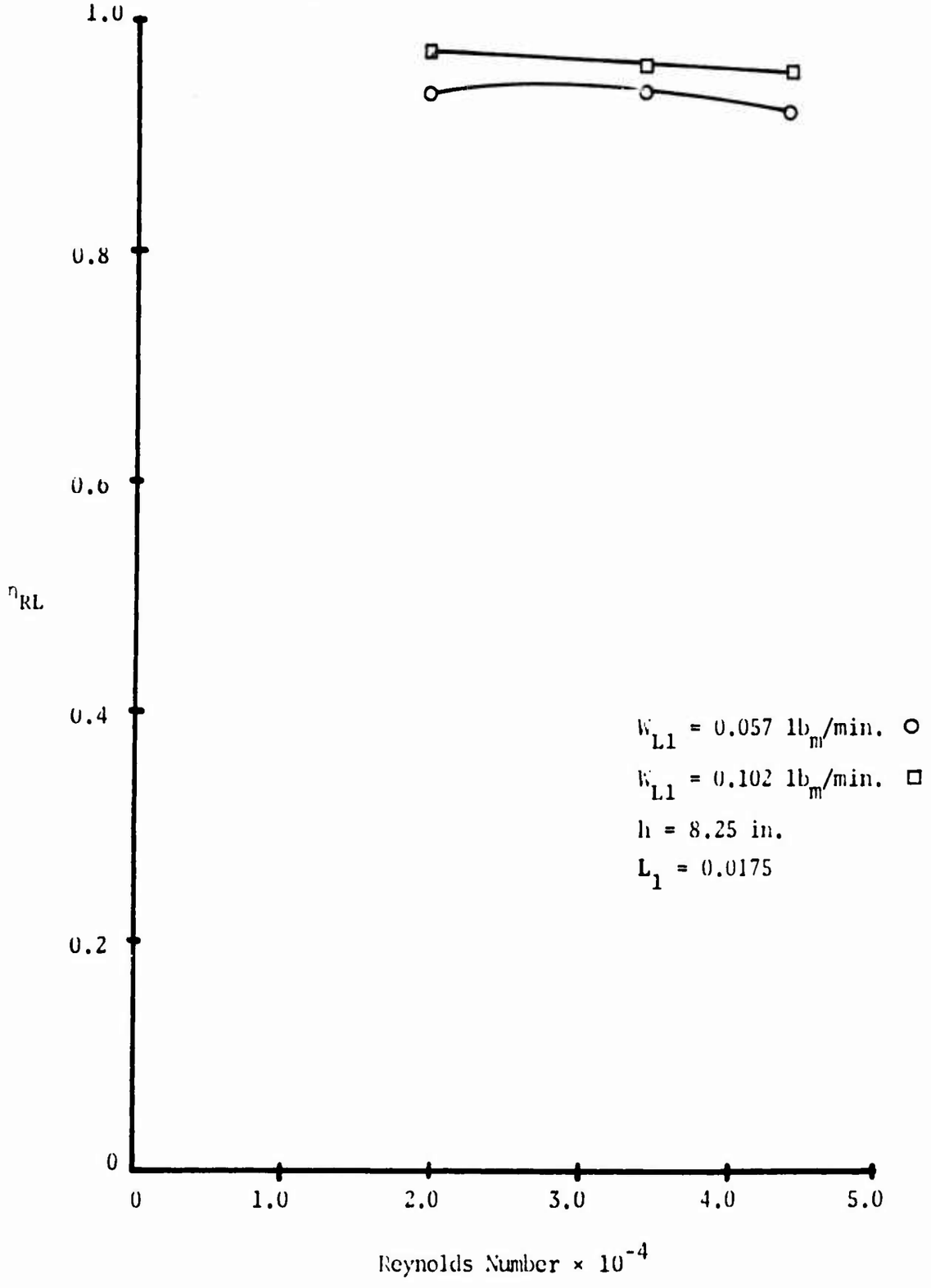

Figure 45

Pressure Drop vs. Reynolds Number For Oil With ν = 10.0 Centistokes At Various Oil Flow Rates For 45° Cone

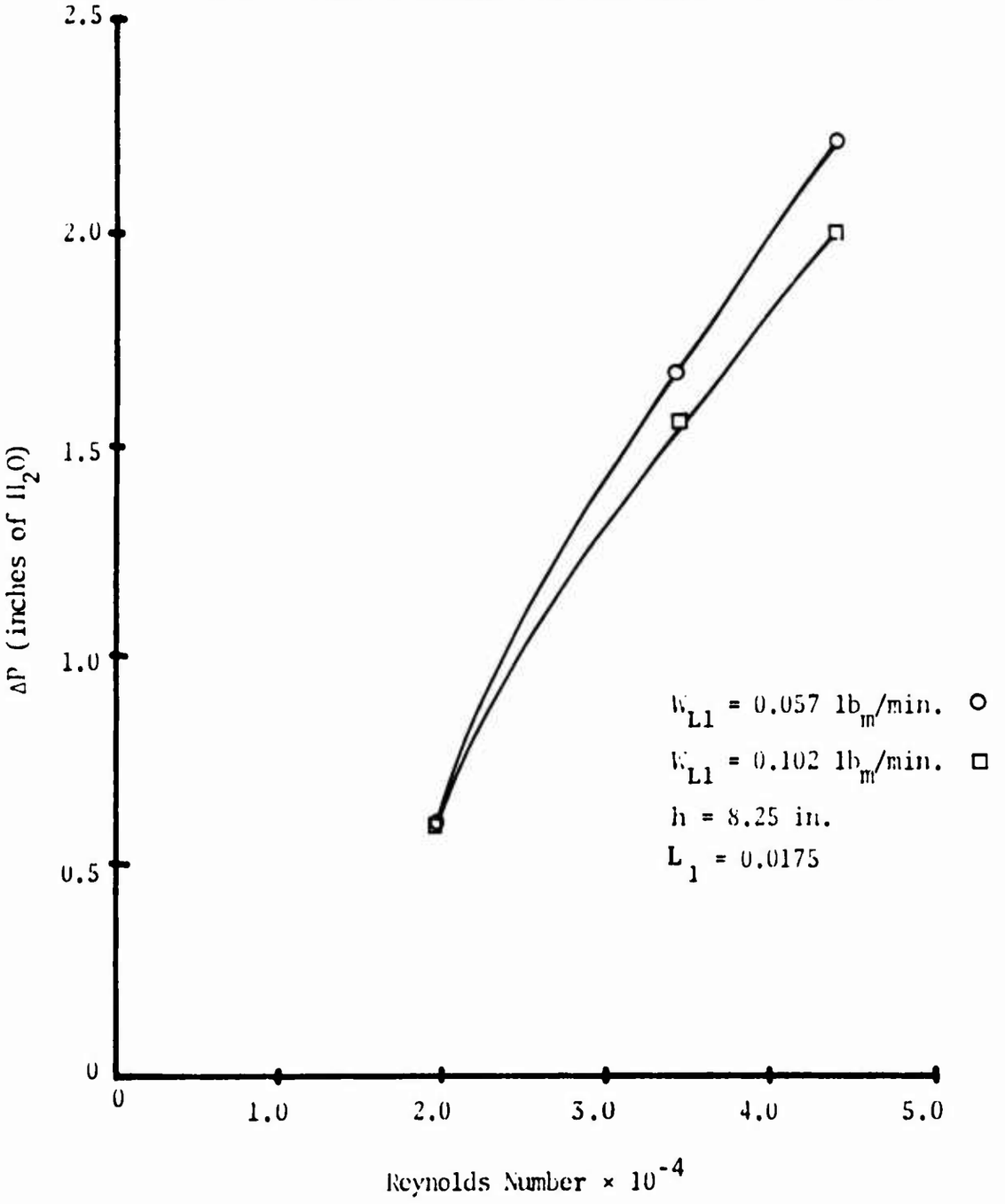

Figure 46

Efficiency vs. Reynolds Number For Oil With ν = 10.0 Centistokes

At Various Underflow Diameters For 45° Cone

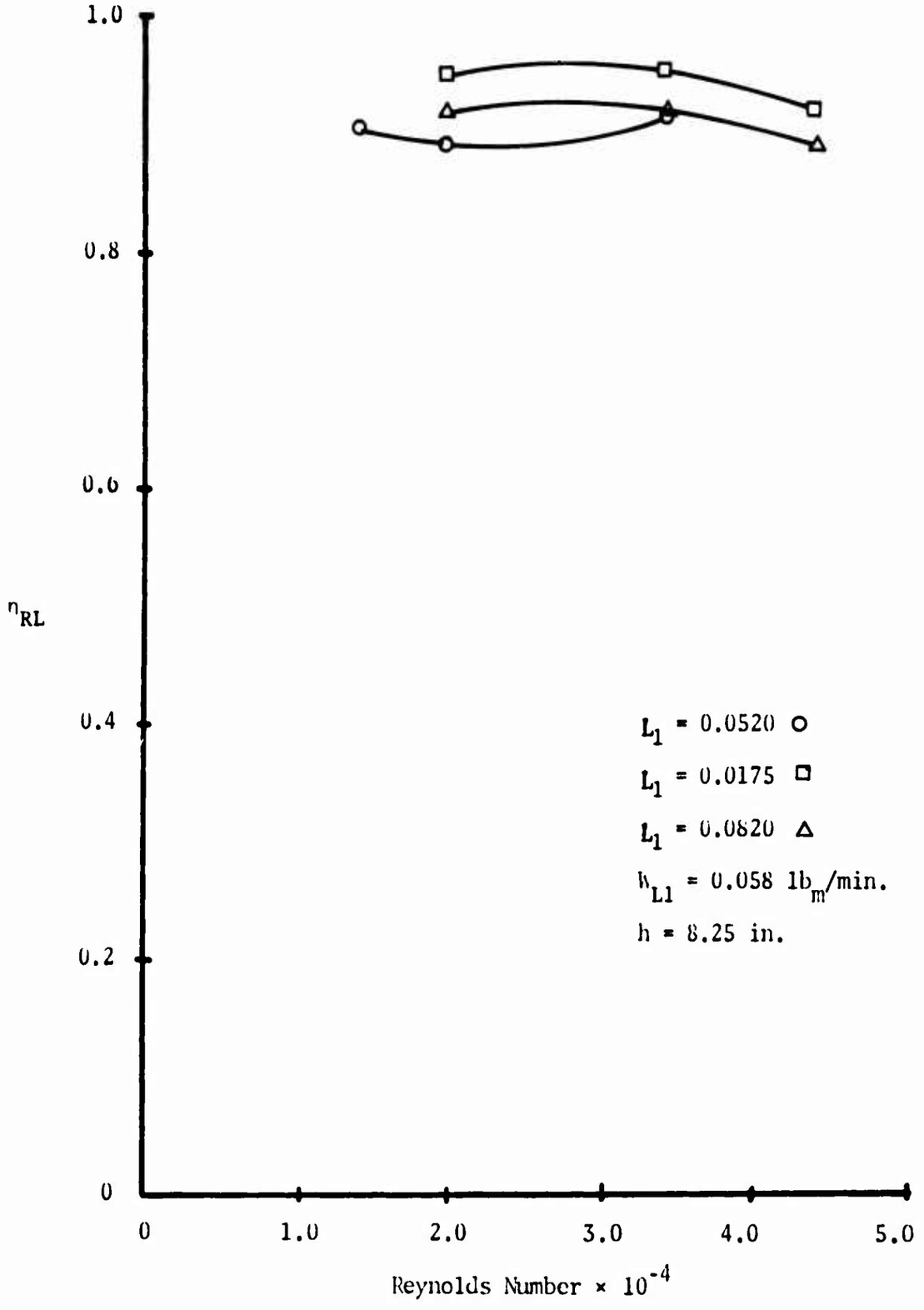

Figure 47

Pressure Drop vs. Reynolds Number For Oil With ν = 10.0 Centistokes

At Various Underflow Diameters For 45° Cone

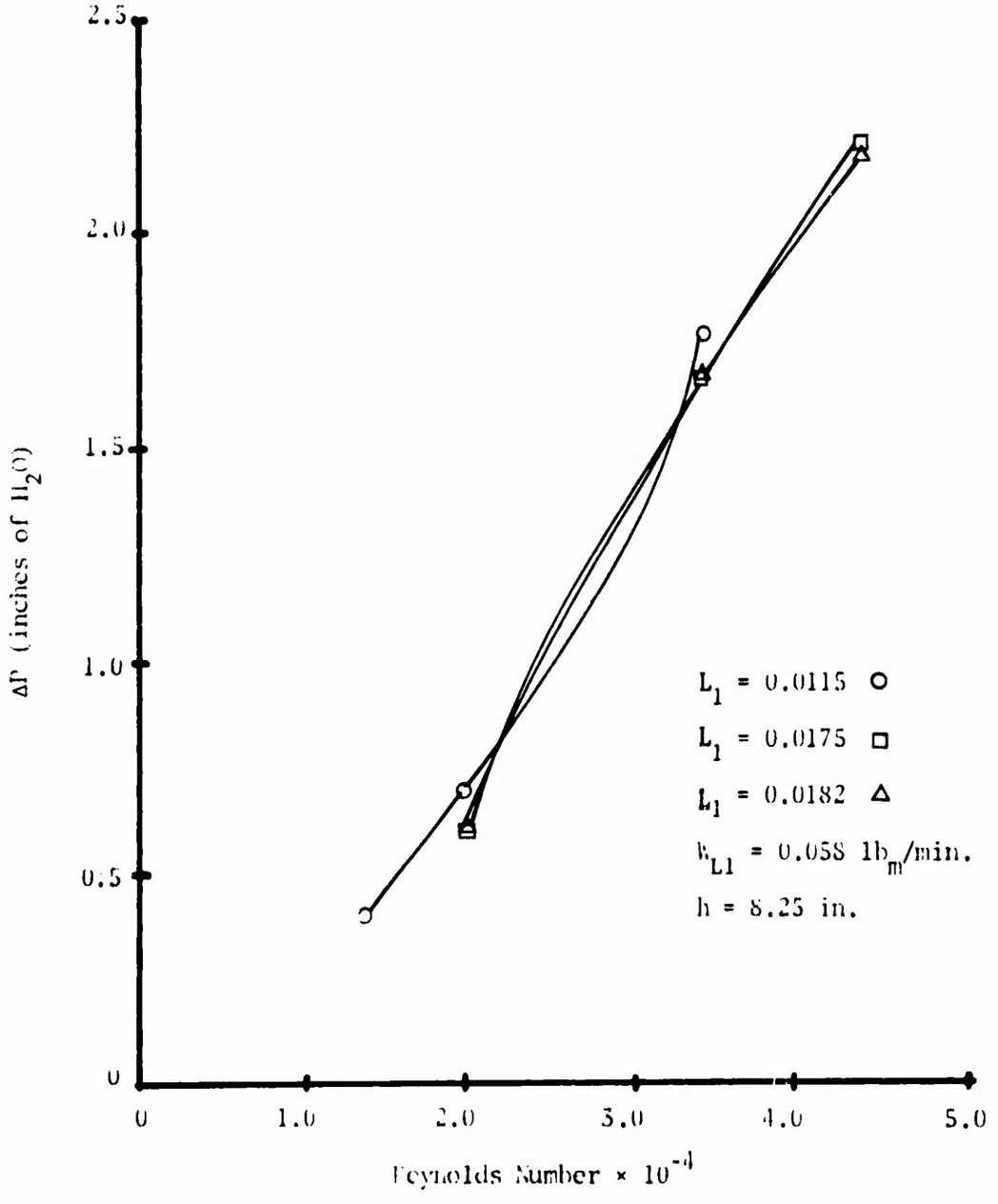

Figure 48

The separator was also run in an "upside down" position (against gravity) as indicated in Figure 2. At the exit of the cone, there was, as found and discussed by Lawler, an adverse static pressure gradient. Because of this static pressure gradient it was not possible to maintain experimental operation which gave a liquid purity of one in this position. Thus, no data is presented for "upside down" operation. However these tests do indicate that the secondary flow is an important part of the discharging of the heavier component because it was possible to see the oil spiral up the inside surface of the cone, against gravity, and then sputter out the exit. The secondary flow was able to overcome the unfavorable body force (gravity) but was unable to flow freely out the exit due to the adverse static pressure gradient.

CHAPTER IV

CONCLUSIONS

This paper considered the boundary layer discharge of the heavier component of a two-phase mixture. An approximation to this secondary flow rate was obtained, making use of an experimental velocity profile which had been determined by ter Linden. This approximation appears to be physically more realistic than Lawler's.

The experimental work, performed on the same separator as used by Lawler, was done both with and against gravity. The influence of certain geometric factors and various operating conditions on separation over a relatively wide range of Reynolds and Weber numbers is presented. From the experimental results with gravity it can be stated that without evaporation, it is possible to obtain nearly 100% efficiency of removal. Operating the separator against gravity gives evidence that the effect of the secondary flow is great enough to overcome an adverse body force, even though there is a problem in the exiting of this flow because of an adverse static pressure gradient. This seems to indicate that such a cyclone separator would perform effectively in an environment of micro-or-no gravity conditions. To summarize the experimental results: i) increasing the separator height has no effect on efficiency and decreases the pressure drop; ii) decreasing the underflow diameter increases the efficiency and slightly increases the pressure drop; iii) increasing the inlet oil flow rates

slightly increases the efficiency and decreases the pressure drop;
iv) increasing the cone angle has no effect on efficiency and increases the pressure drop.

APPENDIX I

Soultion Of The Boundary Layer Equations By Integral Means

The boundary layer equations for a cone can be written as:

$$u \frac{\partial u}{\partial x} - \frac{v^2}{x} + w \frac{\partial u}{\partial z} = - \frac{1}{\rho} \frac{\partial p}{\partial x} + \nu \frac{\partial^2 u}{\partial z^2} \tag{I.1a}$$

$$w \frac{\partial v}{\partial z} + u \frac{\partial v}{\partial x} + \frac{uv}{x} = \nu \frac{\partial^2 v}{\partial z^2} \tag{I.1b}$$

$$\frac{\partial p}{\partial z} = 0 \tag{I.1c}$$

$$\frac{\partial}{\partial x} (ux) + \frac{\partial}{\partial z} (wx) = 0 \tag{I.1d}$$

The reader is referred to Lawler's paper for a detailed derivation of the above boundary layer equations.

Let $v = K(R)$ where $R = x\sin\theta$

$$\therefore v = K(x) \tag{I.2}$$

The inviscid equations give:

$$\frac{1}{\rho} \frac{\partial p}{\partial x} = \frac{v^2}{x}$$

$$\therefore \quad - \frac{1}{\rho} \frac{\partial p}{\partial x} = \frac{v^2}{x} = - \frac{K^2(x)}{x} \tag{I.3}$$

Equations (I.1a)- (I.1d) become:

$$u \frac{\partial u}{\partial x} - \frac{v^2}{x} + w \frac{\partial u}{\partial z} = - \frac{K^2(x)}{x} + \nu \frac{\partial^2 u}{\partial z^2} \tag{I.4a}$$

$$w \frac{\partial v}{\partial z} + u \frac{\partial v}{\partial x} + \frac{uv}{x} = \nu \frac{\partial^2 v}{\partial z^2} \tag{I.4b}$$

$$\frac{\partial}{\partial x} (ux) + \frac{\partial}{\partial z} (xw) = 0 \tag{I.4c}$$

The appropriate boundary conditions are:

$$\text{At } z = 0 : \quad u = V = 0 \tag{I.5a}$$

$$\text{At } z = \delta : \quad u = \frac{\partial u}{\partial z} = \frac{\partial v}{\partial z} = 0 \; ; \; v = K(x) \tag{I.5b}$$

Integrating the x-momentum equation, (I.4a), from 0 to d with respect to z :

$$\int_0^{\delta} u \frac{\partial u}{\partial x} + w \frac{\partial u}{\partial z} - \frac{v^2}{x} + \frac{K^2(x)}{x} \, d_z = \nu \frac{\partial u}{\partial z} \Big|_0^{\delta} \tag{I.6}$$

But:
$$\int_0^{\delta} w \frac{\partial u}{\partial z} \, dz = \Big[uw \Big]_0^{\delta} - \int_0^{\delta} u \frac{\partial w}{\partial z} \, dz$$

$$= - \int_0^{\delta} u \frac{\partial w}{\partial z} \, dz$$

Also, from equation (I.4a):

$$\frac{\partial w}{\partial z} = - \frac{u}{x} + \frac{\partial u}{\partial x}$$

Substituting these into equation (I.6) the integral form of the x-momentum equation is obtained:

$$\partial \int_0^\delta u \frac{u}{x} d_z + \int_0^\delta \frac{u^2}{x} d_z + \int_0^\delta \frac{1}{x} K^2(x) - v^2 d_z = \nu \frac{\partial u}{\partial z} \Bigg|_0^\delta \qquad (I.7)$$

Integrating equation (I.4b) from 0 to δ with respect to z and making use of the boundary conditions one obtains the y-momentum inegral equation:

$$-K(x) \int_0^\delta \frac{1}{x} \frac{\partial}{\partial x} (ux) d_z + 2 \int_0^\delta \frac{uv}{x} d_z + \int_0^\delta \frac{\partial}{\partial x} (ur) d_z = \nu \frac{\partial v}{\partial z} \Bigg|_0^\delta \qquad (1.8)$$

It is desired that u and v satisfy the boundary conditions, equations (I.5a) and (I.5b) to meet these conditions let:

$$u = E(x) K(x) F(\eta) = E(x) K(x) (\eta - 2\eta^2 + \eta^3) \qquad (I.9a)$$

$$v = K(x) \phi(\eta) = K(x) (2\eta - \eta^2) \qquad (I.9b)$$

where $\eta \equiv \frac{z}{\delta}$ and $E = E(x)$, $\delta = \delta(x)$ are unknowns.

Note that $d\eta = \frac{d_z}{\delta} - \frac{z}{\delta^2} \delta' dx$

$\therefore dz = \delta d\eta$ for integration over z at fixed x. (I.9c)

$$\delta_1 = \delta \frac{K(x)}{\nu L} = \text{dimensionless boundary layer thickness.} \quad \text{(I.9d)}$$

By substituting the appropriate combinations of equations (I.9a) and (I.9b) along with equations (I.9c) - (I.9d) into equations (I. 7) and (I. 8) respectively one obtains:

$$\delta_1^2 \frac{d}{dx}(E^2) + \frac{E^2}{2}\frac{d}{dx}(\delta_1^2) + \frac{E^2\delta_1^2}{x} + 2E^2\delta_1^2 \frac{d}{dx} \ln K(x) + \frac{49\delta_1^2}{x} + 105E = 0 \quad \text{(I.10a)}$$

$$\delta_1^2 \frac{d}{dx}(E^2) + E^2 \frac{d}{dx}(\delta_1^2) - \frac{E^2\delta_1^2}{x} - E^2\delta_1^2 \frac{d}{dx} \ln K(x) - 120E = 0 \quad \text{(I.10b)}$$

By combining these equations and noting that:

$$2\frac{d}{dx}(E\delta^2) = 2\frac{d}{dx}(E)\,\delta^2 + 4E\delta\frac{d\delta}{dx}$$

one obtains the final form of the equations:

$$\frac{d}{dx}(E^2) = -\frac{3E^2}{x} - 5E^2\frac{d}{dx}\ln K(x) - \frac{98}{x} - \frac{330E^2}{E\delta_1^2} \quad \text{(I.11a)}$$

$$\frac{d}{dx}(E\delta_1^2) = \frac{5}{2}\frac{E\delta_1^2}{x} + \frac{7}{2}E\delta_1^2\frac{d}{dx}\ln K(x) + \frac{49E\delta_1^2}{xE^2} + 285 \quad \text{(I.11b)}$$

The initial conditions are: $E = \delta_1 = 0$ at $x = 1.0$ thus, both equation (I.11a) and (I.11b) have singularities at their initial values.

Following Taylor's method (2); Let:

$$E\delta_1^2 = A(x-1) \quad \text{and} \quad E^2 = B(x-1)$$

Substituting these expressions into (I.11a) and (I.11b) and evaluating at $x = 1.0$, it is found that $A = 80$, $B = -19.1$.

Thus $$E\delta_1^2 = 80(x-1) \tag{I.12a}$$

$$E^2 = -19.1(x-1) \tag{I.12b}$$

Assuming these relations (I.12a)-(I.12b) to be valid very near to $x = 1.0$, it is now possible to obtain new, non-singular initial conditions.

APPENDIX II

Samples of the experimental data are presented on the following pages. The inlet pressure and the temperature were measured directly. The heavy fluid outflow rate was determined by measurements of the volume liquid flow, Q, in a time interval, t. The pressure drop across the orifice meter, ΔP, was used to calculate the volume flow rate of air and, from this, the inlet air velocity. The inlet oil flow rate was determined from a knowledge of the nozzle diameter, the pressure drop across the nozzle, P_{LIQ}, and the oil being sprayed.

15° Cone

.011 in. Nozzle ; h = 8.25 in. ; L_1 = .0156 ; ν = 1.0

P in. in. of H_2O	P in. of H_2O	Temp. °F	P_{LIQ} in. of H_g	Q ml.	t sec.
1.75	0.30	93.8	26.5	28.5	60.2
5.70	1.00	94.0	26.5	25.5	60.4
10.0	1.80	91.0	26.5	22.8	61.0
13.7	2.40	89.5	26.5	16.5	60.6
18.9	3.20	90.0	26.5	10.0	61.2
2.90	0.50	94.5	26.5	26.5	60.2
5.70	1.00	93.8	26.5	26.0	60.2
10.1	1.80	90.8	26.5	21.5	60.2
13.6	2.40	89.5	26.5	15.5	60.4
18.9	3.20	90.9	26.5	10.0	60.2
13.7	2.40	89.5	26.5	15.5	61.0
0.6	0.10	95.0	50.0	48.2	60.2
1.70	0.30	96.0	50.0	43.5	60.2
2.80	0.50	96.0	50.0	40.0	60.0
5.20	1.00	93.5	50.0	36.8	60.2
9.10	1.80	91.5	50.0	31.0	60.0
11.20	2.40	95.0	50.0	24.5	60.2
15.80	3.20	89.8	50.0	22.8	60.6
0.60	0.10	94.8	50.0	47.5	60.2

15° Cone

.011 in. Nozzle ; h = 8.25 in. ; L_1 = .0156 ; ν = 1.0

P in. in. of H_2O	ΔP in. of H_2O	Temp. °F	P_{LIQ} in. of H_g	Q ml.	t sec.
1.70	0.30	96.0	50.0	44.2	60.0
2.80	0.50	96.0	50.0	40.5	60.2
5.2	1.00	93.5	50.0	37.5	60.6
9.0	1.80	91.2	50.0	32.8	60.2
11.2	2.40	95.0	50.0	24.5	60.2
8.9	1.80	91.2	50.0	32.8	60.4
11.6	2.40	95.0	50.0	26.0	60.2
15.9	3.20	89.8	50.0	22.2	60.2

.011 in. Nozzle ; h = 4.75 in. ; L_1 = .0174 ; ν = 10.0

P in. in. of H_2O	ΔP in. of H_2O	Temp. °F	P_{LIQ} in. of H_g	Q ml.	t sec.
0.30	0.05	85.0	17.5	23.4	60.0
0.65	0.10	88.6	17.5	24.0	59.8
1.85	0.30	90.0	17.5	24.0	60.2
3.00	0.50	90.0	17.5	24.0	60.0
5.35	1.00	89.0	17.5	24.0	60.0
0.30	0.05	85.0	17.5	24.0	60.2
0.65	0.10	88.6	17.5	24.0	60.2

15° Cone

.011 in. Nozzle ; h = 4.75 in. ; L_1 = 0.174 ; ν = 10.0

P in. in. of H_2O	ΔP in. of H_2O	Temp. °F	P_{LIQ} in. of H_g	Q ml.	t sec.
1.85	0.30	90.1	17.5	24.0	60.0
3.00	0.50	90.0	17.5	24.5	60.2
5.40	1.00	89.0	17.5	23.8	59.6

15° Cone

.011 in. Nozzle ; h = 8.25 in. ; L_1 = .0162 ; ν = 10.0

0.30	0.05	88.0	17.5	23.8	60.0
0.60	0.10	89.2	17.5	24.0	60.0
1.80	0.30	92.5	17.5	24.0	61.0
2.80	0.50	92.5	17.5	24.1	60.0
5.70	1.00	92.0	17.5	24.2	60.0
0.30	0.05	88.0	17.5	24.0	59.6
0.65	0.10	89.2	17.5	24.0	60.0
1.80	0.30	92.5	17.5	24.0	59.6
2.80	0.50	92.5	17.5	24.2	60.0
5.65	1.00	92.0	17.5	24.0	60.2

15° Cone

.011 in Nozzle ; h = 8.25 in : L_1 = .0156 ; ν = 10.0

0.30	0.05	84.2	17.5	24.8	60.2
0.60	0.10	89.9	17.5	24.2	60.0

15° Cone

.011 in Nozzle ; h = 8.25 in. ; L_1 = .0156 ; ν = 10.0

P in. in. of H_2O	ΔP in. of H_2O	Temp. °F	P_{LIQ} in. of Hg	Q ml.	t sec.
1.80	0.30	91.0	17.5	24.2	60.0
2.80	0.50	91.2	17.5	25.0	60.6
5.70	1.00	89.5	17.5	23.2	60.0
0.30	0.05	86.6	17.5	24.2	60.0
0.60	0.10	90.2	17.5	24.0	60.0
1.75	0.30	91.2	17.5	25.0	60.4
2.80	0.50	91.2	17.5	25.0	60.0
5.65	1.00	89.8	17.5	24.0	60.4

15° Cone

.011 in Nozzle ; h = 8.25 in. ; L_1 = .0174 ; ν = 10.0

0.30	0.05	92.0	17.5	24.0	59.8
0.55	0.10	94.0	17.5	23.8	60.2
1.80	0.30	94.8	17.5	23.6	60.2
2.80	0.50	95.0	17.5	23.5	60.0
5.50	1.00	87.0	17.5	23.2	60.2
9.50	1.80	87.5	17.5	24.0	60.0
0.30	0.05	92.0	17.5	24.2	60.4
0.60	0.10	94.1	17.5	24.0	60.2
1.75	0.30	94.8	17.5	23.5	60.0

15°Cone

0.11 in. Nozzle ; h = 8.25 in. ; L_1 = .0174 ; ν = 10.0

P in. in. of H_2O	ΔP in. of H_2O	Temp. °F	P_{LIQ} in. of H_g	Q ml.	t sec.
2.80	0.50	95.0	17.5	23.8	60.0
5.50	1.00	87.0	17.5	23.8	60.0
9.50	1.80	87.5	17.5	24.0	60.4
0.30	0.05	92.5	35.0	38.4	60.6
0.60	0.10	93.0	35.0	38.9	60.0
1.70	0.30	94.0	35.0	40.0	60.4
2.70	0.50	94.5	35.0	40.0	61.0
5.25	1.00	93.5	35.0	39.8	60.2
9.40	1.80	91.0	35.0	40.0	60.4
0.30	0.05	92.5	35.0	39.0	60.0
0.65	0.10	92.0	35.0	39.0	60.4
1.70	0.30	94.0	35.0	39.2	60.0
2.70	0.50	94.5	35.0	39.0	60.0
5.20	1.00	93.5	35.0	40.0	60.6
9.40	1.80	91.0	35.0	39.8	60.4
0.30	0.05	93.2	58.4	54.5	60.2
0.60	0.10	95.0	58.4	54.5	60.0
1.70	0.30	95.8	58.4	54.8	60.0
2.70	0.50	95.4	58.4	54.2	60.2

15° Cone

0.11 in. Nozzle ; h = 8.25 in. ; L_1 = .0174 ; ν = 10.0

P in. in. of H_2O	ΔP in. of H_2O	Temp. °F	P_{LIQ} in. of H_g	Q ml.	t sec.
0.30	0.05	93.2	58.4	53.8	60.0
0.60	0.10	95.0	58.4	54.0	60.0
1.70	0.30	95.8	58.4	54.5	60.4
2.75	0.50	95.2	58.4	54.2	60.4

15° Cone

.011 in. Nozzle ; h = 12.75 in. ; L_1 = .0174 ; ν = 10.0

0.30	0.05	86.5	17.5	23.5	60.2
0.50	0.10	90.0	17.5	24.5	60.2
1.40	0.30	92.5	17.5	24.0	59.6
2.20	0.50	91.0	17.5	24.0	60.0
4.30	1.00	89.6	17.5	24.0	60.4
0.35	0.05	86.5	17.5	23.5	60.0
0.50	0.10	90.0	17.5	24.0	60.6
1.35	0.30	92.5	17.5	24.0	59.8
2.20	0.50	91.0	17.5	24.0	60.2
4.30	1.00	89.6	17.5	24.0	60.4

15° Cone

.011 in. Nozzle ; h = 15.00 in. ; L_1 = .0174 ; ν = 10.0

0.30	0.05	86.9	17.5	23.0	59.6

15° Cone

.011 in. Nozzle ; h = 15.00 in. ; L_1 = .0174 ; ν = 10.0

P in. in. of H_2O	ΔP in. of H_2O	Temp °F	P_{LIQ} in. of H_g	Q ml.	t sec.
0.50	0.10	89.0	17.5	23.8	60.0
1.35	0.30	91.0	17.5	23.6	60.0
2.00	0.50	91.0	17.5	23.5	60.4
4.20	1.00	89.5	17.5]	24.0	60.4
0.30	0.05	86.9	17.5	23.2	60.0
0.50	0.10	89.0	17.5	23.8	60.2
1.30	0.30	91.0	17.5	23.5	60.4
2.00	0.50	91.0	17.5	24.0	60.4
4.20	1.00	89.5]	17.5	24.0	60.6

15° Cone

0.14 in. Nozzle ; h = 8.25 in. ; L_1 = .0506 ; ν = 100.0

0.60	0.10	98.0	46.0	39.6	60.8
1.50	0.30	98.6	46.0	39.5	60.0
2.40	0.50	95.0	46.0	39.5	60.0
3.70	0.80	95.0	46.0	39.0	57.8
0.60	0.10	98.0	46.0	39.6	60.4
1.50	0.30	98.6	46.0	39.5	60.0
2.50	0.50	95.0	46.0	39.5	60.0
3.70	0.80	95.0	46.0	39.5	60.2

15° Cone

.014 in. Nozzle ; h = 12.75 in. ; L_1 = .0506 ; ν = 100.0

P in in. of H_2O	ΔP in. of H_2O	Temp. °F	P_{LIQ} in. of Hg	Q ml.	t sec.
0.90	0.10	92.0	46.0	38.0	60.0
1.20	0.30	93.0	46.0	38.5	60.4
1.80	0.50	94.0	46.0	38.5	60.2
2.80	0.80	94.2	46.0	38.5	60.4
0.9	0.10	92.2	46.0	38.0	60.0
1.20	0.30	93.0	46.0	39.0	60.2
1.85	0.50	94.0	46.0	38.2	60.4
2.80	0.80	94.2	46.0	38.2	60.2

15° Cone

.014 in. Nozzle ; h = 15.00 in. ; L_1 = .0506 ; ν = 100.0

0.30	0.10	86.2	46.0	39.0	60.2
1.20	0.30	91.0	46.0	39.5	60.4
1.70	0.50	91.6	46.0	38.0	60.2
2.60	0.80	91.2	46.0	39.5	60.6
0.40	0.10	86.3	46.0	39.5	60.2
1.15	0.30	91.0	46.0	39.5	60.0
1.70	0.80	91.2	46.0	39.5	60.6
2.65	0.80	91.2	46.0	39.5	60.4

45° Cone

.011 in. Nozzle ; h = 8.25 in. ; L_1 = .0174 ; ν = 10.0

P in in. of H_2O	ΔP in. of H_2O	Temp. °F	P_{LIQ} in. of H_g	Q ml.	t sec.
0.60	0.10	93.0	20.0	26.5	60.2
1.70	0.30	94.5	20.0	27.0	60.0
2.25	0.50	94.0	20.0	26.0	60.2
0.60	0.10	93.0	20.0	27.0	60.0
1.65	0.30	94.6	20.0	26.5	60.0
2.20	0.50	94.0	20.0	25.8	59.8

45° Cone

0.11 in Nozzle ; h = 8.25 in. ; L_1 = .0116 ; ν = 10.0

0.40	0.05	89.2	17.5	23.8	60.6
0.70	0.10	91.0	17.5	22.8	60.0
1.80	0.30	92.0	17.5	23.8	60.2
0.40	0.05	89.2	17.5	23.0	60.2
0.70	0.10	91.0	17.5	23.0	60.2
1.75	0.30	92.0	17.5	23.6	61.0

45° Cone

.014 in. Nozzle ; h = 8.25 in. ; L_1 = .0182 ; ν = 10.0

0.60	0.10	95.6	20.0	26.0	60.2
1.70	0.30	96.6	20.0	26.0	60.0
2.20	0.50	97.0	20-0	25.0	60.2

45° Cone

.014 in. Nozzle ; h = 8.25 in. ; L_1 = .0182 ; ν = 10.0

P in. in. of H_2O	ΔP in. of H_2O	Temp. °F	P_{LIQ} in. of Hg	Q ml.	t sec.
0.55	0.10	95.6	20.0	26.0	60.2
1.70	0.30	96.6	20.0	26.0	60.6
2.20	0.50	97.0	20.0	25.2	60.4

45° Cone

.014 in. Nozzle ; h = 8.25 in. ; L_1 = .0174 ; ν = 10.0

0.6	0.10	95.6	50.0	49.0	60.6
1.5	0.30	96.0	50.0	48.5	60.8
2.0	0.50	95.0	50.0	48.5	60.8
0.6	0.10	95.6	50.0	49.0	60.4
1.6	0.30	96.0	50.0	49.0	61.0
2.0	0.50	95.0	50.0	48.0	60.2

45° Cone

.011 in. Nozzle ; h = 12.75 in. ; L_1 = .0174 ; ν = 10.0

0.40	0.10	94.0	20.0	27.0	60.0
1.35	0.30	94.2	20.0	26.5	60.2
2.00	0.50	94.5	20.0	25.0	60.2
0.50	0.10	94.0	20.0	27.0	60.0
1.40	0.30	94.2	20.0	26.0	60.0
2.00	0.50	94.4	20.0	25.0	60.4

45° Cone

.011 in. Nozzle ; h = 15.00 in. ; L_1 = .0175 ; ν = 10.0

P in in. of H_2O	ΔP in. of H_2O	Temp. °F	P_{LIQ} in. of Hg	Q ml.	t sec.
0.35	0.10	91.0	22.0	25.0	60.4
1.20	0.30	93.8	22.0	24.0	60.4
1.80	0.50	94.0	22.0	22.0	60.2
0.40	0.10	91.0	22.0	24.0	60.2
1.80	0.50	94.0	22.0	23.0	60.2

BIBLOGRAPHY

1. Stromquist, A.J.:"Zero Gravity Development For Re-generation Fuel Cell", ASD-TDR-62-240, (by Thompson Ramo Wooldridge, Inc. For The Flight Accessories Laboratory, ASD, Wright-Patterson AFB, Ohio) 1962.

2. Taylor, G.I.:" The Boundary Layer in The Conveying Nozzle of a Swirl Atomizer", Qwart. Jour. Mech. and Appl. Math., Vol. III, Pt. 2, pp. 129-139, 1950.

3. ter Linden, A.J.:"Investigations into Cyclone Dust Collectors", Proc. Inst. Mech. Eng. London, Vol. 160, No. 2, pp 233-251, 1949.

4. Van Dongen, J.R.J.; and ter Linden, A.J.:"The Application of Gas/Liquid Cyclone in Oil Refining", Trans. ASME, pp. 245-251, Jan., 1958.

5. Moore, F.K.: "Three-Dimensional Boundary Layer Theory", Advances in Applied Mechanics, Vol. IV, pp. 159-228, Academic Press Inc., New York, 1956.

6. Lawler, M.T., "A Study of Cyclonic Two-Fluid Separation", Master's Thesis, Case Institute of Technology, 1965.

Security Classification

DOCUMENT CONTROL DATA - R&D

(Security classification of title, body of abstract and indexing annotation must be entered when the overall report is classified)

1. ORIGINATING ACTIVITY (Corporate author) Case Institute of Technology Fluid, Thermal and Aerospace Sciences Group Cleveland, Ohio	2a. REPORT SECURITY CLASSIFICATION UNCLASSIFIED 2b GROUP

3. REPORT TITLE

LIQUID-GAS CYCLONE SEPARATION

4. DESCRIPTIVE NOTES (Type of report and inclusive dates)

Scientific.----------Interim.

5. AUTHOR(S) (Last name, first name, initial)

Sanford Fleeter
Simon Ostrach

6. REPORT DATE	7a. TOTAL NO. OF PAGES	7b. NO. OF REFS
June 1966	113	6

8a. CONTRACT OR GRANT NO.	9a. ORIGINATOR'S REPORT NUMBER(S)
AF-AFOSR 194-66 b. PROJECT NO. 9781-01 c. 61445014 d. 681307	FTAS/TR-66-12 9b. OTHER REPORT NO(S) (Any other numbers that may be assigned this report) AFOSR 66-1400

10. AVAILABILITY/LIMITATION NOTICES

1. Distribution of this document is unlimited.

11. SUPPLEMENTARY NOTES	12. SPONSORING MILITARY ACTIVITY
	AF Office of Scientific Research (SREM) 1400 Wilson Boulevard Arlington, Virginia 22209

13. ABSTRACT

This paper considers the secondary-flow in a liquid-gas mixture in a cyclone separator. By means of a momentum integral method, an engineering approximation to the secondary (heavy fluid) flow rate is obtained which makes use of an experimental velocity profile determined by ter Linden. This flow rate approximation is physically realistic and is partially verified in the laboratory. Tests were run on a separator to determine the effect of the variation of certain operating conditions and geometric factors on the separation of a liquid-gas mixture. The effect of these variations on the efficiency of separation and pressure drop across the separator as functions of the Reynolds and Weber numbers is presented.

DD FORM 1 JAN 64 1473

Security Classification

Security Classification

14. KEY WORDS	LINK A		LINK B		LINK C	
	ROLE	WT	ROLE	WT	ROLE	WT
Fluid Mixtures Fluid Separation Vortex Flows						

INSTRUCTIONS

1. ORIGINATING ACTIVITY: Enter the name and address of the contractor, subcontractor, grantee, Department of Defense activity or other organization *(corporate author)* issuing the report.

2*a*. REPORT SECURITY CLASSIFICATION: Enter the overall security classification of the report. Indicate whether "Restricted Data" is included. Marking is to be in accordance with appropriate security regulations.

2*b*. GROUP: Automatic downgrading is specified in DoD Directive 5200.10 and Armed Forces Industrial Manual. Enter the group number. Also, when applicable, show that optional markings have been used for Group 3 and Group 4 as authorized.

3. REPORT TITLE: Enter the complete report title in all capital letters. Titles in all cases should be unclassified. If a meaningful title cannot be selected without classification, show title classification in all capitals in parenthesis immediately following the title.

4. DESCRIPTIVE NOTES: If appropriate, enter the type of report, e.g., interim, progress, summary, annual, or final. Give the inclusive dates when a specific reporting period is covered.

5. AUTHOR(S): Enter the name(s) of author(s) as shown on or in the report. Enter last name, first name, middle initial. If military, show rank and branch of service. The name of the principal author is an absolute minimum requirement.

6. REPORT DATE: Enter the date of the report as day, month, year; or month, year. If more than one date appears on the report, use date of publication.

7*a*. TOTAL NUMBER OF PAGES: The total page count should follow normal pagination procedures, i.e., enter the number of pages containing information.

7*b*. NUMBER OF REFERENCES: Enter the total number of references cited in the report.

8*a*. CONTRACT OR GRANT NUMBER: If appropriate, enter the applicable number of the contract or grant under which the report was written.

8*b*, 8*c*, & 8*d*. PROJECT NUMBER: Enter the appropriate military department identification, such as project number, subproject number, system numbers, task number, etc.

9*a*. ORIGINATOR'S REPORT NUMBER(S): Enter the official report number by which the document will be identified and controlled by the originating activity. This number must be unique to this report.

9*b*. OTHER REPORT NUMBER(S): If the report has been assigned any other report numbers *(either by the originator or by the sponsor)*, also enter this number(s).

10. AVAILABILITY/LIMITATION NOTICES: Enter any limitations on further dissemination of the report, other than those imposed by security classification, using standard statements such as:

(1) "Qualified requesters may obtain copies of this report from DDC."

(2) "Foreign announcement and dissemination of this report by DDC is not authorized."

"U. S. Government agencies may obtain copies of this report directly from DDC. Other qualified DDC users shall request through

_____."

(4) "U. S. military agencies may obtain copies of this report directly from DDC. Other qualified users shall request through

_____."

(5) "All distribution of this report is controlled. Qualified DDC users shall request through

_____."

If the report has been furnished to the Office of Technical Services, Department of Commerce, for sale to the public, indicate this fact and enter the price, if known.

11. SUPPLEMENTARY NOTES: Use for additional explanatory notes.

12. SPONSORING MILITARY ACTIVITY: Enter the name of the departmental project office or laboratory sponsoring *(paying for)* the research and development. Include address.

13. ABSTRACT: Enter an abstract giving a brief and factual summary of the document indicative of the report, even though it may also appear elsewhere in the body of the technical report. If additional space is required, a continuation sheet shall be attached.

It is highly desirable that the abstract of classified reports be unclassified. Each paragraph of the abstract shall end with an indication of the military security classification of the information in the paragraph, represented as *(TS)*, *(S)*, *(C)*, or *(U)*.

There is no limitation on the length of the abstract. However, the suggested length is from 150 to 225 words.

14. KEY WORDS: Key words are technically meaningful terms or short phrases that characterize a report and may be used as index entries for cataloging the report. Key words must be selected so that no security classification is required. Identifiers, such as equipment model designation, trade name, military project code name, geographic location, may be used as key words but will be followed by an indication of technical context. The assignment of links, rules, and weights is optional.

GPO 886-551